2023

Exploring Pah Partitioning In Oysters Using Immunological Techniques

Kristen Madison Prossner
College of William and Mary - Virginia Institute of Marine Science, kprossner@gmail.com

Exploring PAH Partitioning in Oysters Using Immunological Techniques

---

A Dissertation

Presented to

The Faculty of the School of Marine Science

William & Mary

In Partial Fulfillment

of the Requirements for the Degree of

Doctor of Philosophy

---

by

Kristen Madison Prossner

May 2023

APPROVAL PAGE

This Dissertation is submitted in partial fulfillment of

the requirements for the degree of

Doctor of Philosophy

Kristen Madison Prossner

Approved by the Committee, May 2023

Michael A. Unger, PhD
Committee Chair / Advisor

Ryan B. Carnegie, PhD

Roger L. Mann, PhD

Jeffrey D. Shields, PhD

Upal Ghosh, PhD
University of Maryland Baltimore Country
Baltimore, MD, USA

This Ph.D. is dedicated to the educators in my life who inspired me to stay curious and love learning.

TABLE OF CONTENTS

ACKNOWLEDGEMENTS

First, I would like to thank my incredible advisor Mike Unger for his guidance, support, and enthusiasm throughout this endeavor. I would also like to thank him for building numerous parts in his garage to repair ornery biosensors and keep things going. His willingness to entertain my curiosity and ideas is what ultimately shaped the objectives of this Ph.D., and it is a trait I hope to carry in a future leadership role. I would also like to thank my wonderful committee, Ryan Carnegie, Upal Ghosh, Roger Mann, and Jeff Shields, for their dedication to improving my research. To Kim Reece, thank you for all your work as the Aquatic Health Sciences Department chair. Thank you to Academic Studies, Linda, Jen, Cathy, and John for supporting the graduate student body. I would also like to acknowledge my funding sources: NIEHS Superfund Research Program, Exxon-Mobil Biomedical Sciences, Inc. (EMBSI), and VIMS.

Next, I would like to thank our external collaborators. Thank you to Chris Prosser and Aaron Redman at EMBSI and Tom Parkerton at EnviSci Consulting, LLC for providing expertise and support in our crude oil WAF exposure experiment. Thank you to Joe Rieger and the Elizabeth River Project for providing expertise in the Elizabeth River Watershed oyster survey and for allowing me to be a part of the State of the River Report and Watershed Action Plan steering committee. Having grown up in Hampton Roads, it was really rewarding to contribute to making the Elizabeth River a more beautiful place. Also, thank you to Todd Egerton with VDH for his support in the oyster survey. Many thanks to Tommy Leggett for providing oysters for several experiments.

So many amazing VIMS researchers generously donated their time to help me carry out this research. First, I'd like to say a huge thank you to Hamish Small, a fantastic mentor in science and in life, for helping me build a tissue processing and immunohistochemistry protocol from the ground up and for providing so much scientific inspiration and encouragement throughout my time at VIMS. Thank you for bringing many laughs as well. Thank you to George Vadas for having patience when teaching me wet chemistry skills and for captaining numerous excursions to hunt for oysters. To Mary Ann, thank you for teaching me all about the immunological side of this work. Thanks for helping me troubleshoot misbehaving biosensors, and for all your support in the lab. I'd also like to thank Frances Knight for assistance with running our SRL experiment and data collection. Thank you to Matt Mainor for helping me in the SRL, captaining excursions in the field, as well as helping with sample preparation as an all-star tissue homogenizer and freeze drier. To Ellen Harvey, thank you for being the mass spectrometry wizard and for guidance in the lab. Thank you to Drew Luellen for support in sample processing and for helping me work smarter not harder. I would also like to thank Rita Crockett and Melanie Kolacy for providing expertise and preparing histological slides. Thank you to Jess Small for providing her expertise and generously donating oysters for experiments.

I am so lucky to have had such a strong support system throughout this experience. Thank you to my parents, Carla and Jim, for their encouragement throughout this endeavor, even in the face of a several health complications. Thanks to my brother, James, for showing me that science is cool. I also appreciate the support from my sister-in-law, Kristen, and my niblings, Lila and Matthew. I am so thankful for my incredible friends and chosen family who provided

community, countless laughs and a space for venting. There are too many people to recognize. Also, thank you all for your patience when I have been less-than-responsive to texts.

Finally, I am eternally grateful for my partner and best friend, Ryan. Thank you for helping me keep things in perspective and for carrying the heavier load when needed, especially in these last few months. Your love and support through it all, for both me and Kano, has meant everything, I am also so lucky to have you in my life – and your family, as an added bonus. I love you (so does Kano).

ABSTRACT

Anthropogenic activities such as oil spills are major sources of polycyclic aromatic hydrocarbon (PAH) pollution in the environment. Bivalves such as *C. virginica* can accumulate high levels of PAHs in tissue due to a limited metabolic capacity for these compounds. Accordingly, bivalves have served as key biomonitoring species for contaminants and exposure to PAH through seafood consumption can also be an important risk to human health due to the toxic and carcinogenic potential of these compounds. For evaluating bivalve PAH levels, conventional analyses are limited due to extensive time and expense and unreliability. This work demonstrates the application of immunological techniques to overcome such limitations in conventional techniques and to explore PAH kinetics and partitioning mechanisms within oysters.

Biosensor technology coupled with a PAH antibody was employed to rapidly and inexpensively screen PAH levels in adult oysters in an Elizabeth River watershed monitoring survey. Through a novel extension of a fundamental chemistry theory, PAH concentrations measured in oyster fluid by biosensor were used to predict tissue concentrations. Biosensor-derived predictions had a strong association with tissue concentrations measured by conventional chemical analysis. A strong association between the biosensor and tissue concentrations when compared against regulatory PAH thresholds and efficient mapping of PAH levels throughout the watershed, demonstrates the real-world value of the method. The biosensor was also employed in PAH kinetics studies. Oysters were exposed to crude oil water accommodated fractions (WAF) in the laboratory to explore the application of the biosensor in oil spill response; however, further work is needed to improve the precision of biosensor-derived predictions at non-steady state. In a field exposure study, PAH levels in cultured triploid and diploid oysters deployed at a PAH hotspot in the Elizabeth River were compared to wild oysters inhabiting the site. Differences in PAH kinetic trends were observed between oyster fluid and tissue. When combined with the observed differences in PAH levels in specific tissue types between transplanted and wild oysters, there is evidence that internal partitioning and tissue-specific kinetic rates may be important factors in determining the overall PAH body burden in an oyster and warrants further investigation to improve precision in future biomonitoring efforts.

The fluorescently tagged PAH antibody was also employed in an immunohistochemical (IHC) technique to visualize complex PAH mixtures within oyster tissue. Oysters were collected throughout the laboratory WAF exposure, and the observed change in signal intensity in tissue followed a similar trend to measured PAH concentrations. In visualizing transplanted vs. wild oyster tissue, the trends in signal intensity supported the differences observed in tissue-specific PAH concentrations between groups.

Overall, the biosensor shows promise as a tool to overcome current analytical challenges faced in environmental monitoring of biota. While further work is needed to understand the influence of chemical and biological factors on PAH kinetics and biosensor-derived tissue predictions, the unique analytical features of these technologies are valuable for addressing these mechanistic questions. When coupled with IHC, these immunologic techniques can provide new insight to address complexities in environmental pollution and health risk assessments that cannot be as feasibly and inexpensively answered by standard methods.

Exploring PAH Partitioning in Oysters Using Immunological Techniques

Introduction

Polycyclic aromatic hydrocarbons

PAHs are ubiquitous environmental organic contaminants for both fresh and marine environments. They are a large class of chemically related compounds consisting of two or more aromatic rings in their structure composed of primarily carbon and hydrogen atoms which are fused together by the sharing of two carbon atoms between rings (Douben 2003; Neff et al. 2005). PAHs exist in the environment as complex mixtures often from fossil fuel sources (petrogenic PAHs) and sources of incomplete combustion of organic matter (pyrogenic PAHs), which are the largest contributor of PAHs to the environment (Abdel-Shafy and Mansour 2016). Chemical fingerprinting techniques can be used to discern whether PAHs are of pyrogenic or petrogenic origin as compound concentrations and distribution greatly differs between sources (Kasiotis and Emmanouil, 2015). Petrogenic sources typically contain a higher proportion of alkylated 2– and 3–ring compounds and lower molecular weight PAHs, whereas pyrogenic sources generally contain a higher proportion of high molecular weight PAHs (4-6–ring PAHs). The formation of PAHs can occur by natural processes such as volcanic activity and natural petroleum seepage; however, emissions from increased anthropogenic activity such as fossil fuel burning, production of coal-tar derivatives, and oil spills are the dominate source of PAH pollution in the environment (Neff et al. 2005). Prior to the 1972 US Clean Water Act, unregulated discharge of industrial waste was a major source of the legacy PAH contamination seen today. However, increased PAH loads from non-point sources (e.g. vehicle fuel exhaust and stormwater run-off) attributed to increased urbanization and continued reliance on fossil fuels are a major source of current PAH pollution (Wolfe et al., 1996, Van Metre et al., 2000, Walker et al., 2005, Minick and Anderson, 2017). In the aquatic environment, organically rich sediment serves as a significant repository for PAHs. Although hydrophobic, PAHs are not completely

insoluble and are dissolved in the water column and sediment porewaters at low concentrations (Abdel-Shafy and Mansour 2016).

As of 2019, PAHs are ranked in the top ten priority pollutants according to the Agency for Toxic Substances and Disease Registry (ATSDR) due to their frequency of detection, toxicity, and potential for human exposure at Superfund sites and other hazardous sites (ATSDR, 2020). PAHs are of environmental concern because several compounds can have toxic, mutagenic, and carcinogenic properties, depending on molecular weight and number of aromatic rings (Latimer & Zheng 2003). Additionally, these compounds persist in the environment for long periods of time due to a relatively stable nonpolar molecular structure (Abdel-Shafy and Mansour 2016).

The International Agency on Cancer Research has classified specific PAH compounds as known, possible, or probable human carcinogens (Group 1, 2A, and 2B) (IARC 2010). Of them, benzo [a] pyrene is considered a known human carcinogen and benz [a] anthracene, benzo [b] fluoranthene, benz [k] fluoranthene, chrysene, dibenz [a,h] anthracene, and indeno [1,2,3-cd] pyrene are considered probable human carcinogens (IARC 2010; Abdel Shafy and Mansour 2016). In humans, PAHs are considered causative agents for more cancers, particularly lung cancer, than any other carcinogen (Lawal 2017). In addition, exposure to PAHs is attributed to other health effects in humans including localized skin effects; pulmonary and respiratory issues; genetic, reproductive, and developmental issues; and behavioral and neurological issues among others (Lawal 2017). Metabolic activation of PAHs and subsequent formation of diol-epoxides and other metabolites is required to induce carcinogenic effects; activation can occur via multiple metabolic pathways (Moorthy et al. 2015; Lawal 2017).

Although PAHs exist in the environment as complex mixtures of hundreds of different PAH compounds, regulatory thresholds for maximum acceptable levels are typically based on the concentrations of a subset of target PAHs. The subsets of target compounds can vary depending on the regulatory agency and endpoint of interest. The U.S Environmental Protection Agency (EPA) has developed a list of 16 priority PAHs to target for environmental risk assessments and monitoring (Andersson and Achten, 2015). As of 2011, the European Food Safety Authority within the European Union set maximum acceptable levels for a variety of different types and preparation of food (e.g. different levels have been set for smoked vs. fresh bivalves) entering the market (European Union, 2011). For human health risk assessments, PAH concentrations are converted to their toxic equivalent concentration relative to benzo [a] pyrene (BaPE) to assess cancer risk (EPA, 1984, Nisbet and LaGoy, 1992, ATSDR, 1995). Following major oil spills such as the 1990 Exxon Valdez spill in Prince William Sound in Alaska and the 2010 Deepwater Horizon incident in the Gulf of Mexico, seafood risk assessments conducted by the Food and Drug Administration have used BaPE concentrations to assess cancer risk (FDA 2010). As more research is being conducted on this class of compounds, studies have revealed that alkylated PAH isomers can have higher toxicities relative to their parent forms, warranting a reevaluation of priority PAH lists (Andersson and Achten 2015; Wise et al. 2015; da Silva Junior et al. 2021).

PAH partitioning and equilibrium partitioning theory

The distribution of PAHs in the environment is driven by their hydrophobicity and solubility (Latimer & Zheng 2003). PAHs can exist in different environmental compartments (phases) including bound solid phases such as particle-bound, NAPL (non-aqueous phase liquid)-bound, and bound within biological tissues through organismal uptake, as well as existing

in the freely dissolved aqueous phase in interstitial sediment pore water and water column (Neff et al. 2005; Burgess et al. 2003). Sediment serves as a significant repository for PAHs as these compounds more readily sorb to the nonpolar, organic regions of suspended sediment particles or to black (soot) carbon, the particulate fraction of exhaust from fossil fuel combustion, and settle to depth via sedimentation (Neff et al. 2005). Sediment composition, such as organic carbon type in the sediment and grain size, is also important in determining the bioavailable fraction (Burgess et al. 2003). Residence time of the contaminant in the environment also plays a role in partitioning. PAHs in contact with sediment for prolonged periods of time tend to be less bioavailable and have slower desorption rates than sediments freshly spiked with PAHs (Chung & Alexander 1998).

Desorption rates, and ultimately the distribution of the bioavailable fraction of PAHs in the environment, is a function of the binding affinities of individual compounds for various phases. The octanol-water partition coefficient or K_{ow} for a compound is measure of hydrophobicity and lipophilicity. The coefficient is often expressed as log K_{ow} since untransformed values span orders of magnitude and because log K_{ow} increases linearly with increasing hydrophobic structural elements of the molecule (Cumming and Rucker 2017). It serves as an important predictor for fate and partitioning and determines chemical behavior, bioavailability, and toxicity (Meador 2003; Honda and Suzuki 2020). Increasing hydrophobicity is correlated with increasing log K_{ow} values and molecular weight of the contaminant. Accordingly, compounds with a higher log K_{ow} have a higher affinity for non-polar phases, such as organics-rich sediment or lipid, and a great potential for bioconcentration in organisms (Burgess et al. 2003).

Chemical partitioning is a dynamic process and exchange of PAHs between different phases occurs via sorption and desorption. PAHs in the freely dissolved aqueous phase are most readily available for exchange between phases or passing through organismal membranes and are, therefore, considered most bioavailable. The net flow of molecules from one phase to another is based on differences in chemical potential. Molecular transfer between phases continues until dynamic equilibrium is reached within the system, when forward and reverse rates of reaction are equal. This is the central principle of the equilibrium partitioning theory (EqP) (DiToro et al. 1991; Burgess et al. 2003). When phases are at assumed equilibrium, the distribution of PAHs in the environment are proportional to each other via partitioning coefficients, or equilibrium constants. By using a simple ratio calculation, an unknown concentration of PAHs in one phase can be deduced by dividing the partition coefficient by the known concentration in another phase.

PAHs in bivalves

Routes of uptake and exposure

Routes of uptake of PAHs in oysters include respiration via gills, sorption through soft tissues, and ingestion into the digestive tract. The gill system is main site for direct exchange with the environment and is therefore an important route for uptake and elimination of environmental contaminants. As suspension-feeders, bivalves possess complex gill structures with large surface areas to serve key functions including gas exchange, feeding, digestion, among others. Oysters pump bioavailable PAHs dissolved in water over their gills. Upon entry, PAHs can bind to lipids within the gill structure as well as circulate through the rest of the body. The lipid-rich hepatopancreas (digestive gland) is an important structure for PAH accumulation and often contains the highest concentration of PAHs relative to other organs. The digestive

gland is also the main site for detoxification and metabolism, though bivalves limited metabolic ability relative to other organisms (Wang et al. 2020; Gan et al. 2021). Transfer of PAH in the dissolved phase to tissue is thought to mainly occur via passive diffusion across lipid-rich cell membrane along a concentration gradient until equilibrium is reached (Meador 2003; Beyer et al. 2012). Another important route is active contaminant uptake via ingestion of PAH sorbed to food and sediment particles. Contaminated food particles can be taken up in the gut wall via endocytosis or captured by mucus cells and transported through the digestive system (Beyer et al. 2012). Studies have found that uptake via ingestion can be a significant contribution to overall body burden; however, this route is not well studied (Meador 2003; Beyer et al. 2017; Gan et al. 2021). For chronically exposed bivalves that have been assumed to reach steady-state with the environment, the route of uptake is generally considered less important relative to acutely exposed organisms (Meador 2003).

Bioconcentration factors (BCFs), the ratio of contaminant concentration in the organism relative to concentrations in water, and bioaccumulation factors (BAFs), the ratio of contaminant concentration relative to the concentrations found in contaminated seawater and diet, are important for risk assessments. Many environmental, biological, and chemical factors can contribute to the level of bioavailable PAH in a system and ultimately the final concentrations observed in an organism. Chemical factors include but are not limited to PAH composition and hydrophobicity, kinetics, sorption efficiency, and formation of more soluble photo-products via UV photo-oxidation. Environmental factors include salinity, temperature, pH, sediment composition and resuspension, hydrodynamic processes such as upwelling, currents, and advective porewater flux via tidal pumping. Biological factors include bivalve feeding rate, reproductive and spawning status, size, sex, disease status, and lipid content (Chu et al. 1990;

Ellis et al. 1993; Meador 2003; Koelmans et al. 2010; Greenfield et al. 2014; Beyer et al. 2017; Gan et al. 2021).

Elimination and biotransformation

Several routes are available for elimination of PAHs including depuration along a concentration gradient, biotransformation, and excretion. Spawning is also considered an important seasonal mechanism of PAH elimination as PAH bound to lipid-rich gametes can be released from oysters (Chu et al. 1990; Ellis et al. 1993). The gill is an important structure in elimination as well. Depuration is considered the main route of elimination as bivalves including oysters have a limited ability to metabolize PAHs. However, studies have shown that the cytochrome p450 pathway for detoxifying PAHs can be activated in response to PAH exposure and that some PAHs may be preferentially metabolized over others (Ertl et al. 2016). In this pathway, stage I enzymes, shown to be upregulated in response to PAH accumulation, reduce PAHs into more water-soluble derivatives which can then be conjugated by stage II enzymes and excreted (Gan et al. 2021).

Notably, metabolic transformation activates PAH toxicity and can promote oxidative tissue damage such as lipid peroxidation. Additional sublethal toxic effects include changes in immune function including hemocyte toxicity and possible increases in disease susceptibility as well as physiological changes including prolonged shell closure and subsequent starvation, narcosis, and lysosomal destabilization (Chu and Hale 1994; Bado-Nilles et al. 2008; Vignier et al. 2018; Gan et al. 2021). In its toxic form, PAHs has been shown to also induce DNA damage in oysters. When exposed to 20mg/L suspension of contaminated sediment from Black Rock Harbor, NY, in both a laboratory and field experiment, tissue neoplasms developed in *C. virginica* after 30-60 days of continuous exposure including tumor development in renal epithelia

and water tube and gill filaments, and gastrointestinal adenocarcinoma among other tissue types (Gardner et al. 1991; Gan et al. 2021). However, various contaminants were measured in sediment at high concentrations including PAHs, polychlorinated biphenyls, heavy metals, and chlorinated pesticides, making it difficult to establish a causal relationship between the observed neoplastic effects and a specific chemical class. The upregulation of stress biomarkers in bivalves including antioxidant and metabolic enzymes in response to chemical exposure has led to their incorporation into bivalve biomonitoring strategies for a more holistic evaluation of chemical exposure and organismal effects; however, more work is needed to attribute such biomarkers specifically to PAH exposure and improve reliability (Beyer et al. 2017).

Biomonitoring

Bivalve molluscs are considered ideal sentinel organisms for monitoring pollution for the following reasons (Boening 1999; Farrington et al. 2016; Gan et al. 2021): 1) many species are widely distributed; 2) they are good integrators of localized pollution; 3) they concentrate PAHs to levels that are orders of magnitude greater than surrounding water concentrations; 4) pollutant concentrations in bivalves can be used to assess bioavailability; 5) most species are tolerant of moderate pollution levels without suffering mortality but are still sensitive to changes in exposure; 6) they have a low ability to metabolize organic contaminants relative to fish; 7) they have a long life span for long-term sampling; and 8) many bivalves are important commercial seafood species. Selection of bivalve species is also an important consideration in biomonitoring because different species will accumulate different levels of contaminants. Oysters accumulate the highest PAH concentrations relative to other bivalves (Oros and Ross 2005).

C. virginica have served as key biomonitoring species in large-scale monitoring programs including the NOAA Mussel Watch since its establishment in 1975 (Goldberg et al. 1978;

Farrington et al., 1983, Farrington et al., 2016, Wade et al., 1998). Two methods of biomonitoring are employed, and each has advantages and limitations. In passive biomonitoring, wild bivalve populations at sites of interest are sampled for measurement of contaminants of concern. This method has been historically employed in long-term monitoring efforts (Farrington et al. 1983; Sericano et al. 1995). Bivalves can be immediately sampled since it is assumed wild populations have sufficiently reached equilibrium with the surrounding environment. In active biomonitoring, bivalves are collected from pristine sites or purchased from aquaculture facilities and relocated to sites of interest deployed in cages. This method can overcome the limitations of a heterogenous distribution of wild bivalves at a site or the complete absence of bivalves (Beyer et al. 2017; Lacroix et al. 2015). In addition, various biological parameters such as stock, origin, size, and sex can be controlled to reduce variability and enhance experimental replication (Besse et al. 2012). However, transplanted bivalves must be deployed at the site for an extended period to equilibrate with the environment (Sericano et al. 1996), and discrepancies are observed among studies regarding the optimal length of time required for equilibration, ranging from 3 weeks to 2 years (Bodin et al. 2004; Marigomez et al. 2013; Beyer et al. 2017).

Analytical Techniques

Three analytical techniques were employed throughout this dissertation. Each method is described in more detail in relevant chapters. General overviews are provided below.

Gas chromatography–mass spectrometry

Gas chromatography coupled with a mass spectrometer (GC–MS) is considered the ‘gold standard’ analytical technique for measuring environmental contaminants in biota, including PAHs in oysters. Fundamentally, individual analytes within a complex mixture can be separated and isolated by gas chromatography, and then identified based on their unique signature, or mass

spectra, by a mass spectrometer. For GC–MS analysis, samples are typically held in organic solvent, such as 100% dichloromethane. In the gas chromatograph, the sample is injected, vaporized, and introduced to a carrier gas (e.g. hydrogen or helium), the mobile phase, which transports the sample from the sample injector through a long, thin capillary column coated with a stationary phase (Sparkman and Kitson 2011). The separation of individual compounds is determined based on its partitioning between the mobile and stationary phase. Higher molecular weight and less soluble compounds (e.g. higher-ringed PAHs) typically spend a longer time in the stationary phase. The column eluate is ionized upon entering the mass spectrometer and separated based on mass-to-charge ratio (*m/z*). Ions are accelerated out of the ion source into the *m/z* analyzer for detection. A mass spectrum is generated containing mass spectral peaks. The coordinates of each peak represent the m/z value of an ion as a function of time (x-axis) and the relative intensity (y-axis) which is a function of the amount of analyte present. Compounds will produce characteristic mass spectrum or fingerprints. GC–MS provides both qualitative (analyte identification based on retention time and *m/z* value where the peak occurs in the chromatogram) and quantitative data (concentration of analyte based on area of peak) (Sparkman and Kitson 2011; Karasak and Clement 2012).

Gas chromatography-mass spectrometry (GC–MS) is a highly vetted quantitative technique able to produce accurate, reliable, and reproducible data. An important feature of this method is the ability to measure concentrations of individual compounds in a complex mixture—critical data for determining sources of contaminants, particularly aromatic hydrocarbons (Sportsol et al., 1983). This method is an established analytical technique; however, there are two important limitations: time and cost. Preparing samples for GC–MS analysis is a highly involved process and time-consuming (Zhang et al., 2018). GC–MS analysis itself is also time-limited as

long retention times are typically required to gain the resolution levels needed for precise measurement of analytes. This limits the number of samples that can feasibly be analyzed and makes real-time detection unattainable. At any point in the preparation process, there is a high risk of losing analyte in the sample—also losing time and money. Additionally, large volumes of hazardous and expensive organic solvents are required throughout sample extraction, separation, and cleaning steps that are harmful to the environment. From sample preparation to analysis, several sophisticated and expensive instruments are required (Lux et al., 2015).

Accordingly, following major PAH contamination events such the Deepwater Horizon incident in 2010, screening methods have been employed to prioritize samples for more extensive analysis such as high-performance liquid chromatography coupled with fluorescence detection (HPLC–FLD). This screening method offers a more streamlined sample preparation protocol to reduce time and cost; however, HPLC–FLD analysis yields semi-quantitative estimates of concentrations, limiting the sensitivity and accuracy of this method (Yender 2002; Plaza-Bolanos et al. 2010). Like GC–MS, sample preparation requires sample extraction via hazardous organic solvents. Therefore, laboratory space and specialized expertise are necessary which limits the utility of this method in remote, on-site settings (Yender 2002; Gratz et al. 2011). Another screening method that has been employed is sensory analysis (Moller 1999; FDA 2010). Sensory testing requires the employment of a panel of trained specialists to detect the tainting of seafood taste or odor due to oil contamination. The qualitative results of such testing has shown some correlation to petroleum concentrations; however, to date, seafood taint has not been attributed to specific compounds in petroleum and may be contingent on specific oil characteristics or specific seafood species (Yender 2002). Further, the reliability of sensory testing results may be impacted by the sensitivity and experience of the panel and adulteration of

the seafood sample due to factors unrelated to oil contamination such as fecal odor or decay (Mauseth and Challenger 2001).

Antibody-based biosensor technology

In the healthcare and biomedical field, monoclonal antibody-based immunoassays have proven to be successful as rapid, inexpensive, user-friendly screening techniques for on-site or non-laboratory testing (Posthuma-Trumpie et al. 2009; Gao et al. 2018; Di Nardo et al. 2021). With features including high selectivity and sensitivity, immunosensors such as antibody-based biosensor technologies can quantify fluorescent signal based on antigen-antibody interactions and have proven to be valuable analytical screening tools for environmental monitoring of contaminants, including PAHs (EPA 1996a; EPA 1996b; Plaza et al. 2000; Baeumner 2003; Spier et al. 2012; Wang et al. 2014; Justino et al. 2017; Behera et al. 2018; da Costa Filho et al. 2022).

Biosensor technology combines a bioreceptor such as enzymes, antibodies, DNA, plant or animal cells, or microorganisms that can interact with a target analyte (‘bio’) with an instrument capable of detecting and converting the bioreceptor response into an analytical signal (‘sensor’) (da Costa Filho et al. 2022). The KinExA Inline Sensor coupled with a murine monoclonal antibody with uniform selectivity for 3-5–ring PAHs, mAb 2G8, is the biosensor technology employed in this work and has been described in detail previously (Spier et al. 2011; Spier et al. 2011; Li et al. 2016). A fluorescent tag, AlexaFluor 647 (AF647), is covalently bound to mAb 2G8. The instrument will detect the fluorescent signal response of PAH-bound antibody which can then be converted to PAH concentration. The sensor functions as a kinetic assay: mAb 2G8 mixes with an aqueous sample and binds to free PAHs. Then, this solution is passed over a PAH antigen in a stationary phase (1-pyrene-butyric acid) held in a glass flow cell in front of the

detector. Remaining free antibody not bound to PAHs in the aqueous sample will bind to the stationary antigen and elicit a signal response (dV) that is measured by the instrument. Thus, the level of signal response is inversely proportional to PAH concentration. A calibration curve is generated at the start of analysis using a series of phenanthrene standards and laboratory blank to establish the linear range of signal response. Samples are diluted with double deionized water to stay within the calibration range, if necessary. The measured signal response and required dilution factor are then used to calculate the PAH concentration for the sample (µg/L).

The biosensor technology discussed above has been successfully employed as a quantitative screening technique for monitoring of environmental contaminants in water or porewater samples (Li et al. 2016; Hartzell et al. 2017; Conder et al. 2021; Camargo et al. 2022). The work presented in this dissertation explores a novel application of the Inline Sensor coupled with mAb 2G8 to screen PAH concentrations in oysters.

Immunohistochemistry

Immunohistochemistry (IHC) is a powerful tool for visualizing cell- or tissue-specific localization of an antigen based on highly specific antibody binding and immunofluorescent staining (Aziz and Mehta, 2016). Use of IHC methods has become routine within a wide range of disciplines including disease research and diagnosis, drug development, and toxicology (Dugger & Dickson, 2017; Hawes et al., 2009). Despite such a broad applicability, very few studies on bioaccumulation at environmentally impacted sites have incorporated IHC techniques in detecting environmental chemical contaminants within specific tissues of aquatic organisms (Strandberg et al., 1998; Kerr Lobel and Davis, 2002; Eisporn and Koehler, 2008; Sforzini et al., 2014). Many studies have been limited in detecting the accumulation of one or a few individual PAH compounds in tissue via laboratory exposure (Rodríguez & Bishop, 2005; Sforzini et al.,

2014; Speciale et al., 2018; Subashchandrabose et al., 2014; Wang et al., 2012). Extrapolation of the results from such studies is also limited as biota are exposed to a complex mixture of contaminants in the environment.

Confocal microscopy is a common imaging technique for characterizing immunofluorescently stained tissue specimens. This imaging technique produces sharp images through point-by-point illumination of the specimen and removal of excess, out-of-focus light. A thin planar section of the specimen is created through a pinhole aperture: a process known as optical sectioning (Robinson, 2001). Confocal microscopy offers several advantages over conventional light microscopy including sharper, more detailed 2D images with higher contrast. These 2D sections can also be compiled to create 3D images of the specimen with an adjustable *z*-scale for optimized imaging.

IHC techniques and confocal microscopy rely on the presence of a fluorescently tagged antibody with specific binding affinity for an antigen of interest. A highly specific monoclonal antibody (2G8) tagged with Alexa Fluor 647 has already been developed for use with the biosensor technology – its use in visualizing PAH in specific tissues is a novel application for the antibody.

Dissertation Structure

Chapter 1 describes the method development and exploration of real-world application for using biosensor technology to quantitatively screen PAH concentration in oysters in near real-time. This work was published in *Environmental Technology and Innovation* in 2022 (Prossner et al. 2022). As an extension of the first chapter, Chapter 2 explores the utility of the biosensor to screen PAH concentrations in oysters in an oil spill response scenario via a PAH

uptake and depuration kinetics experiment. Chapter 3 describes the protocol and proof-of-concept for the novel application of mAb 2G8 in immunohistochemistry to visualize the accumulation of PAH mixtures in oyster tissue. This work was published in *Environmental Toxicology and Chemistry* in 2023 (Prossner et al. 2023). Chapter 4 combines both immunological techniques to compare PAH uptake and depuration in wild oysters native to a PAH-impacted site in the Elizabeth River to cultured triploid and diploid oysters transplanted to the site. The work presented in this dissertation is formatted in the form of manuscripts ready for publication or previously published.

References

Abdel-Shafy, H.I., Mansour, M.S., 2016. A review on polycyclic aromatic hydrocarbons: Source,environmental impact, effect on human health and remediation. *Egyptian Journal of Petroleum* 25, 107–123.

Andersson, J.T., Achten, C., 2015. Time to say goodbye to the 16 EPA PAHs? Toward an up-to-date use of PACs for environmental purposes. *Polycyclic Aromatic Compounds* 35, 330–354.

ATSDR (Agency for Toxic Substances and Disease Registry), 1995. Toxicological Profile for Polycyclic Aromatic Hydrocarbons: Technical Report. U.S. Department of Health and Human Services, Public Health Service, Agency for Toxic Substances and Disease Registry Atlanta, GA, USA

ATSDR (Agency for Toxic Substances and Disease Registry), 2020. The ATSDR 2019 Substance Priority List. Agency for Toxic Substances and Disease Registry, Division of Toxicology and Human Health Services, Atlanta, GA, USA.

Aziz S.A., Mehta R., 2016. Immunohistochemistry: Overview, Its Potential, and Challenges. In: Aziz S., Mehta R. (eds) Technical Aspects of Toxicological Immunohistochemistry. Springer, New York, NY

Bado-Nilles, A., Gagnaire, B., Thomas-Guyon, H., Le Floch, S., & Renault, T., 2008. Effects of 16 pure hydrocarbons and two oils on haemocyte and haemolymphatic parameters in the Pacific oyster, Crassostrea gigas (Thunberg). *Toxicology in Vitro 22*, 1610-1617.

Baeumner, A. J., 2003. Biosensors for environmental pollutants and food contaminants. *Analytical and Bioanalytical Chemistry*, 377, 434-445.

Behera, B.K., Das, A., Sarkar, D.J., Weerathunge, P., Parida, P.K., Das, B.K., Thavamani, P., Ramanathan, R. and Bansal, V. (2018). Polycyclic Aromatic Hydrocarbons (PAHs) in inland aquatic ecosystems: Perils and remedies through biosensors and bioremediation. *Environmental Pollution* 241, 212-233.

Besse, J. P., Geffard, O., & Coquery, M., 2012. Relevance and applicability of active biomonitoring in continental waters under the Water Framework Directive. *TrAC Trends in Analytical Chemistry* 36, 113-127.

Beyer, J., Green, N.W., Brooks, S., Allan, I.J., Ruus, A., Gomes, T., Bråte, I.L.N. and Schøyen, M., 2017. Blue mussels (Mytilus edulis spp.) as sentinel organisms in coastal pollution monitoring: a review. *Marine Environmental Research* 130, 338-365.

Bodin, N., Burgeot, T., Stanisiere, J.Y., Bocquené, G., Menard, D., Minier, C., Boutet, I., Amat, A., Cherel, Y. and Budzinski, H., 2004. Seasonal variations of a battery of biomarkers and physiological indices for the mussel Mytilus galloprovincialis transplanted into the

northwest Mediterranean Sea. *Comparative Biochemistry and Physiology Part C: Toxicology & Pharmacology* 138, pp.411-427.

Boening, D. W., 1999. An evaluation of bivalves as biomonitors of heavy metals pollution in marine waters. *Environmental Monitoring and Assessment* 55, 459-470.

Burgess, R., Ahrens, M., Hickey, C., 2003. Geochemistry of PAHs in aquatic environments: source, persistence and distribution. In: Douben, PET (Ed.), PAHs: An Ecotoxicological Perspective. Wiley, Chichester, West Sussex, England, pp. 35–45.

Camargo, K., Vogelbein, M.A., Horney, J.A., Dellapenna, T.M., Knap, A.H., Sericano, J.L., Wade, T.L., McDonald, T.J., Chiu, W.A. and Unger, M.A., 2022. Biosensor applications in contaminated estuaries: Implications for disaster research response. *Environmental Research 204*, 111893.

Conder, J., Jalalizadeh, M., Luo, H., Bess, A., Sande, S., Healey, M., & Unger, M. A., 2021. Evaluation of a rapid biosensor tool for measuring PAH availability in petroleum-impacted sediment. *Environmental Advances 3*, 100032.

Chu, F. L. E., Webb, K. L., & Chen, J., 1990. Seasonal changes of lipids and fatty acids in oyster tissues (Crassostrea virginica) and estuarine particulate matter. *Comparative Biochemistry and Physiology Part A: Physiology 95*, 385-391.

Chu, F. L., & Hale, R. C., 1994. Relationship between pollution and susceptibility to infectious disease in the eastern oyster, Crassostrea virginica. *Marine Environmental Research 38*, 243-256.

Chung, N., Alexander, M., 1998. Differences in sequestration and bioavailability of organic compounds aged in disimilar soils. *Environmental Science and Technology* 32, 855-860.

Cumming, H., & Rücker, C., 2017. Octanol–water partition coefficient measurement by a simple 1H NMR method. *ACS omega 2*, 6244-6249.

da Costa Filho, B. M., Duarte, A. C., & Santos, T. A. R., 2022. Environmental monitoring approaches for the detection of organic contaminants in marine environments: a critical review. *Trends in Environmental Analytical Chemistry*, e00154.

da Silva Junior, F.C., Felipe, M.B.M.C., Castro, D.E.F., Araújo, S.C.D.S., Sisenando, H.C.N., Batistuzzo de Medeiros, S.R., 2021. A look beyond the priority: A systematic review of the genotoxic, mutagenic, and carcinogenic endpoints of non-priority PAHs. *Environmental Pollution* 278, 116838.

Di Nardo, F., Chiarello, M., Cavalera, S., Baggiani, C., & Anfossi, L., 2021. Ten years of lateral flow immunoassay technique applications: Trends, challenges and future perspectives. *Sensors* 21, 5185.

Di Toro, D., Zarba, C., Hansen, D., Berry, W., Swartz, R., Cowan, C., Pavlou, S., Allen, H., Paquin, P., 1991. Technical basis for establishing sediment quality criteria for nonionic organic chemicals using equilibrium partitioning. *Environmental Toxicology and Chemistry* 10, 1541-1583.

Douben, P. Introduction., 2003. In: Douben, PET (Ed.), PAHs: An Ecotoxicological Perspective. Wiley, Chichester, West Sussex, England, pp. 3–6.

Dugger, B. N., & Dickson, D. W., 2017. Pathology of neurodegenerative diseases. *Cold Spring Harbor Perspectives in Biology* 9, a028035.

Einsporn, S., & Koehler, A., 2008. Immuno-localisations (GSSP) of subcellular accumulation sites of phenanthrene, aroclor 1254 and lead (Pb) in relation to cytopathologies in the gills and digestive gland of the mussel Mytilus edulis. *Marine Environmental Research* 66, 185– 186.

Ellis, M. S., Choi, K. S., Wade, T. L., Powell, E. N., Jackson, T. J., & Lewis, D. H., 1993. Sources of local variation in polynuclear aromatic hydrocarbon and pesticide body burden in oysters (Crassostrea virginica) from Galveston Bay, Texas. *Comparative Biochemistry and Physiology Part C: Pharmacology, Toxicology and Endocrinology* 106, 689-698.

EPA (US Environmental Protection Agency), 1984. Health Effects Assessment for Polycylic Aromatic Hydrocarbons (PAH) : EPA-540/1-86-013 . Environmental Criteria and Assessment Office, Cinncinnati, OH

EPA (US Environmental Protection Agency)., 1996a. SW-846 Test Method 4000:Immunoassay. https://www.epa.gov/hw-sw846/sw-846-test-method-4000-immunoassay

EPA (US Environmental Protection Agency)., 1996b. SW-846 Test Method 4030: Soil Screening for Petroleum Hydrocarbons by Immunoassay. https://www.epa.gov/hw-sw846/sw-846-test-method-4030-soil-screening-petroleum-hydrocarbons-immunoass

Ertl, N. G., O'Connor, W. A., Brooks, P., Keats, M., & Elizur, A., 2016. Combined exposure to pyrene and fluoranthene and their molecular effects on the Sydney rock oyster, Saccostrea glomerata. *Aquatic Toxicology* 177, 136-145.

European Union, 2011. Commission regulation (EU) no 835/2011. Off. J. Eur. Union L214/5 835/2011.

Farrington, J. W., Goldberg, E. D., Risebrough, R. W., Martin, J. H., & Bowen, V. T., 1983. US" Mussel Watch" 1976-1978: an overview of the trace-metal, DDE, PCB, hydrocarbon and artificial radionuclide data. *Environmental Science & Technology* 17, 490-496.

Farrington, J.W., Tripp, B.W., Tanabe, S., Subramanian, A., Sericano, J.L., Wade, T.L., Knap, A.H., 2016. Edward D. Goldberg's proposal of the mussel watch: reflections after 40 years. *Marine Pollution Bulletin* 110, 501–510.

FDA (US Food and Drug Administration), 2010. Protocol for Interpretation and Use of Sensory Testing and Analytical Chemistry Results for Re-Opening Oil-Impacted Areas Closed to Seafood Harvesting Due to the Deepwater Horizon Oil Spill : Technical Report . 2010 US Food and Drug Administration Washington, DC

Gan, N., Martin, L., & Xu, W. (2021). Impact of polycyclic aromatic hydrocarbon accumulation on oyster health. *Frontiers in Physiology* 12, 734463.

Gao, Huang, X., Zhu, Y., & Lv, Z., 2018. A brief review of monoclonal antibody technology and its representative applications in immunoassays. *Journal of Immunoassay & Immunochemistry* 39, 351–364.

Gardner, G. R., Yevich, P. P., Harshbarger, J. C., & Malcolm, A. R., 1991. Carcinogenicity of Black Rock Harbor sediment to the eastern oyster and trophic transfer of Black Rock Harbor carcinogens from the blue mussel to the winter flounder. *Environmental Health Perspectives* 90, 53-66.

Goldberg, E.D., Bowen, V.T., Farrington, J.W., Harvey, G., Martin, J.H., Parker, P.L., Risebrough, R.W., Robertson, W., Schneider, E. and Gamble, E., 1978. The mussel watch. *Environmental Conservation* 5, 101-125.

Gratz, S.R., Ciolino, L.A., Mohrhaus, A.S., Gamble, B.M., Gracie, J.M., Jackson, D.S., Roetting, J.P., McCauley, H.A., Heitkemper, D.T., Fricke, F.L. and Krol, W.J., 2011. Screening and determination of polycyclic aromatic hydrocarbons in seafoods using QuEChERS-based extraction and high-performance liquid chromatography with fluorescence detection. *Journal of AOAC International* 94, 1601-1616.

Greenfield, R., Brink, K., Degger, N., & Wepener, V., 2014. The usefulness of transplantation studies in monitoring of metals in the marine environment: South African experience. *Marine Pollution Bulletin* 85, 566-573.

Hartzell, S. E., Unger, M. A., McGee, B. L., & Yonkos, L. T., 2017. Effects-based spatial assessment of contaminated estuarine sediments from Bear Creek, Baltimore Harbor, MD, USA. *Environmental Science and Pollution Research* 24, 22158-22172.

Hawes, D., Shi, S. R., Dabbs, D. J., Taylor, C. R., & Cote, R. J., 2009. Immunohistochemistry. In N. Weidner, R. J. Cote, S. Suster, & L. M. Weiss (Eds.), Modern surgical pathology (Vol. 1, pp. 48– 70). Elsevier.

Honda, M., & Suzuki, N., 2020. Toxicities of polycyclic aromatic hydrocarbons for aquatic animals. *International Journal of Environmental Research and Public Health* 17, 1363.

IARC (IARC Working Group on the Evaluation of Carcinogenic Risks to Humans), 2010. Some non-heterocyclic polycyclic aromatic hydrocarbons and some related exposures. *IARC Monographs on the evaluation of carcinogenic risks to humans* 92, 1.

Justino, C. I., Duarte, A. C., & Rocha-Santos, T. A., 2017. Recent progress in biosensors for environmental monitoring: A review. *Sensors* 17, 2918.

Karasek, F. W., & Clement, R. E. 2012. Basic gas chromatography-mass spectrometry: principles and techniques. Amsterdam, The Netherlands: Elsevier. 210 p.

Kasiotis, K. M., & Emmanouil, C., 2015. PAHs Pollution Monitoring by Bivalves. *Pollutants in buildings, water and living organisms*, 169-234.

Koelmans, A. A., Poot, A., Lange, H. J. D., Velzeboer, I., Harmsen, J., & Noort, P. C. V., 2010. Estimation of in situ sediment-to-water fluxes of polycyclic aromatic hydrocarbons, polychlorobiphenyls and polybrominated diphenylethers. *Environmental Science & Technology* 44, 3014-3020.

Lacroix, C., Richard, G., Seguineau, C., Guyomarch, J., Moraga, D., & Auffret, M., 2015. Active and passive biomonitoring suggest metabolic adaptation in blue mussels (Mytilus spp.) chronically exposed to a moderate contamination in Brest harbor (France). *Aquatic Toxicology* 162, 126-137.

Latimer, J., Zheng, J., 2003. The sources, transport, and fate of PAHs in the marine environment. In: Douben, PET (Ed.), PAHs: An Ecotoxicological Perspective. Wiley, Chichester, West Sussex, England, pp. 7–33.

Lawal, A.T., 2017. Polycyclic aromatic hydrocarbons. A review. Rev. *Cogent Environmental Science* 3, 1339841.

Li, X., Kaattari, S. L., Vogelbein, M. A., Vadas, G. G., & Unger, M. A., 2016. A highly sensitive monoclonal antibody based biosensor for quantifying 3–5 ring polycyclic aromatic hydrocarbons (PAHs) in aqueous environmental samples. *Sensing and bio-sensing research* 7, 115-120.

Lobel, L. M. K., & Davis, E. A., 2002. Immunohistochemical detection of polychlorinated biphenyls in field collected damselfish (Abudefduf sordidus; Pomacentridae) embryos and larvae. *Environmental Pollution* 120, 529– 532.

Lux, G., Langer, A., Pschenitza, M., Karsunke, X., Strasser, R., Niessner, R., Knopp, D. and Rant, U., 2015. Detection of the carcinogenic water pollutant benzo [a] pyrene with an electro-switchable biosurface. *Analytical Chemistry* 87, 4538-4545.

Marigómez, I., Zorita, I., Izagirre, U., Ortiz-Zarragoitia, M., Navarro, P., Etxebarria, N., Orbea, A., Soto, M. and Cajaraville, M.P., 2013. Combined use of native and caged mussels to assess biological effects of pollution through the integrative biomarker approach. *Aquatic toxicology* 136, 32-48.

Mauseth, G.S., Challenger, G.E., 2001. Trends in rescinding seafood harvest closures following oil spills. In: Proceedings, 2001 International Oil Spill Conference, Tampa, FL, USA, March 26-29, 2001. 679–684.

Meador, J., 2003.Bioaccumulation in Marine Invertebrates. In: Douben, PET (Ed.), PAHs: An Ecotoxicological Perspective. Wiley, Chichester, West Sussex, England, pp. 147-171.

Minick, D.J., Anderson, K.A., 2017. Diffusive flux of PAHs across sediment–water and water–air interfaces at urban superfund sites. *Environmental Toxicology and Chemistry* 36, 2281–2289.

Moller, T.H., Dicks, B., Whittle, K.J. and Girin, M., 1999. Fishing and harvesting bans in oil spill response. In *International Oil Spill Conference* (Vol. 1999, No. 1, 693-699). American Petroleum Institute.

Moorthy, B., Chu, C., & Carlin, D. J., 2015. Polycyclic aromatic hydrocarbons: from metabolism to lung cancer. *Toxicological Sciences* 145, 5-15.

Neff, J.M., Stout, S.A., Gunster, D.G., 2005. Ecological risk assessment of polycyclic aromatic hydrocarbons in sediments: Identifying sources and ecological hazard. *Integrated Environmental Assessment and Management* 1, 22–33.

Nisbet, I.C., LaGoy, P.K., 1992. Toxic equivalency factors (TEFs) for polycyclic aromatic hydrocarbons (PAHs). *Regulatory Toxicology and Pharmacology* 16, 290–300.

Oros, D. R., & Ross, J. R., 2005. Polycyclic aromatic hydrocarbons in bivalves from the San Francisco estuary: spatial distributions, temporal trends, and sources (1993–2001). *Marine Environmental Research* 60, 466-488.

Plaza, G., Ulfig, K., & Tien, A. J., 2000. Immunoassays and environmental studies. *Polish Journal of Environmental Studies* 9, 231-236.

Posthuma-Trumpie, G. A., Korf, J., & van Amerongen, A. (2009). Lateral flow (immuno) assay: its strengths, weaknesses, opportunities and threats. A literature survey. *Analytical and Bioanalytical Chemistry* 393, 569-582.

Prossner, K. M., Vadas, G. G., Harvey, E., & Unger, M. A., 2022. A novel antibody-based biosensor method for the rapid measurement of PAH contamination in oysters. *Environmental Technology & Innovation* 28, 102567.

Prossner, K.M., Small, H.J., Carnegie, R.B. and Unger, M.A., 2023. Immunofluorescence Visualization of Polycyclic Aromatic Hydrocarbon Mixtures in the Eastern Oyster Crassostrea virginica. *Environmental Toxicology and Chemistry* 42, 475-480.

Robinson, J.P. 2001. Principles of confocal microscopy. *Methods in Cell Biology* 63, 89–106

Rodríguez, S. J., & Bishop, P. L., 2005. Competitive metabolism of polycyclic aromatic hydrocarbon (PAH) mixtures in porous media biofilms. *Water Science and Technology* 52, 27– 34.

Sericano, J.L., Wade, T.L., Jackson, T.J., Brooks, J.M., Tripp, B.W., Farrington, J.W., Mee, L.D., Readmann, J.W., Villeneuve, J.P. and Goldberg, E.D., 1995. Trace organic contamination in the Americas: an overview of the US National Status & Trends and the International 'Mussel Watch' programmes. *Marine Pollution Bulletin* 31, 214-225.

Sericano, J. L., Wade, T. L., & Brooks, J. M., 1996. Accumulation and depuration of organic contaminants by the American oyster (Crassostrea virginica). *Science of the Total Environment* 179, 149-160.

Sforzini, S., Moore, M. N., Boeri, M., Benfenati, E., Colombo, A., & Viarengo, A., 2014. Immunofluorescence detection and localization of B[a]P and TCDD in earthworm tissues. *Chemosphere* 107, 282– 289.

Sparkman, Penton, Z., & Kitson, F. G., 2011. *Gas Chromatography and Mass Spectrometry.* (2nd ed.). Elsevier Science & Technology.

Speciale, A., Zena, R., Calabrò, C., Bertuccio, C., Aragona, M., Saija, A., & Cascio, P. L., 2018. Experimental exposure of blue mussels (Mytilus galloprovincialis) to high levels of benzo[a]pyrene and possible implications for human health. *Ecotoxicology and Environmental Safety* 150, 96– 103.

Spier, C. R., Vadas, G. G., Kaattari, S. L., & Unger, M. A., 2011. Near real-time, on-site, quantitative analysis of PAHs in the aqueous environment using an antibody-based biosensor. *Environmental Toxicology and Chemistry* 30, 1557-1563.

Spier, C.R., Unger, M.A. and Kaattari, S.L., 2012. Antibody-based biosensors for small environmental pollutants: Focusing on PAHs. *Biosensors and Environmental Health*, p. 273.

Sporstol, S., Gjos, N., Lichtenthaler, R.G., Gustavsen, K.O., Urdal, K., Oreld, F. and Skei, J., 1983. Source identification of aromatic hydrocarbons in sediments using GC/MS. *Environmental Science & Technology* 17, 282-286.

Strandberg, J. D., Rosenfield, J., Berzins, I. K., & Reinisch, C. L., 1998. Specific localization of polychlorinated biphenyls in clams (Mya arenaria) from environmentally impacted sites. *Aquatic Toxicology* 41, 343– 354.

Subashchandrabose, S. R., Krishnan, K., Gratton, E., Megharaj, M., & Naidu, R., 2014. Potential of fluorescence imaging techniques to monitor mutagenic PAH uptake by microalga. Environmental Science & Technology 48, 9152– 9160.

Van Metre, P.C., Mahler, B.J., Furlong, E.T., 2000. Urban sprawl leaves its PAH signature. *Environmental Science and Technology* 34, 4064–4070.

Vignier, J., Rolton, A., Soudant, P., Chu, F. L. E., Robert, R., & Volety, A. K., 2018. Evaluation of toxicity of Deepwater Horizon slick oil on spat of the oyster Crassostrea virginica. *Environmental Science and Pollution Research* 25, 1176-1190.

Wade, T. L., Sericano, J., Gardinali, P. R., Wolff, G., & Chambers, L., 1998. NOAA's 'Mussel Watch'project: Current use organic compounds in bivalves. *Marine Pollution Bulletin* 37, 20-26.

Walker, S.E., Dickhut, R.M., Chisholm-Brause, C., Sylva, S., Reddy, C.M., 2005. Molecular and isotropic identification of PAH sources in a highly industrialized urban estuary. *Organic Geochemistry* 36, 619–632.

Wang, H., Huang, W., Gong, Y., Chen, C., Zhang, T., & Diao, X., 2020. Occurrence and potential health risks assessment of polycyclic aromatic hydrocarbons (PAHs) in different tissues of bivalves from Hainan Island, China. *Food and Chemical Toxicology* 136, 111108.

Wang, P., Wu, T. H., & Zhang, Y., 2012. Monitoring and visualizing of PAHs into mangrove plant by two-photon laser confocal scanning microscopy. *Marine Pollution Bulletin* 64, 1654– 1658.

Wang, X., Lu, X., & Chen, J., 2014. Development of biosensor technologies for analysis of environmental contaminants. *Trends in Environmental Analytical Chemistry* 2, 25-32.

Wise, S.A., Sander, L.C., Schantz, M.M., 2015. Analytical methods for determination of polycyclic aromatic hydrocarbons (PAHs) — A historical perspective on the 16 U.S. EPA priority pollutant PAHs. *Polycyclic Aromatic Compounds* 35, 187–247.

Wolfe, D.A., Long, E.R., Thursby, G.B., 1996. Sediment toxicity in the hudson-raritan estuary: Distribution and correlations with chemical contamination. *Estuaries* 19, 901–912.

Yender, R., Michel, J.M. and Lord, C., 2002. *Managing seafood safety after an oil spill*. US Department of Commerce, National Oceanic and Atmospheric Administration, National Ocean Service, Office of Response and Restoration.

Zhang, W., Liu, Q.X., Guo, Z.H. and Lin, J.S., 2018. Practical application of aptamer-based biosensors in detection of low molecular weight pollutants in water sources. *Molecules* 23, 344

Chapter 1: A Novel Antibody-Based Biosensor Method for the Rapid Measurement of PAH Contamination in Oysters

Prossner, K. M., Vadas, G. G., Harvey, E., & Unger, M. A., 2022. A novel antibody-based biosensor method for the rapid measurement of PAH contamination in oysters. *Environmental technology & innovation*, *28*, 102567.

Introduction

Polycyclic aromatic hydrocarbons (PAHs) are a class of organic contaminants known for their ubiquity and persistence in the environment and their toxic, mutagenic, and carcinogenic potential (Chapman, 1990, Latimer and Zheng, 2003, Lawal, 2017). In the environment, PAHs exist as complex mixtures comprised of hundreds of different compounds. Natural processes such as volcanic eruptions, forest fires, and oil seeps release PAHs, but emissions from anthropogenic sources such as fossil fuel burning, production of coal-tar derivatives, and oil spills are major sources of PAH pollution in the environment (Neff et al., 2005, Abdel-Shafy and Mansour, 2016). Of particular concern is legacy contamination related to unregulated industrial discharge of PAHs prior to the US Clean Water Act of 1972, as well as increased PAH loads from non-point sources (e.g. vehicle exhaust) due to urbanization and continued reliance on fossil fuels (Wolfe et al., 1996, Van Metre et al., 2000, Walker et al., 2005, Minick and Anderson, 2017). As of 2019, PAHs are ranked within the top ten pollutants on the substance priority list of the Agency for Toxic Substances and Disease Registry (ATSDR) based on their frequency of detection, toxicity, and potential for human exposure at Superfund sites (ATSDR, 2020).

The distribution of PAHs in the aquatic environment is driven by their hydrophobicity and lipophilicity (Latimer and Zheng, 2003). PAHs can exist in different environmental phases including bound to organic sediments, lipid-bound within biological tissues via bioaccumulation, or freely dissolved in water at very low concentrations (Neff et al., 2005, Burgess et al., 2003). Sediment serves as a significant repository for PAHs as they readily sorb to the nonpolar, organic regions of sediment particles (Neff et al., 2005). When phases are at assumed equilibrium, the distribution of PAHs in the environment is proportional between phases via partitioning

coefficients, or equilibrium constants. By using a simple ratio calculation, an unknown concentration of PAHs in one phase can be deduced by dividing the partition coefficient by the known concentration in another phase. The utility of the equilibrium partitioning (EqP) theory is observed in previous assessments of PAH bioavailability in which known concentrations in hydrophobic phases are used to estimate low PAH concentrations in the dissolved aqueous phase. The dissolved phase has the most potential for biological uptake but is difficult to measure by conventional analytical methods due to limitations in sample volume requirements. A prominent example of the utility of the EqP theory in bioavailability assessments is its fundamental role in techniques using polymer-based passive sampling devices (PSD). Based on the contaminant concentration sorbed within the PSD and the known partition coefficient, the freely dissolved PAH fraction can be estimated (DiToro et al., 1991, Leslie et al., 2002, Vrana et al., 2005, Ghosh et al., 2014, Mayer et al., 2014).

As sessile benthic filter feeders, bivalve molluscs such as oysters are highly sensitive to bioaccumulation of lipophilic PAH due to their detritivore feeding habits as well as their low metabolic capacity (James, 1989). PAH levels in bivalve tissue are among the highest observed in all food products, posing a potential human health risk (EFSA, 2008). Accordingly, oysters are a well-known biomonitoring species with widespread ecological significance and have served as a key sentinel species in the NOAA Mussel Watch Program since its establishment in 1975 (Farrington et al., 1983, Farrington et al., 2016, Wade et al., 1998). For degraded estuarine sites, oyster restoration is a valuable remediation strategy that provides an array of ecosystem services such as stabilizing shorelines and supplying protective habitat for epibenthic fauna and juvenile fish (Grabowski et al., 2012). With a native habitat distribution ranging 8000 km from Canadian maritime provinces to the Gulf of Mexico as well as Panama and the Caribbean islands, the

eastern oyster (*Crassostrea virginica*) is an internationally important commercial seafood product (NMFS, 2007). In 2020, *C. virginica* commercial fishery landings garnered over $140 million in the United States alone (NMFS, 2015).

While a multitude of PAH compounds exist in the environment, regulatory bodies often base maximum acceptable levels on the concentrations of a subset of target PAHs. The subset of compounds analyzed in such assessments are considered priority pollutants due to their frequency and occurrence in environmental samples as well as their toxicity and potential for human exposure (ATSDR, 2020). Subsets of priority PAHs can vary depending on the regulatory agency and endpoint of concern. The list of 16 priority PAHs issued by the U.S. Environmental Protection Agency (EPA) is commonly analyzed for environmental risk assessments and monitoring. This list was originally developed to assess human health risk from drinking water, but these compounds have since served as target analytes in food-related risk assessments (Andersson and Achten, 2015). Although there is no legislation on maximum acceptable PAH levels in food in the United States, the European Food Safety Authority (EFSA) within the European Union regulates PAH levels in a wide variety of food products entering the market. As of 2011, maximum levels have been set for benzo [a] pyrene and the sum of 4 PAH compounds, benzo [a] pyrene, benz [a] anthracene, benzo [b] fluoranthene, and chrysene (PAH4), in fresh, chilled, or frozen bivalves (EC 835/2011) through the European Committee for Standardization (CEN)-accepted gas chromatography–mass spectrometry (GC–MS) method (EN 16619: 2015) (European Union, 2011). Adopted by the EPA in 1984, the toxic equivalency factor approach to human health risk assessments considers carcinogenic potency of individual PAH compounds (EPA, 1984, Nisbet and LaGoy, 1992). In this technique, individual PAH concentrations are converted to their toxic equivalent concentration relative to benzo [a] pyrene (BaPE) and used to

assess cancer risk from exposure (EPA, 1984, Nisbet and LaGoy, 1992, ATSDR, 1995). This method has also been utilized by the FDA following the Deepwater Horizon oil spill in 2010 and the Virginia Department of Health's Division of Shellfish Sanitation (VDH-DSS) in 2012 (VDH, 2012).

Standard chemical analyses such as GC–MS to quantify PAH levels in seafood are often time-consuming, labor-intensive, and expensive on a per sample basis (Mauseth and Challenger, 2001, Mastovska et al., 2015, Zhang et al., 2018, Felemban et al., 2019). Additionally, complex sample extraction and clean up methods prior to analysis require large volumes of hazardous organic solvents (Farré et al., 2010). In large scale surveys or in rapid response scenarios (e.g. oil spills or flooding events), employment of GC–MS alone is inefficient due to slow assessment time and cost. Methods exist to quickly and inexpensively screen samples for further GC–MS analysis such as high-performance liquid chromatography coupled with fluorescence detection (HPLC-FLD); however, this method is limited in its sensitivity and accuracy and it still requires multiple steps of sample processing and preparation (Plaza-Bolaños et al., 2010, Zelinkova and Wenzl, 2015). For seafood contamination assessment following an oil spill, sensory analysis (i.e. sniff-testing) has been used to prioritize samples for further GC–MS analysis based on the detection of petroleum taint in the seafood sample (US Food and Drug Administration (FDA), 2010, Moller et al., 1999). This testing is conducted by a panel of experts that have undergone highly specialized training (Yender et al., 2002); however, results may be unreliable due to the sensitivity and experience of panel members as well as compromised sample integrity due to factors unrelated to petroleum (e.g. putrefaction or fecal contamination) (Mauseth and Challenger, 2001). Additionally, sensory analysis is not a quantitative approach — PAH levels and relative toxicity remain unknown until GC–MS analysis. Faster, more cost-effective, and

reliable screening methods that can measure PAH levels in seafood are needed to better assess human health risk.

In an effort to provide faster, economical and reliable PAH analyses, a variety of immunoassay methods have been examined for the detection and quantification of PAH in environmental samples (EPA, 1996a, EPA, 1996b, Spier et al., 2012, Behera et al., 2018). Our lab has developed a rapid, near-real-time method for PAH quantitation using the KinExA Inline Biosensor (Sapidyne Instruments, Boise, ID) and a mouse-derived anti-pyrene-butyric acid monoclonal antibody, 2G8, with previously demonstrated uniform selectivity for a range of 3–5 ring PAHs (Li et al., 2016). Additionally, the biosensor is a user-friendly instrument that can directly analyze environmental samples (i.e requires minimal sample preparation). It has been used to quantify PAH in porewater samples in the Chesapeake Bay and Houston ship channel and has demonstrated strong positive correlation with PAH measurements of sediment porewater when using passive sampling and GC–MS (Hartzell et al., 2017, Conder et al., 2021, Camargo et al., 2022).

Serving as the study area, the Elizabeth River is a tidal estuary in southeastern Virginia (USA) surrounded by four major cities and comprised of the Eastern, Western, and Southern branches and the Lafayette River. The Elizabeth River was selected on the basis of significantly elevated PAH levels observed in sediment throughout the river due to numerous military and industrial activities. Coal and petroleum storage and transport, shipbuilding and repair activities, as well as creosote-based wood treatment facilities active until the 1990s were predominant sources of PAH pollution. Atlantic Wood Industries, a designated Superfund Site, was one of three major wood treatment facilities located in this river. In 2004, the Elizabeth River had the

highest known PAH concentrations in sediment worldwide and has been a site for ongoing remediation efforts (DiGiulio and Clark, 2015).

The purpose of this study is to evaluate antibody-based biosensor technology as a rapid screening method to measure PAH concentrations in adult oysters (*C. virginica*) and assist in regulatory assessments and environmental monitoring. Through a novel extension of the equilibrium phase partitioning theory, we hypothesize that a strong association will be observed between biosensor measurement of aqueous phase concentrations and GC–MS measurement of tissue concentrations in field-collected oysters. Based on this association, near real-time biosensor measurements can be used to predict tissue concentrations for rapid quantitative screening. Evaluation of the biosensor screening method consisted of a linear regression analysis comparing biosensor measurements of PAH concentrations to that of GC–MS. To relate the PAH totals screened by biosensor to human health risk, mean biosensor measurements of total PAH concentration per site were then compared to the respective summations of several regulatory PAH subsets involved in determining human health risk. Lastly, to demonstrate the utility of the biosensor screening method in environmental monitoring efforts, biosensor-derived concentrations in oysters throughout the Elizabeth River watershed were mapped and compared to known historic sediment concentrations.

Materials and Methods

Sample collection

Oysters were sampled from beach shorelines as well as bridge and pier pilings at twenty-one sites throughout the Elizabeth River watershed (listed in Tables 1 and 2) and transported from the field on ice. In the laboratory, whole oysters were stored at −20 °C and thawed at room temperature for processing. Oyster interstitial fluid, defined as the fluid pooled in the shell cavity

upon opening of the thawed oyster, was collected from individual oysters with a glass disposable Pasteur pipet, filtered through a 0.45μm PTFE syringe filter and then stored in 20 mL glass scintillation vials. Biosensor analysis (see below) was employed to measure PAH concentration in interstitial fluid from six individual animals per site. Soft tissues from the same six individual oysters per site were homogenized and pooled to provide sufficient sample material to achieve a sensitive detection limit for GC–MS analysis. The composite tissue samples were stored at −20 °C until extraction and further preparation for GC–MS analysis. A schematic of the experimental design is presented in Fig. 1.

Biosensor analysis of PAHs

Features and design for the KinExA Inline Sensor as well as development and screening procedures for the monoclonal anti-PAH antibody (mAb 2G8) employed in this study have been previously described (Bromage et al., 2007, Spier et al., 2011, Li et al., 2016). The Inline instrument uses computer programmable fluidics to process up to eight samples in series and provides precise quantitative measurements of the total concentration of 3–5 ring PAHs when using the 2G8 monoclonal antibody (Li et al., 2016). The instrument functions as a kinetic assay: the antibody binds to PAH in the aqueous sample initially, then the sample-antibody mixture is passed over a stationary antigen in the detector flow cell where free unbound antibody is retained and measured. The 2G8 antibody used in this study contains a covalently bound fluorescent tag (648 nm) measured by the instrument so the biosensor signal response (dV) is inversely proportional to the PAH content in the sample. The automated sample processing cycle takes less than ten minutes and includes steps for mixing the sample with the antibody, rinsing the flow cell and replacing and loading of antigen coated beads for the next sample in the cycle. Each day prior to sample analysis a six-point calibration curve is generated using double-deionized water

(ddH2O) as an analytical blank and a dilution series of phenanthrene standards with concentrations ranging from 0.5 to 2.5 µg/L to determine the linear range of the detector's dV response via log-linear regression analysis. Based on the signal response measured in the oyster interstitial fluid sample, PAH concentrations were calculated and reported in µg/L.

GC–MS analysis

GC–MS analyses were conducted using standard protocols described previously (Unger et al., 2008, Li et al., 2016). In brief, composite tissue samples were freeze-dried in pre-cleaned glass troughs. Samples and laboratory blanks were spiked with a deuterated surrogate PAH standard and extracted using a Dionex® (Bannockburn, IL) accelerated solvent extractor (ASE 300) with 100% dichloromethane. The sample volumes were reduced under a gentle stream of nitrogen at 40 °C in a TurboVap® evaporator. Following a standard protocol, a high-performance liquid chromatograph with a gel permeation column was used for size exclusion separation. The samples were fractionated, and polar compounds removed via open column chromatography containing 10.0 g of deactivated silica gel eluted with 100% hexane followed by an elution with 80/20% hexane/dichloromethane. The extracts were solvent exchanged to 100% dichloromethane, concentrated to a final volume. Calibration standards and samples were spiked with 0.1 mL of internal standard, p-terphenyl. A 7- to 10-point calibration curve was generated for analysis of individual PAH analytes and surrogate standards. A total of 64 analytes — both methylated and parent compounds were measured and include the priority PAHs utilized in subsequent calibrations to regulatory subset lists (Table S1). PAH measurements in tissue are reported in µg/kg wet weight. Average surrogate standard recoveries are also reported.

Statistical methods

Using R statistical computing and graphics software, simple linear regression models were used to examine associations. A 95% confidence band around the regression was determined through *t*-based approximation in R. The regression line of best fit is described by the following equation:

$$y = bx + a$$

Where *x* and *y* serve as independent and dependent variables, respectively. For this study, *x* represents biosensor-measured PAH concentrations in oyster interstitial fluid and *y* serves as the GC–MS-measured PAH concentrations in oyster tissue. The regression slope, *b*, serves as the partition coefficient between interstitial fluid and soft tissues. The y-intercept for the model is *a*.

Evaluation of instrument precision and method detection limit for biosensor

An aliquot of oyster interstitial fluid was measured in triplicate for six oysters from three sites (3 samples per oyster; 18 samples per site; 54 samples total). The three sites, MP2, JCBR, and RS, were selected to represent high-, mid-, and low-range PAH concentrations of the dataset to assess the biosensor's performance at each level. The method detection limit (MDL) was determined following the EPA standard procedure described in EPA 821–R–16–006 (EPA 2016). Briefly, an initial MDL was estimated by subtracting three times the standard deviation of a set of method blanks from the mean-determined concentration. A spiking level of 0.5 µg/L was selected based on the estimated MDL. A minimum of 7 spiked samples and 7 method blanks (ddH2O) were prepared on 6 separate calendar days and analyzed on 6 separate calendar days. A Welch's t-test was conducted to compare means of method blanks to spiked samples, to ensure spiking levels were significantly different from zero. Based on a $p < 0.05$, the null hypothesis of equal means could be rejected. An MDL was calculated based on spiked samples and method

blanks, MDL_s and MDL_b respectively. The greater of MDL_s and MDL_b was selected as the initial MDL.

Method Calibration to Priority PAH Subsets

Calibration to EU Regulations (EFSA-4)

From the total 64 analytes targeted for GC–MS analysis of Elizabeth River oysters, concentrations for the EFSA-4 subset (benz[a]anthracene, chrysene, benzo[b]fluoranthene, benzo[a]pyrene) were summed for each site (see Table S3 for calculations). The maximum acceptable level for the sum of the 4 PAHs is 30 µg/kg wet weight (Regulation (EU) No. 835/2011) (European Union, 2011). Dry weight concentrations were converted to wet weight by multiplying by the total percent moisture loss from freeze-dried tissue samples. Elizabeth River oyster sampling sites were evaluated against this regulatory limit.

Calibration to VDH oyster consumption advisory guidelines (VDH-15)

Calibration for this assessment was based on the 2012 Health Consultation released by VDH (VDH 2012). Fifteen PAH compounds were selected on the basis of their known toxicity through evaluations by the Agency for Toxic Substances and Disease Registry (ATSDR) (ATSDR 1995). The Division of Environment Epidemiology (DEE) of the VDH used toxicity equivalency factors (TEF) to assess the carcinogenic potential of the 15 PAHs analyzed (acenanapthylene, acenapthene, fluorene, phenanthrene, anthracene, fluoranthene, pyrene, benz[a]anthracene, chrysene, benzo[b]fluoranthene, benzo[k]fluoranthene, benzo[a]pyrene, ideno[1,2,3-cd]pyrene, dibenz[a,h]anthrancene, benzo[g,h,i]perylene) (Table S2). By multiplying the concentration of each compound by its respective TEF, the benzo [a] pyrene equivalent concentration can be determined (BaPE). A calibrated model was generated comparing the summation of 15 BaPEs (VDH-15) and biosensor measurements across sites (Figure S2).

Concentrations at each Elizabeth River site were evaluated under the advisory guidelines determined by VDH (VDH 2012). Guidelines developed by the VDH for consumption of PAH-contaminated oysters based on BaPE concentrations are as follows: less than 25 µg/kg — no advisory, 25-50 µg/kg — two meals per month, 50-100 µg/kg — one meal per month, greater than 100 µg/kg — do not eat oysters from advisory area. A meal consists of a dozen 14 g oysters for an adult with an average weight of 80kg.

Calibration to EPA's list of 16 priority PAHs (EPA-16)

Unlike EFSA-4 and VDH-15, consumption guidelines or regulatory limits for this subset of priority PAHs in food do not exist but this list is often used in environmental monitoring efforts. Therefore, the association between EPA-16 PAH subset and biosensor measurements of total 3- to 5-ring PAHs across sites was evaluated. Table S4 provides respective compound concentrations and totals for each site.

Results and Discussion

Linear regression analysis of biosensor vs. GC–MS technique

A strong association between PAH concentrations measured by biosensor and conventional GC–MS supports the role of biosensor technology as a screening method to assess tissue contamination in oysters via the application of the equilibrium partitioning theory. There was a strong positive relationship ($R^2 = 0.88$) between interstitial fluid PAH concentrations measured by the biosensor and tissue PAH concentrations (64 analytes) measured via GC–MS (Figure 2). The following equation was determined from linear regression analysis:

$$y = 47.0\,x - 316.0$$

The slope of the fitted regression line, 47.0, serves as the model-derived equilibrium partition coefficient which can be used to predict tissue concentrations (y) from oyster interstitial fluid (x).

The *y*-intercept is –316.0. Additionally, the mean surrogate standard recoveries for GC–MS analysis were as follows: d8-napthalene: 13%; d10-acenaphthene: 26%; d10-phenanthrene: 48%; 1,1’ binaphthyl: 52%; d12-chrysene: 78%; d12-perylene: 66%.

With the development and validation of a steady-state equilibrium partitioning model, unknown phase concentrations can be predicted, particularly if they are within concentration range evaluated. An order of magnitude difference observed between PAH concentrations measured in interstitial fluid versus soft tissue suggests an adherence to equilibrium phase partitioning principles within the organism. Hydrophobic organic contaminants will more readily bind to lipid-rich sites such as fatty tissue; thus, tissue PAH concentrations will be comparatively higher than those in interstitial fluids. Although biosensor measurements are precise (see below), several data points fall outside the 95% confidence band around the regression line (Figs. 2 and 5). The observed variation is reasonable and expected for this study as two entirely different matrices are being compared: average interstitial fluid concentrations of individual oysters and concentrations measured in pooled oyster tissue homogenate. Nonetheless, the strong association indicates that measuring PAH levels in interstitial fluid alone can give reasonably precise estimates of whole animal exposure. Biosensors have had previously demonstrated success as rapid, low-cost methods to analyze pathogens and marine biotoxins in shellfish (Nordin et al. 2017; Campàs et al. 2007; Tian et al. 2021). To our knowledge, this the first study to demonstrate the application of biosensors for measuring environmental contaminants in shellfish, an equally important food safety threat, through a novel implementation of the equilibrium partitioning theory.

Method performance

Small standard deviations observed in the analytical replicates demonstrates the precision of the biosensor measurements (Fig. 3). Moreover, estimated differences between animals within stations indicate that individual variation in uptake is far greater than the precision of the method (Fig. 4).

Notably, because of the high sensitivity, reproducibility, and small sample volume requirement of the biosensor, PAH concentrations can now be measured rapidly and at the scale of individual oysters. With this feature, variability between individual oysters within the population at a specific site can be determined (Fig. 4). An efficient means to measure concentrations in individual animals is valuable as contamination at sites occurs heterogeneously and sample variation is obscured when data are pooled (Bignert et al., 1993). Analysis of individuals also allows for detection of single outliers which may influence the overall trends observed or reveal unknown hotspots. Evaluation of the method detection limit shows that the limit for detecting PAH in interstitial fluid is 0.39 µg/L, an order of magnitude below the lowest concentration measured in any oyster interstitial fluid to date. Previous studies have investigated commercial enzyme-linked immunoassay (ELISA) kits to rapidly screen PAH levels in biological samples such as oiled seabird sera and crab urine and hemolymph (Fritcher et al., 2002, Fillmann et al., 2002). While the applications of these tests were deemed promising for monitoring PAH exposure in biota, these immunoassays were much less sensitive with detection limits in the ppm range. Furthermore, the results from these assays are only semi-quantitative and still required several sample preparation and extraction steps prior to analysis. We present a method that can accurately quantify total PAH concentrations in the sub-ppb range with minimal sample preparation.

Assessment of sites in context of priority PAH subsets

As revealed in the original regression (targeting 64 PAH analytes for analysis), a significant positive association between mean biosensor measurements of PAH concentration in oyster interstitial fluid were significantly positively associated and the summation of the EPA-16 PAHs in oyster tissues at each site, still held for this subset of PAH compounds (y=37.1 x -303.5, R^2 = 0.88, df=23) (Fig. 5). Because of the strong association, the regression equation can be used to rapidly estimate total tissue concentrations for this particular subset of PAH compounds. This information then can assist in streamlining environmental monitoring assessments that frequently target these 16 priority compounds.

Across all Elizabeth River sample sites, predicted oyster tissue concentrations at only 2 sites fell below the EFSA-4 threshold of a maximum of 30.0 µg/kg. From the model calibrated to fit EFSA guidelines, with a partition coefficient of 15.8 (Figure S1), concentrations in oyster interstitial fluid must be below 11.5µg/L to adhere to these regulations. When considering the VDH multi-tier advisory approach, 19 of 21 sample sites had predicted tissue concentrations within acceptable levels for human consumption. Oysters at 9 sites met tier 1 VDH guidelines of no advisory; oysters at 5 sites met tier 2 guidelines; and oysters at 5 sites met tier 3 guidelines. Based on the partition coefficient of 2.3 from the model calibrated for the metrics used in the VDH assessment (Figure S2), interstitial fluid concentrations must be below the following thresholds: 17.2 µg/L for no advisory (tier 1), 28.1 µg/L for 2 meals per month (tier 2); and 49.9 µg/L for 1 meal per month (tier 3). If the oyster interstitial fluid is greater than 49.9 µg/L, oysters should not be consumed in that area (tier 4).

The estimates for tissue concentrations based on interstitial fluid concentrations showed a very high accuracy and correspondence (Tables 1 and 2). Respective regressions used to

determine tissue concentration predictions are provided in the supplemental data (Figs. S1 and S2). For 18 out of 21 sites, individual tissue concentrations were successfully predicted by this screening method as falling above or below the EFSA threshold (80% accuracy or greater). For the VDH multi-tier regulatory approach, individual oysters at 10 out of 21 sites successfully predicted the correct tier in which the oysters at a site fell. The low prediction accuracy (0-33%) at some sites can be attributed to specific PAH composition and compound variability in individual oysters. For example, in Table 1, individual oysters at site MP2 predicted that the site would fall below the 30 µg/kg limit. However, the concentrations of the 4 individual PAH compounds considered for the threshold comprised almost 30% of the overall concentration of PAH analyzed for the site. The total PAH concentration was low compared to the rest of the sites throughout the Elizabeth River. In another example, predictions for site HS failed across all individuals (Table 2). This was the only site that had a high concentration of dibenz [a,h] anthracene, which has a TEF of 5 (VDH, 2012). When converted to its BaPE concentration, this specific PAH compound accounted for over 50% of the total VDH-15 concentration. Other cases in which individual concentrations inaccurately predicted a site's performance in meeting regulations included those which were on the cusp of the threshold value such as GR and CLY in Table 1. When screening sample results are approaching regulatory concerns, conducting more extensive compound specific analyses and further monitoring may be necessary. At present, oysters are not to be consumed from the Elizabeth River or its tributaries; therefore, the interpretations drawn from this assessment are for demonstration purposes only. They do, however, serve as reference points for ongoing studies.

Survey of PAH concentrations in oysters throughout the river watershed

Since biosensor technology allows for rapid and inexpensive data assessment, a map of concentrations throughout the entire Elizabeth River watershed was efficiently produced (Fig. 6). This could be particularly valuable for documenting concentration gradients, focusing on hot spots, and prioritizing samples for further compound-specific analyses or source identification using GC–MS. Efficient mapping also assists in establishing baseline levels. Baseline measurements are critical for the development of realistic remediation goals as well as impact assessment following environmental disturbances (e.g oil spills, dredging, flood events). The concentrations observed in Fig. 6 show that regression-based predictions of PAH concentrations are good bioindicators of legacy sediment contamination in the system and can be a cost-effective monitoring tool used to map gradients and document remediation effectiveness. The resulting map from this study also elucidated new target areas for future monitoring and remediation as elevated levels were observed in oysters where previous data are limited. A common logistical issue observed in hazardous waste remediation programs such as Superfund is inefficient detection and mapping of contamination at specific sites (US Congress Office of Technology Assessment, 1991). Additionally, increased urbanization and changing land use can greatly impact spatial distribution of contaminants such as PAH and ultimately exposure risk (Chalmers et al. 2007; Nowell et al. 2013). Simplistic, user-friendly, high-throughput methods to rapidly quantify PAH levels allows for more efficient monitoring to track these changes in distribution and bioavailability on a greater spatiotemporal scale.

Conclusions

In this era of global change, tenacious monitoring and assessment of legacy organic contaminants such as PAHs is as vital as ever. Although PAHs have been well-documented as

contaminants of interest in a multitude of previous environmental assessments, they are still some of the most commonly detected toxic chemicals of concern at hazardous sites (ATSDR 2020). The onslaught of more frequent and extreme weather events can lead to the mobilization of these contaminants, shifting their environmental distribution (Knap and Rusyn 2016; Kibria et al. 2021). Additionally, the continued reliance on oil makes the possibility of oil spills and the resulting PAH contamination a looming threat. The need for cost-effective analytical methods that can operate within a refined spatiotemporal scope is apparent, particularly when human health is at risk. Immunoassays such as antibody-based biosensor technology show great promise in this regard. Although compound-specific analysis is unattainable with this technology, the biosensor can serve as rapid quantitative screening tool to document contamination and prioritize samples or sampling strategies for further GC–MS analysis when needed. With features including near real-time analysis and low-cost per sample, the biosensor screening method can be a valuable tool in the assessment of seafood safety for human consumption or as a monitoring tool to document PAH levels at sites throughout an entire watershed. When biosensor measurements were compared against different regulatory subsets of priority PAHs (EPA-16, EFSA-4, VDH-15), similar trends were observed across sites suggesting that it is highly adaptable. The demonstrated flexibility of the biosensor screening method to different PAH subsets will become more apparent as new toxicity studies redefine priority PAHs (da Silva Junior et al. 2021). In particular, alkylated PAH isomers have garnered increased attention as they have shown higher toxicities than their parent forms but have not been previously included on regulatory PAH lists (Andersson and Achten 2015; Wise et al. 2015). Reducing the time and expense of conventional analytical methods, antibody-based biosensor technology expands the

spatiotemporal scope of real-world applications for these hydrophobic organic contaminants in the aquatic environment.

References

Andersson, J.T., Achten, C., 2015. Time to say goodbye to the 16 EPA PAHs? Toward an up-to-date use of PACs for environmental purposes. *Polycyclic Aromatic Compounds* 35, 330–354.

Abdel-Shafy, H.I., Mansour, M.S., 2016. A review on polycyclic aromatic hydrocarbons: Source,environmental impact, effect on human health and remediation. *Egyptian Journal of Petroleum* 25, 107–123.

ATSDR (Agency for Toxic Substances and Disease Registry), 1995. Toxicological Profile for Polycyclic Aromatic Hydrocarbons : Technical Report . U.S. Department of Health and Human Services, Public Health Service, Agency for Toxic Substances and Disease Registry Atlanta, GA, USA

ATSDR (Agency for Toxic Substances and Disease Registry), 2020. The ATSDR 2019 Substance Priority List. Agency for Toxic Substances and Disease Registry, Division of Toxicology and Human Health Services, Atlanta, GA, USA.

Behera, B.K., Das, A., Sarkar, D.J., Weerathunge, P., Parida, P.K., Das, B.K., Thavamani, P., Ramanathan, R., Bansal, V., 2018. Polycyclic Aromatic Hydrocarbons (PAHs) in inland aquatic ecosystems: Perils and remedies through biosensors and bioremediation. *Environmental Pollution* 241, 212–233.

Bignert, A., Göthberg, A., Jensen, S., Litzén, K., Odsjö, T., Olsson, M., Reutergårdh, L., 1993. The need for adequate biological sampling in ecotoxicological investigations: A retrospective study of twenty years pollution monitoring. *Science of the Total Environment* 128, 121–139.

Bromage, E.S., Vadas, G.G., Harvey, E., Unger, M.A., Kaattari, S.L., 2007. Validation of an antibody- based biosensor for rapid quantification of 2, 4, 6-trinitrotoluene (TNT) contamination in groundwater and river water. *Environmental Science and Technology* 41, 7067–7072.

Burgess, R., Ahrens, M., Hickey, C., 2003. Geochemistry of PAHs in aquatic environments: source, persistence and distribution. In: Douben, PET (Ed.), PAHs: An Ecotoxicological Perspective. Wiley, Chichester, West Sussex, England, pp. 35–45.

Camargo, K., Vogelbein, M.A., Horney, J.A., Dellapenna, T.M., Knap, A.H., Sericano, J.L., Wade, T.L., McDonald, T.J., Chiu, W.A., Unger, M.A., 2022. Biosensor applications in contaminated estuaries: Implications for disaster research response. *Environmental Research* 204, 111893.

Campàs, M., Prieto-Simón, B., Marty, J.L., 2007. Biosensors to detect marine toxins: Assessing seafood safety. *Talanta* 72, 884–895.

Chalmers, A.T., Van Metre, P.C., Callender, E., 2007. The chemical response of particle-associated contaminants in aquatic sediments to urbanization in New England, USA. *Journal of Contaminant Hydrology* 91, 4–25.

Chapman, P.M., 1990. The sediment quality triad approach to determining pollution-induced degradation. *Science of the Total Environment* 97 (98), 815–825.

Conder, J., Jalalizadeh, M., Luo, H., Bess, A., Sande, S., Healy, M., Unger, M.A., 2021. Evaluation of a rapid biosensor tool for measuring PAH availability in petroleum-impacted sediments. *Environmental Advances* 3, 1–6.

da Silva Junior, F.C., Felipe, M.B.M.C., Castro, D.E.F., Araújo, S.C.D.S., Sisenando, H.C.N., Batistuzzo de Medeiros, S.R., 2021. A look beyond the priority: A systematic review of the genotoxic, mutagenic, and carcinogenic endpoints of non-priority PAHs. *Environmental Pollution* 278, 116838.

DiGiulio, R.T., Clark, B.W., 2015. The Elizabeth River story: a case study in evolutionary toxicology. *Journal of Toxicology and Environmental Health, Part B* 18, 259–298.

DiToro, D., Zarba, C., Hansen, D., Berry, W., Swartz, R., Cowan, C., Pavlou, S., Allen, H., Paquin, P., 1991. Technical basis for establishing sediment quality criteria for nonionic organic chemicals using equilibrium partitioning. *Environmental Toxicology and Chemistry* 10, 1541–1583.

DIVER, 2020. Web application: Data integration visualization exploration and reporting application, national oceanic and atmospheric administration. Retrieved: July, 22, 2021, from https://www.diver.orr.noaa.gov.

EFSA (European Food Safety Authority), 2008. Scientific Opinion of the Panel on Contaminants in the Food Chain on a request from the European Commission on Polycyclic Aromatic Hydrocarbons in Food, EFSA J. 724, 1–114.

EPA (US Environmental Protection Agency), 1984. Health Effects Assessment for Polycylic Aromatic Hydrocarbons (PAH) : EPA-540/1-86-013 . Environmental Criteria and Assessment Office, Cinncinnati, OH

EPA (US Environmental Protection Agency), 1996a. SW-846 Test Method 4000: Immunoassay. https://www.epa.gov/hw-sw846/sw-846-test-method-4000-immunoassay.

EPA (US Environmental Protection Agency), 1996b. SW-846 Test Method 4030: Soil Screening for Petroleum Hydrocarbons by Immunoassay. https://www.epa.gov/hw-sw846/sw-846-test-method-4030-soilscreening-petroleum-hydrocarbons-immunoass.

EPA (US Environmental Protection Agency), 2016. Definition and Procedure for the Determination of the Method Detection Limit, Revision 2 : EPA 821-R-16-006. Technical Report. US Environmental Protection Agency Washington, DC

European Union, 2011. Commission regulation (EU) no 835/2011. Off. J. Eur. Union L214/5 835/2011.

Farré, M., Pérez, S., Gonçalves, C., Alpendurada, M.F., Barceló, D., 2010. Green analytical chemistry in the determination of organic pollutants in the aquatic environment. *TRAC Trends in Analytical Chemistry*. 29, 1347–1362.

Farrington, J.W., Goldberg, E.D., Risebrough, R.W., Martin, J.H., Bowen, V.T., 1983. US mussel watch 1976–1978: an overview of the trace-metal, DDE, PCB, hydrocarbon and artificial radionuclide data. *Environmental Science and Technology* 17, 490–496.

Farrington, J.W., Tripp, B.W., Tanabe, S., Subramanian, A., Sericano, J.L., Wade, T.L., Knap, A.H., 2016. Edward D. Goldberg's proposal of the mussel watch: reflections after 40 years. *Marine Pollution Bulletin* 110, 501–510.

Felemban, S., Vazquez, P., Moore, E., 2019. Future trends for in situ monitoring of polycyclic aromatic hydrocarbons in water sources: The role of immunosensing techniques. *Biosensors* 9, 142.

Fillmann, G., Watson, G.M., Francioni, E., Readman, J.W., Depledge, M.H., 2002. A non-destructive assessment of the exposure of crabs to PAH using ELISA analyses of their urine and haemolymph. *Marine Environmental Research* 54, 823–828.

Fritcher, D.L., Mazet, J.A., Ziccardi, M.H., Gardner, I.A., 2002. Evaluation of two direct immunoassays for rapid detection of petroleum products on marine birds. *Marine Pollution Bulletin* 44, 388–395.

Ghosh, U., Driscoll, S.K., Burgess, R.M., Jonker, M.T.O., Reible, D., Gobas, F., Choi, Y., Spitz, S.E., Maruya, K.A., Gala, W.R., Mortimer, M., Beegan, C., 2014. Passive sampling methods for contaminated sediments: Practical guidance for selection, calibration, and implementation. *Integrated Environmental Assessment and Management* 10, 210–223.

Grabowski, J.H., Brumbaugh, R.D. Robert D., Conrad, R.F., Keeler, A.G., Opaluch, J.J., Peterson, C.H., Piehler, M.F., Powers, S.P., Smyth, A.R., 2012. Economic valuation of ecosystem services provided by oyster reefs. *BioScience* 62, 900–909.

Hartzell, S., Unger, M., McGee, B., Yonkos, L., 2017. Effects-based spatial assessment of contaminated estuarine sediments from Bear Creek, Baltimore Harbor, MD, USA. *Environmental Science and Pollution Research* 24, 22158–22172.

James, M., 1989. Biotransformation and disposition of PAH in aquatic invertebrates. In: Varanasi, U. (Ed.), Metabolism of Polycyclic Aromatic Hydrocarbons in the Aquatic Environment. CRC Press, Boca Raton, FL, USA, pp. 69–92.

Kibria, G., Nugegoda, D., Rose, G., Yousuf Haroon, A.K., 2021. Climate change impacts on pollutants mobilization and interactive effects of climate change and pollutants on toxicity and bioaccumulation of pollutants in estuarine and marine biota and linkage to seafood security. *Marine Pollution Bulletin* 167, 112364.

Knap, A.H., Rusyn, I., 2016. Environmental exposures due to natural disasters. *Reviews on Environmental Health* 31, 89–92.

Latimer, J., Zheng, J., 2003. The sources, transport, and fate of PAHs in the marine environment. In: Douben, PET (Ed.), PAHs: An Ecotoxicological Perspective. Wiley, Chichester, West Sussex, England, pp. 7–33.

Lawal, A.T., 2017. Polycyclic aromatic hydrocarbons. A review. *Cogent Environmental Science* 3, 1339841.

Leslie, H.A., ter Laak, T.L., Busser, F.J., Kraak, M.H., Hermens, J.L., 2002. Bioconcentration of organic chemicals: Is a solid-phase microextraction fiber a good surrogate for biota? *Environmental Science and Technology* 36, 5399–5404.

Li, X., Kaattari, S.L., Vogelbein, M.A., Vadas, G.G., Unger, M.A., 2016. A highly sensitive monoclonal antibody-based biosensor for quantifying 3–5 ring polycyclic aromatic hydrocarbons (PAHs) in aqueous environmental samples. *Sensing and Bio-Sensing Research* 7, 115–120.

Mastovska, K., Sorenson, W.R., Hajslova, J., 2015. Determination of polycyclic aromatic hydrocarbons (PAHs) in seafood using gas chromatography-mass spectrometry: Collaborative study. *Journal of AOAC International* 98, 477–505.

Mauseth, G.S., Challenger, G.E., 2001. Trends in rescinding seafood harvest closures following oil spills. In: Proceedings, 2001 International Oil Spill Conference, Tampa, FL, USA, March 26-29, 2001. pp. 679–684.

Mayer, P., Parkerton, T., Adams, R., Cargill, J., Gan, J., Gouin, T., Gschwend P. Hawthorne, S., Helm, P., Witt, G., You, J., Escher, B., 2014. Passive sampling methods for contaminated sediments: Scientific rationale supporting use of freely dissolved concentrations. *Integrated Environmental Assessment and Management* 10, 197–209.

Minick, D.J., Anderson, K.A., 2017. Diffusive flux of PAHs across sediment–water and water–air interfaces at urban superfund sites. *Environmental Toxicology and Chemistry* 36, 2281–2289.

Moller, T.H., Dicks, B., Whittle, K.J., Girin, M. 1999. Fishing and harvesting bans in oil spill response. In: Proceedings, 1999 International Oil Spill Conference. Seattle, WA, USA, March 8-11, 1999. pp. 693–699.

Neff, J.M., Stout, S.A., Gunster, D.G., 2005. Ecological risk assessment of polycyclic aromatic hydrocarbons in sediments: Identifying sources and ecological hazard. *Integrated Environmental Assessment and Management* 1, 22–33.

Nisbet, I.C., LaGoy, P.K., 1992. Toxic equivalency factors (TEFs) for polycyclic aromatic hydrocarbons (PAHs). *Regulatory Toxicology and Pharmacology* 16, 290–300.

NMFS (National Marine Fisheries Service), 2007. Eastern Oyster Biological Review Team Status Review of the Eastern Oyster (Crassostrea Virginica) : NOAA Tech. Memo. NMFS F/SPO-88. Report to the National Marine Fisheries Service, Northeast Regional Office 105 February 16, 2007

NMFS (National Marine Fisheries Service), 2015. Annual Commercial LandIng Statistics. NOAA, Silver Spring, MD www.st.nmfs.noaa.gov/commercial-fisheries/commercial-landings/annual-landings/index. Viewed 20 Dec 2021.

Nordin, N., Yusof, N.A., Abdullah, J., Radu, S., Hushiarian, R., 2017. A simple, portable, electrochemical biosensor to screen shellfish for vibrio parahaemolyticus. *Amb Express* 7, 1–9.

Nowell, L.H., Moran, P.W., Gilliom, R.J., Calhoun, D.L., Ingersoll, C.G., Kemble, N.E., Kuivila, K.M., Phillips, P.J., 2013. Contaminants in stream sediments from seven United States metropolitan areas: part I: Distribution in relation to urbanization. *Archives of Environmental Contamination and Toxicology* 64, 32–51.

Plaza-Bolaños, P., Frenich, A.G., Vidal, JLM., 2010. Polycyclic aromatic hydrocarbons in food and beverages. Analytical methods and trends. *Journal of Chromatography A* 1217, 6303–6326.

Spier, C.S., Unger, M.S., Kaattari, S.L., 2012. Antibody-based biosensors for small environmental pollutants: Focusing on PAHs. In: Preedy, V.R., Patel, V.B. (Eds.), Biosensors and Environmental Health. CRC Press, Boca Raton, FL, pp. 273–295.

Spier, C.R., Vadas, G.G., Kaattari, S.L., Unger, M.A., 2011. Near real-time, on-site, quantitative analysis of PAHs in the aqueous environment using an antibody-based biosensor. *Environmental Toxicology and Chemistry* 30, 1557–1563.

Tian, Y., Du, L., Zhu, P., Chen, Y., Chen, W., Wu, C., Wang, P., 2021. Recent progress in micro/nano biosensors for shellfish toxin detection. *Biosensors and Bioelectronics* 176, 112899.

Unger, M.A., Harvey, E., Vadas, G.G., Vecchione, M., 2008. Persistent pollutants in nine species of deep-sea cephalopods. *Marine Pollution Bulletin* 56, 1498–1500.

US Congress, Office of Technology Assessment, 1991. Complex Cleanup: The Environmental Legacy of Nuclear Weapons Production, OTA-O-484. U.S. Government Printing Office, Washington, DC.

US Food and Drug Administration (FDA), 2010. Protocol for Interpretation and Use of Sensory Testing and Analytical Chemistry Results for Re-Opening Oil-Impacted Areas Closed to Seafood Harvesting Due to the Deepwater Horizon Oil Spill : Technical Report . 2010 US Food and Drug Administration Washington, DC

Van Metre, P.C., Mahler, B.J., Furlong, E.T., 2000. Urban sprawl leaves its PAH signature. *Environmental Science and Technology* 34, 4064–4070.

VDH (Virginia Department of Health), 2012. Health Consultation: Consumption Advisory Guidelines for Oysters Contaminated with Polycyclic Aromatic Hydrocarbons for the Lafayette River: Technical Report. Virginia Department of Health Richmond, Virginia, USA

Vrana, B., Allan, I.J., Greenwood, R., Mills, G.A., Dominiak, E., Svensson, K., Knutsson, J., Morrison, G. 2005. Passive sampling techniques for monitoring pollutants in water. *Trends in Analytical Chemistry* 24, 845–868.

Wade, T.L., Sericano, J., Gardinali, P.R., Wolff, G., Chambers, L., 1998. NOAA's 'Mussel Watch' project: Current use organic compounds in bivalves. *Marine Pollution Bulletin* 37, 20–26.

Walker, S.E., Dickhut, R.M., Chisholm-Brause, C., Sylva, S., Reddy, C.M., 2005. Molecular and isotropic identification of PAH sources in a highly industrialized urban estuary. *Organic Geochemistry* 36, 619–632.

Wise, S.A., Sander, L.C., Schantz, M.M., 2015. Analytical methods for determination of polycyclic aromatic hydrocarbons (PAHs) — A historical perspective on the 16 U.S. EPA priority pollutant PAHs. *Polycyclic Aromatic Compounds* 35, 187–247.

Wolfe, D.A., Long, E.R., Thursby, G.B., 1996. Sediment toxicity in the hudson-raritan estuary: Distribution and correlations with chemical contamination. *Estuaries* 19, 901–912.

Xia, K., Hagood, G., Childers, C., Atkins, J., Rogers, B., Ware, L., Armburst, K., Jewell, J., Diaz, D., Gatian, N., Folmer, H., 2012. Polycyclic aromatic hydrocarbons (PAHs) in Mississippi seafood from areas affected by the Deepwater Horizon oil spill. *Environmental Science and Technology* 46, 5310–5318.

Yender R. Michel J. Lord C, 2002. Managing Seafood Safety after an Oil Spill : Technical Report. National Oceanic and Atmospheric Administration, Office of Response and Restoration, Hazardous Materials Response Division Seattle, WA, USA

Zelinkova, Z., Wenzl, T., 2015. The occurrence of 16 EPA PAHs in food–a review. *Polycyclic Aromatic Compounds* 35, 248–284.

Zhang, W., Liu, Q., Guo, Z.H., Lin, J.S., 2018. Practical application of aptamer-based biosensors in detection of low molecular weight pollutants in water sources. *Molecules* 23, 344.

Figures

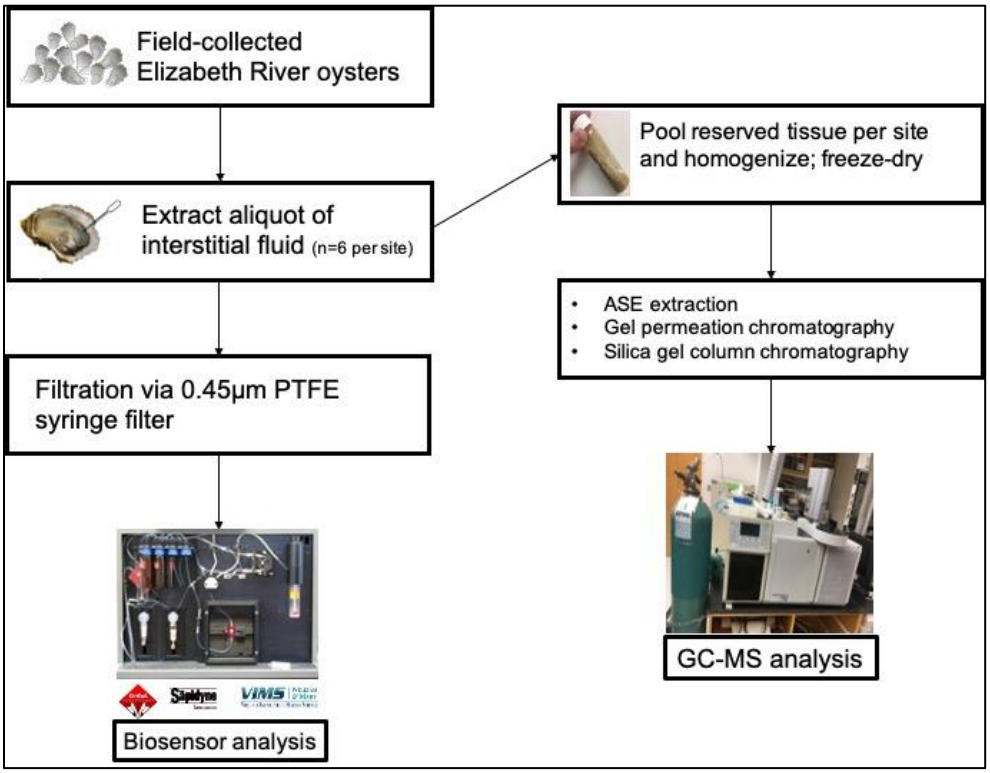

Figure 1. Schematic of study design

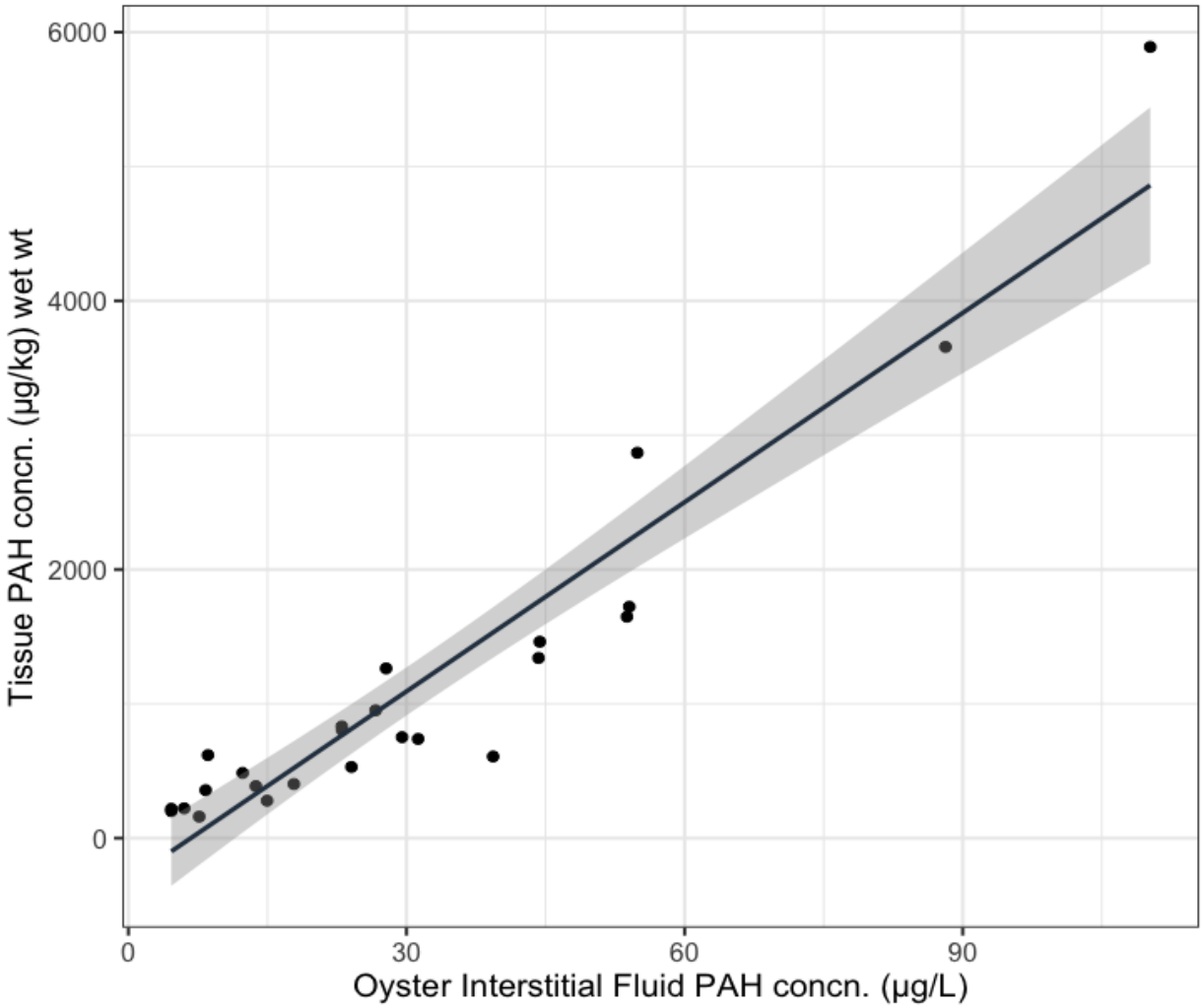

Figure 2. PAH levels in oyster soft tissues in relation to interstitial fluids. Linear regression comparing mean oyster interstitial fluid PAH concentration (n=6) to pooled, composite tissue samples of the same oysters (64 PAH analytes; y=47.0 x-316.0; R^2 = 0.88; df=23). Gray band denotes 95% confidence interval around regression.

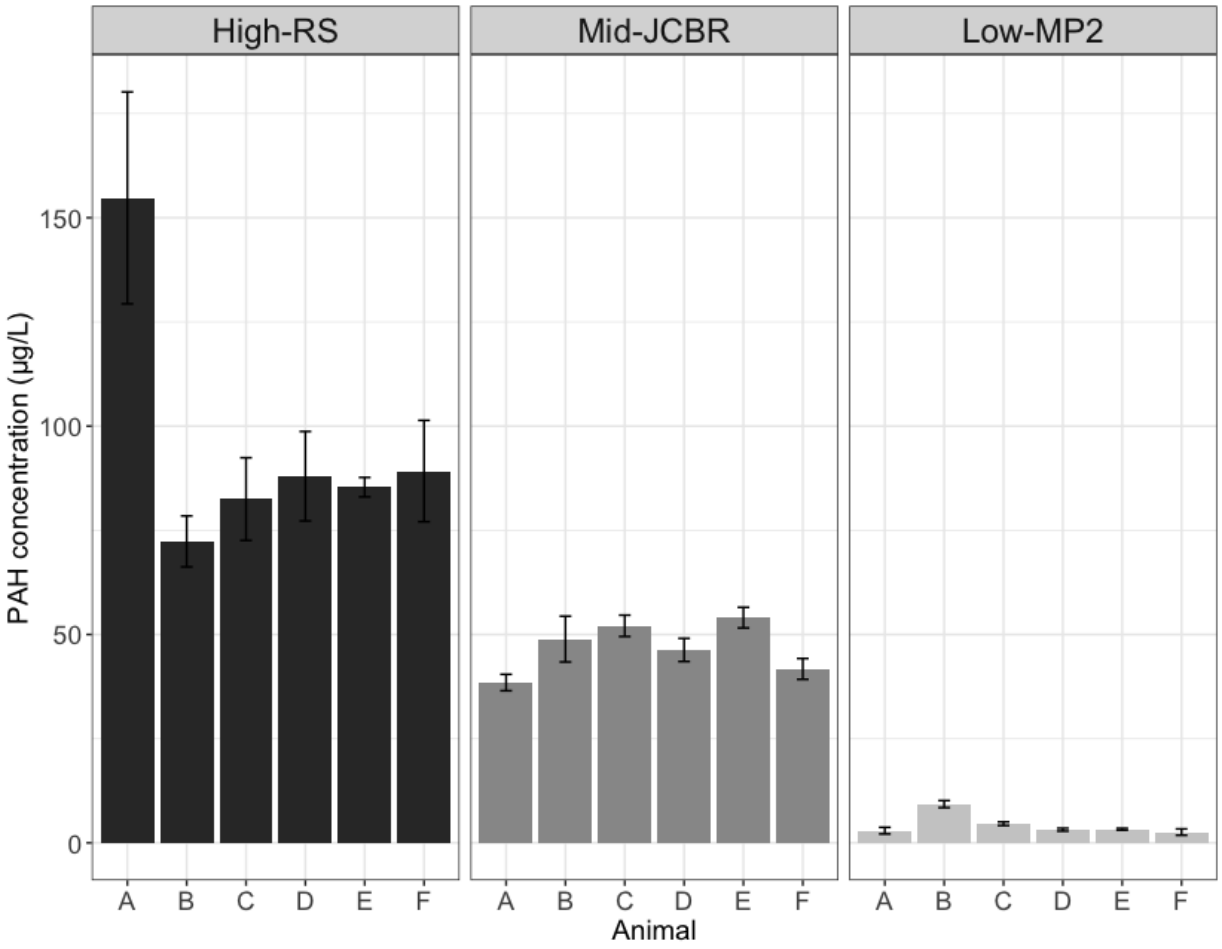

Figure 3. Analytical replication of interstitial fluids from 6 individual oysters at sites with high-, mid-, and low ranging PAH concentrations using the biosensor method. Triplicate aliquots of interstitial fluid per oyster (A-F) at each site were measured; mean concentrations for each animal are reported. Error bars depict standard deviations.

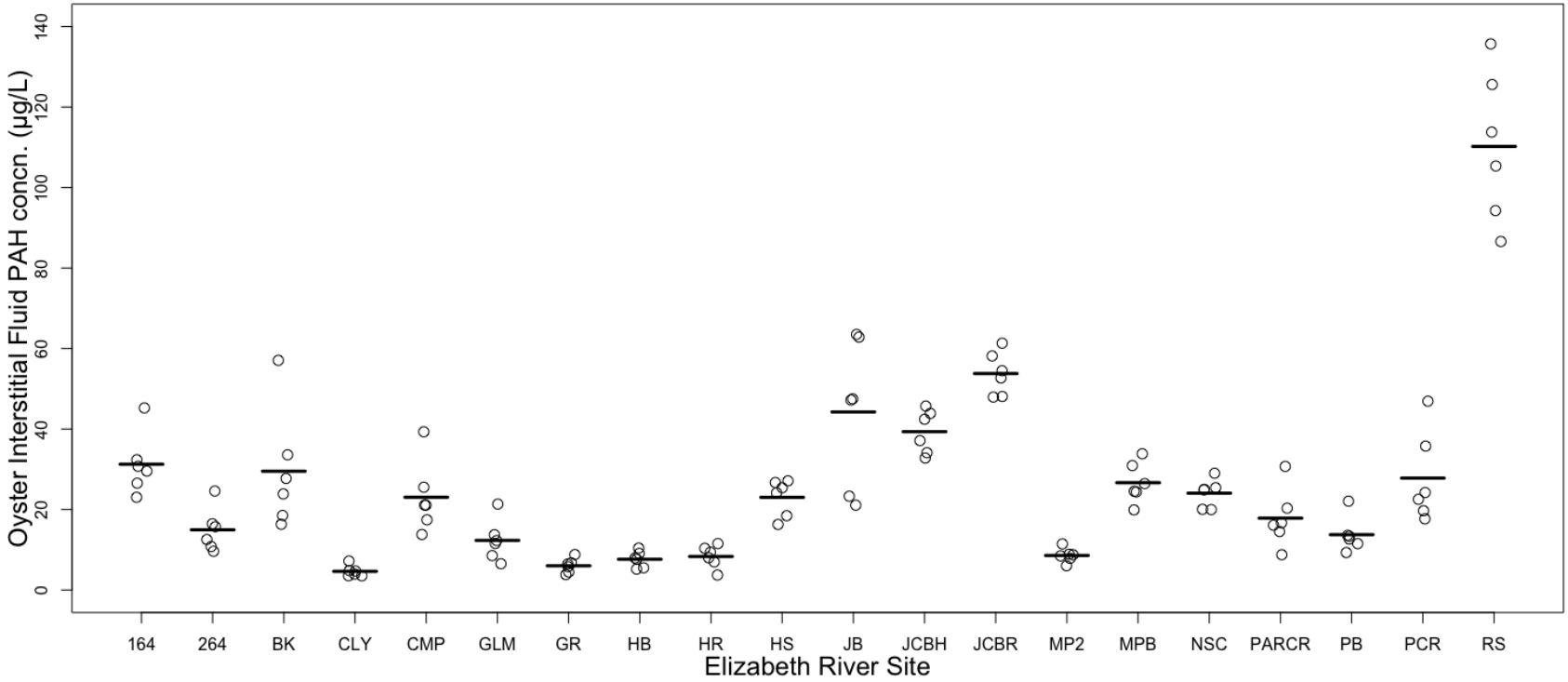

Figure 4. Measurements of PAH concentrations among individual oysters at each site using the biosensor method (n=6 per site). Line indicates mean for each site.

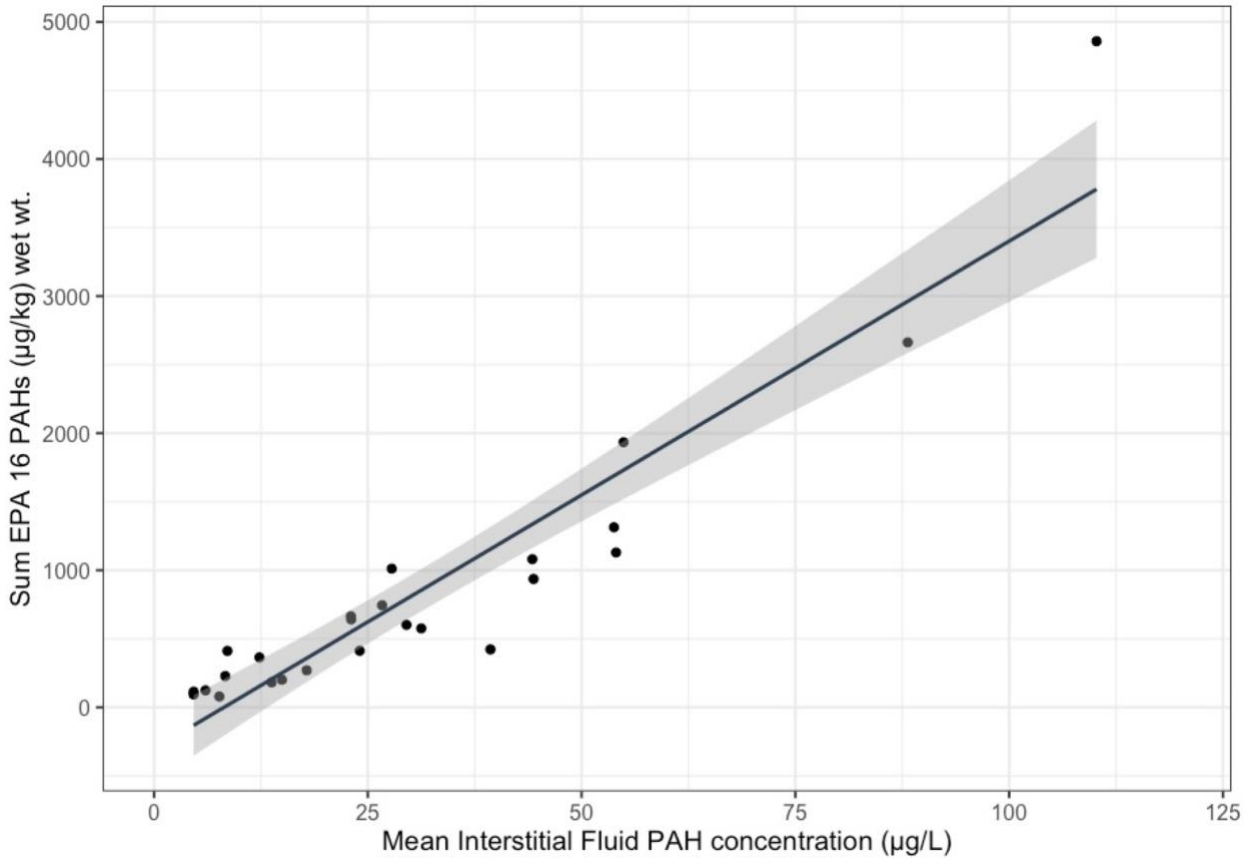

Figure 5. Combined data for PAH analytes (sum EPA 16 PAHs) in oyster soft tissues in relation to mean PAH levels in interstitial fluids. Linear regression comparing mean oyster interstitial fluid PAH concentration (n=6) to pooled, composite tissue sample

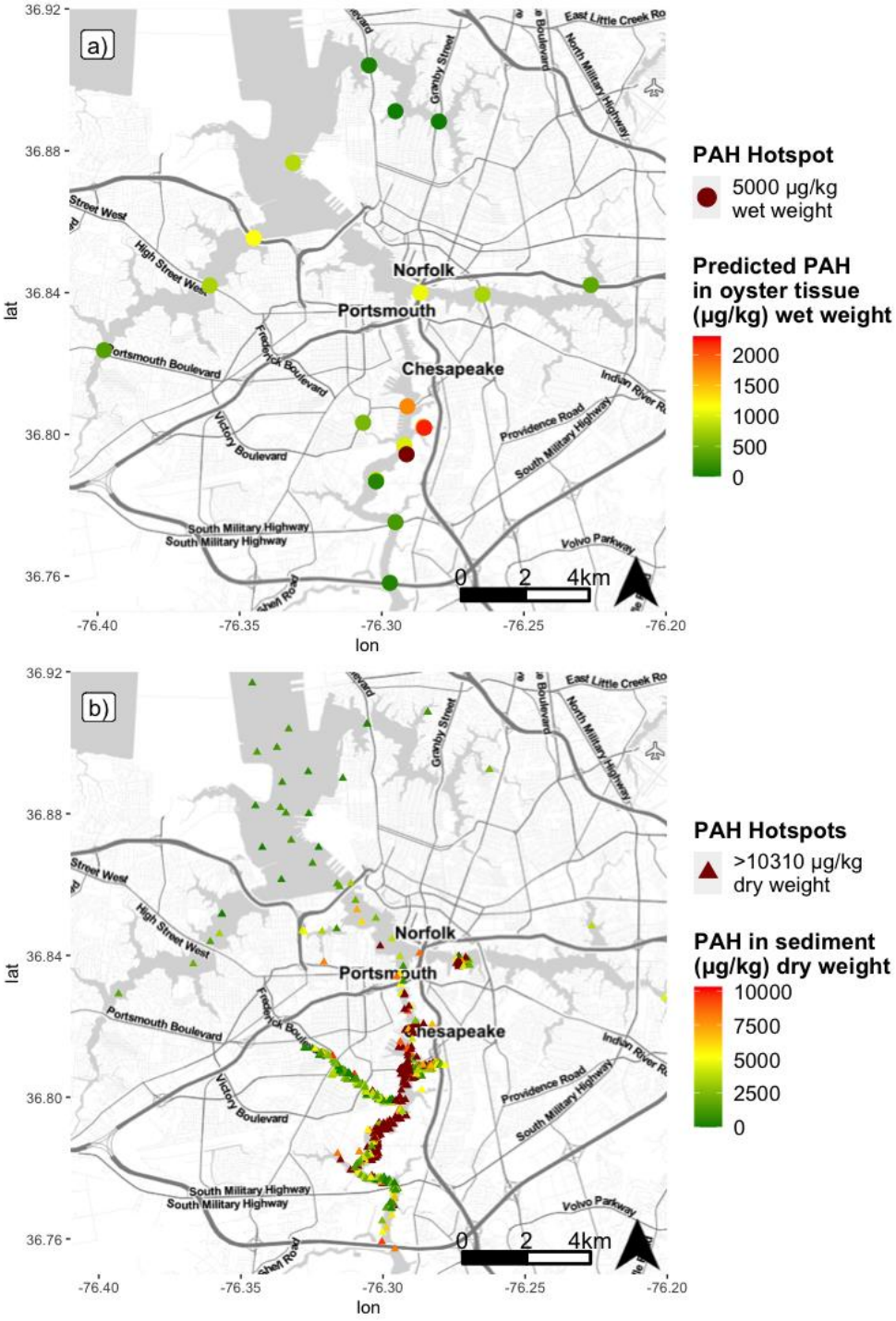

Figure 6. Comparison of **a)** mapped predicted oyster tissue concentrations based on regression from present study to **b)** mapped historic datasets on total PAH concentration in sediment from 1985 to 2012 (DIVER 2020). Similar concentration trends and PAH hotspots throughout the watershed are observed across both maps. Concentrations below detection limit were treated as zero for mapping clarity. Note change in scale between maps due to higher concentrations typically observed in sediment.

Tables

Table 1. Evaluation of risk assessment accuracy under EU regulation based on predicted individual oyster tissue concentrations at Elizabeth River sites.

SITE ID	Predicted individual oyster concn.[a]						Measured PAH4 concn.[a]	Measured 64 PAHs concn.[a]	Prediction accuracy
	A	B	C	D	E	F			
MP2	U	U	U	U	U	U	168.7	618.3	0%
JRWS	U	U	U	U	U	U	23.6[b]	201.8	100%
PARCR	74.9	108.9	331.0	U	166.8	99.9	98.3	402.8	83%
JCBH	363.9	432.6	568.2	539.5	384.8	516.5	162.1	607.9	100%
JCBR	603.6	707.2	765.3	815.5	678.8	606.0	443.5	1648.6	100%
RS	1992.0	1645.4	1215.2	1512.0	1336.7	1832.2	1883.6	5889.7	100%
GR	U	U	U	U	U	U	33.2	221.9	0%
CLY	U	U	U	U	U	U	33.7	219.0	0%
HB	U	U	U	U	U	9.9	19.1[b]	160.1	100%
HR	27.6	U	U	U	U	9.11	79.0	357.4	17%
PB	60.0	U	56.4	45.5	194.4	27.3	41.6	387.2	83%
GLM	39.5	28.1	62.4	U	183.0	U	126.2	485.8	67%
264	105.4	234.2	94.1	43.8	U	16.1	49.2	279.0	67%
HS	102.9	267.8	274.2	247.2	227.1	137.1	168.5	831.4	100%
NSC	304.1	162.4	241.0	247.4	161.3	238.7	106.7	530.1	100%
CMP	467.1	178.9	249.3	121.1	63.4	179.2	183.5	804.9	100%
BK	283.7	103.6	138.2	748.1	222.8	376.6	204.6	751.8	100%
MPB	380.7	263.5	334.4	160.0	233.1	230.7	285.1	951.4	100%
PCR	201.8	587.5	410.9	228.4	124.9	156.7	380.4	1263.8	100%
164	265.1	331.5	312.5	209.7	560.9	357.3	230.7	738.7	100%
JB	592.1	596.5	839.2	214.0	178.7	850.1	512.1	1341.1	100%

U=below range of regression model (Figure S1)

[a] µg/kg wet wt

[b] below EU regulatory limit

Table 2. Evaluation of risk assessment accuracy under VDH multi-tier advisory based on predicted individual oyster tissue concentrations at Elizabeth River sites.

SITE ID	Predicted individual oyster concn.[a]						Measured 15B*a*PE concn.[a]	Advisory tier[b]	Prediction accuracy
	A	B	C	D	E	F			
MP2	U	11.7	4.8	3.4	5.5	5.8	65.3	3	0%
JRWS	2.3	U	1.2	U	U	U	16.2	1	100%
PARCR	18.7	23.7	56.0	5.5	32.1	22.4	20.2	1	67%
JCBH	60.7	70.7	90.4	86.3	63.8	82.9	40.6	2	0%
JCBR	95.6	110.7	119.1	126.4	106.5	95.9	54.3	3	33%
RS	297.4	247.0	184.5	227.7	202.2	274.2	323.0	4	100%
GR	U	U	U	0.8	0.2	5.6	3.8	1	100%
CLY	U	U	U	1.9	U	U	4.5	1	100%
HB	U	6.2	2.9	3.6	U	9.3	2.2	1	100%
HR	11.8	6.9	1.4	U	3.7	9.2	11.5	1	100%
PB	16.6	6.7	16.0	14.4	36.1	11.8	5.3	1	83%
GLM	13.6	11.9	16.9	0.3	34.4	5.0	23.4	1	83%
264	23.2	41.9	21.5	14.2	7.5	10.2	3.7	1	83%
HS	22.8	46.8	47.7	43.8	40.9	27.8	102.0	4	0%
NSC	52.1	31.4	42.9	43.8	31.3	42.5	26.4	2	83%
CMP	75.7	33.8	44.1	25.4	17.0	33.9	56.1	3	17%
BK	49.1	22.9	27.9	116.6	40.2	62.6	30.4	2	50%
MPB	63.2	46.1	56.4	31.1	41.7	41.4	52.3	3	33%
PCR	37.2	93.2	67.6	41.0	26.0	30.6	48.5	2	67%
164	46.4	56.0	53.3	38.3	89.4	59.8	27.8	2	0%
JB	93.9	94.6	129.8	38.9	33.8	131.4	65.6	3	33%

U= below range of regression model (Figure S2)

[a] µg/kg wet wt

[b] Tier allocations: Tier 1: less than 25 µg/kg –no advisory; Tier 2: 25-50 µg/kg –two meals per month; Tier 3: 50-100 µg/kg –one meal per month; Tier 4: greater than 100 µg/kg –do not eat oysters from advisory area.

Chapter 2: Evaluating Antibody-Based Biosensor Technology as a Rapid PAH Screening Tool for Seafood in Oil Spill Response

Introduction

Global reliance on petroleum and refined petroleum products makes the possibility of oil spills an important ongoing concern. Crude oil is a complex mixture comprised primarily of aliphatic and aromatic hydrocarbons, resins and asphaltenes, as well as trace amounts of heterocyclic compounds containing nitrogen, oxygen, or sulfur and other metals. Polycyclic aromatic hydrocarbons (PAHs) are a key class of crude oil constituents that comprise a large fraction of crude oil and contribute to its toxicity (McGrath and DiToro 2009). Therefore, measuring PAHs in the bioavailable, or dissolved form, at oil-impacted sites is important for evaluating potential risk. Analytical techniques such as gas chromatography coupled with mass spectrometry (GC–MS) can provide reliable quantitative compound-specific concentration measurements and contribute to a robust characterization of an impacted site. However, given the time and expense required for analysis and number of samples often required for site characterization, this technique is not suitable for rapid screening (Christensen and Tomasi, 2007; Mauseth and Challenger 2001; Mastovska et al. 2015; Zhang et al. 2018; Felemban et al. 2019).

As sessile, benthic filter-feeding fauna with a limited ability to metabolize PAHs (James, 1989), oysters, such as *Crassostrea virginica* readily accumulate PAHs in tissues. In fact, PAH levels observed in bivalves are among the highest observed in all food products (EFSA, 2008). Following a PAH contamination event, such as an oil spill, exposure via consumption of commercially important shellfish can pose a significant public health threat. With *C. virginica* commercial fishery landings garnering over $140 million in the United States alone (NMFS, 2015), the potential loss in economic livelihood due to a PAH contamination event can be substantial. Therefore, given such economic considerations, a critical management decision

following an oil spill is determining the threshold at which shellfish tissue concentrations are acceptable to reopen the fishery or aquaculture production to harvest.

Several seafood screening techniques exist to prioritize samples for further GC–MS analysis. Sensory analysis has been used following major spills including the Deepwater Horizon incident in 2010 (US Food and Drug Administration, 2010; Moller 1999). Sensory analysis is conducted by a panel of specialists trained to detect tainting of seafood by oil or oil products. The results of such tests indicate whether the presence of an altered seafood odor or taste has been detected. Although there is some evidence that a correlative relationship between taint and petroleum concentration may exist, specific compounds have yet to be attributed to seafood taint and thresholds may be related to specific species, oil type, or other unknown factors (Yender 2002). Additionally, this test may provide unreliable results depending on the sensitivity and experience of the sensory panel and factors unrelated to oil contamination (e.g. fecal odor and putrefaction) can adulterate the sample (Mauseth and Challenger, 2001). Furthermore, sensory analysis cannot provide quantitative data on the overall concentration of toxic compounds, such as PAHs. Another rapid screening technique currently available is high performance liquid chromatography coupled with UV fluorescence detection (HPLC–FLD). This approach uses a more streamlined sample processing protocol than GC-MS; thereby improving sample throughput, but the results provided by HPLC–FLD are semi-quantitative estimates of concentrations. Thus, the sensitivity and accuracy of this analysis is also limited (Plaza-Bolanos et al. 2010, Yender, 2002). In addition, sample processing requires multiple steps including solvent extraction which limits its utility in remote settings since laboratory availability and specialized expertise are necessary (Yender, 2002; Gratz et al. 2011). Therefore, the need for improved, rapid, on-site screening analyses for biota is imperative to facilitate timely response

and risk characterization as well as to reduce time and cost required for long-term monitoring of residual oil contamination.

Monoclonal antibody-based immunoassays have proven to be valuable analytical screening tools for environmental monitoring of contaminants, including PAHs (EPA 1996a; EPA 1996b; Plaza et al. 2000; Baeumner 2003; Spier et al. 2012; Wang et al. 2014; Justino et al. 2017; Behera et al. 2018; da Costa Filho et al. 2022). A rapid, near real-time PAH quantitation method using a KinExA Inline Biosensor (Sapidyne Instruments, Boise, ID, USA) coupled with a murine anti-PAH monoclonal antibody, 2G8, has been previously demonstrated to have uniform selectivity for parent and alkylated PAH compounds in the 3- to 5-ring range (Li et al. 2016). The biosensor method has been used to directly analyze PAHs in porewater samples (i.e. minimal sample preparation required) from Chesapeake Bay tributaries and the Houston Ship Channel and has shown strong correlation with PAH concentrations determined via GC–MS and passive sampling (Hartzell et al., 2017, Conder et al., 2021, Camargo et al., 2022). The biosensor coupled with mAb 2G8 has also been employed to measure PAH concentrations in oyster (*C. virginica*) interstitial fluid samples, which had a strong positive association with GC–MS-derived PAH concentrations in tissue (Prossner et al. 2022). In that study, oysters were collected from the Elizabeth River, a system in which legacy creosote contamination is a major source of PAH contamination (DiGiulio and Clark 2015). Their findings suggested it was reasonable to assume steady-state conditions between internal interstitial fluid and tissue concentrations. Through a novel extension of the equilibrium partitioning theory, Prossner et al. (2022) demonstrated that PAH concentrations measured via biosensor in oyster interstitial fluid could be used to predict tissue concentrations for rapid human health risk assessment of PAH contaminated oysters and cost-effective field tissue monitoring.

The objective of our study was to further explore the relationship between PAH concentrations measured in *C. virginica* interstitial fluid using the rapid biosensor method with PAH concentrations in tissues measured using conventional GC-MS analysis. This was accomplished by performing a controlled laboratory oyster bioconcentration test involving both uptake and depuration phases. This test was performed twice using two crude oils containing different PAH compositions. By exposing oysters to water accommodated fractions (WAFs) prepared at different oil loadings of each crude oil, this design allowed both the PAH concentration and composition in oyster tissues to be varied and analyzed over time. Based on the oysters collected during the bioconcentration tests, we then evaluated the role of this biosensor technology in screening seafood in in spill response scenarios in which steady state may not be assumed.

Materials and Methods

Test Oils

The two oils investigated in this study, Quintana Hoops crude oil blend and heavy fuel oil (HFO) were provided by ExxonMobil Biomedical Sciences, Inc. Total PAH concentrations of each oil were 10,026 and 145,292 mg/kg, respectively with the individual PAH composition provided in Table S1 and relative percentages of 2, 3 and >4–ring aromatic compounds compared in Figure S1. This figure indicates that the HFO is enriched in heavier PAHs compared to the crude oil.

Experimental design and WAF generation

The experimental set-up was identical for the bioconcentration studies for the two test oils. Oysters were acutely exposed to oil WAFs and allowed to depurate to evaluate the ability of the biosensor to predict tissue concentrations in the kinetic regime. The experiment was designed

to simulate a short-term environmental exposure to an oil spill in a controlled laboratory setting. The dosing system consisted of a hybrid flow-through system in which WAF (generated in a closed system via water recirculation through an oil-loaded generator column, described below) was pumped from the dosing water reservoir to the mixing aquarium in which oil-dosed water and clean unfiltered York River water were mixed at a 1:1 ratio and delivered to the treatment tank. Approximately 5 test aquarium volume exchanges occurred per 24-hour period. The purpose of mixing was to recreate realistic settings and ensure oysters would receive food as supplementary food was not provided. The flow-through set-up for the control oysters was identical with the exclusion of WAF delivery to the tank. Figure 1 depicts a schematic of the experimental set-up. Oysters were exposed to WAF for 3 days. On the third day, flow from the WAF dosing reservoir was stopped and residual water was siphoned out of the test aquarium. Tanks were refilled with clean, unfiltered York River water and volume exchange with fresh unfiltered water proceeded as previously described. The dosing reservoir and all tanks were covered to minimize loss of volatile hydrocarbons during WAF generation.

WAFs were prepared as follows: 40mL of Quintana Hoops oil blend was loaded onto ignited filter sand in a 10 x 70 cm generator column. York River water was passed through a bag filter to remove particulate matter and recirculated for approximately 10-12 days through the sand column and 310 L dosing water reservoir until steady state was achieved, as monitored by near real-time biosensor analysis of water samples as described below (Figure S1). The procedure for WAF generation for the second experiment was identical; however, 40 mL of heavy fuel oil (HFO) was loaded in the generator column. Bag-filtered York River water recirculated through the column for approximately 12 days. Again, the biosensor was used to monitor concentrations to determine steady state (Figure S2).

Oyster acquisition and husbandry

Adult cultured oysters were purchased from a local oyster farm on the York River in Gloucester County, VA. Oysters were transported to the laboratory (~10km away) in a cooler and kept cool with gel ice packs. Immediately upon arrival, oysters were scrubbed clean and shell height (bill edge to umbo) was measured by caliper prior to transfer to clean aquaria filled with unfiltered York River water. The oysters were acclimated to laboratory conditions for approximately 7 days prior to experimentation. Oysters were spread evenly along the bottom of each tank and unnecessary disturbance was avoided during sampling. Supplemental food was not provided; however, unfiltered river water was used to supply natural sources of food to oysters and allow for more realistic environmental conditions in the laboratory study. No mortalities were observed in the Hoops oil bioconcentration experiment or preceding acclimation period. During the HFO experiment, two mortalities occurred during the acclimation period, one control oyster and one treatment oyster; however, no mortalities were observed during the bioconcentration test. For each bioconcentration test, additional oysters were held in the aquaria during the acclimation period. At the start of the exposure, any additional oysters were removed so that a total of 30 oysters were held in both the treatment and control tanks. Water quality parameters including temperature, salinity, pH, dissolved oxygen, and ammonia were monitored throughout each experiment in both the control and treatment tank and maintained at appropriate levels as per ASTM Standard Guide E1022-94 (ASTM International 1994) using a commercial aquarium test kit, refractometer (for salinity), and digital aquarium tank thermometer. No significant deviations in water quality thresholds were observed between experiments or throughout respective experiments (Supplementary Tables S2-S4).

Sample collection

For sampling oil-dosed water from the generator column effluent, dosing reservoir, and test aquaria, aliquots of 10-15 mL water were collected in 20 mL glass screw-top scintillation vials and refrigerated at 4°C until analysis. On the day of analysis, samples were filtered through a 0.45 µm PTFE syringe filter. During uptake, water samples were collected twice a day. During depuration, water samples were collected once a day. For tissue sampling, oysters were carefully retrieved from the tank using stainless steel tongs and disturbance of other test animals was avoided. Whole oysters (i.e. in-shell) were placed in plastic bags and immediately frozen at -20°C until further sample collection. During uptake, oysters were collected once a day. During depuration, oysters were collected every other day. Both treatment and control samples were collected throughout the experiment. Measurements at time 0 (or hour 0) indicate background PAH concentrations measured in oysters prior to start of the experiment. The first sampling of experimental oysters occurred a few hours after the start of the exposure once the treatment tank was filled with WAF of each respective test oil. Prior to biosensor analysis, oysters were thawed, opened with a knife, and an aliquot of pooled fluid encompassing the soft tissue in the individual oyster (i.e. oyster interstitial fluid, per Prossner et al. 2022) was collected using a disposable glass Pasteur pipet. Fluid was collected from 3 individual oysters per sample period. The aliquot of individual oyster interstitial fluid was then transferred to a 20mL glass scintillation vial for a final sample volume of ~5mLs, filtered through a 0.45 µm PTFE syringe filter, and then frozen at -20°C until analysis.

Following interstitial fluid sample collection, soft tissues from individual oysters were retained for GC–MS in glass screw-top jars and frozen at -20°C until further processing. Soft tissues from the three oysters per sample period was pooled, homogenized, and then transferred

to glass screw-top jars and stored frozen at -20°C until overnight shipment of samples to the external lab conducting GC-MS analysis of the oyster tissues.

Biosensor analysis

The procedures for biosensor analysis of PAH concentrations in water samples and oyster interstitial fluid (Conder et al. 2021, Hartzell et al. 2018, Camargo et al. 2022, Spier et al. 2011, Prossner et al. 2022) as well as selection and screening procedure of mAb 2G8 (Li et al. 2016) have been described previously. The murine monoclonal antibody, mAb 2G8, has a uniformly strong affinity for 3-5 ring PAHs, including methylated compounds, measured in aqueous environmental samples with excellent correlation to GC–MS measurements (Li et al., 2016). There is some evidence that mAb 2G8 will bind with lower affinity to 2-ring aromatic hydrocarbons, particularly alkylated compounds (Conder et al. 2021); therefore, the total PAH concentration measured by the biosensor may include a fraction of 2-ring aromatic compounds if present in high concentrations. The KinExA Inline Sensor (Sapidyne Instruments, Boise, ID) uses programmable fluidics to provide precise quantitative measurement of antibody binding for up to eight samples in a cycle. A fluorescent tag, AlexaFluor 647 (Invitrogen), was covalently bound to mAb 2G8 and the signal response (dV) of the fluorescently tagged antibody was measured by the KinExA detector. The KinExA Inline Sensor functions as a kinetic assay: the antibody is mixed with an aqueous sample and binds to free PAH, then the sample-antibody mixture is washed over stationary polymethyl methacrylate (PMMA) beads coated in antigen (1-pyrenebutyric acid, CAS no. 3443-45-6) conjugated to bovine serum albumin (BSA) located in the detector flow cell. Any free mAb 2G8 that did not bind to dissolved PAH in aqueous sample will bind to the antigen-coated beads and the resulting fluorescent signal then measured. Thus, the detected signal response is inversely proportional to the level of total PAH in a sample. The

automated sample handling cycle takes up to ten minutes to measure signal response in a sample and includes time for mixing with the antibody, cleaning of the flow cell, and replacement with a fresh set of antigen-coated beads for the next sample. At the start of a new day of operating the instrument and prior to sample analysis, a six-point calibration curve was generated using a laboratory blank, double deionized water (ddH2O), and a series of phenanthrene standards in ddH2O ranging from 0.5 to 2.5 µg/L to determine the linear range for the dV response from the instrument via log-linear regression analysis. Once calibrated, samples were diluted accordingly with ddH2O to fall within the standard range and the PAH concentration was then quantified based on measured signal response and required dilution factor. Concentrations are reported in µg/L (ppb).

The detection limit for PAH analysis of oyster interstitial fluid by biosensor is reported to be 0.39 µg/L, as determined in Prossner et al. (2022). Signal responses detected outside the lower end of the calibration range (i.e. below the lowest phenanthrene standard, 0.5µg/L) are reported as below the biosensor detection limit. All measurements of oyster interstitial fluid were well-above the reported detection limit, for both treatment and control oysters. The lowest oyster interstitial fluid concentration was measured in a control oyster at 1.11 µg/L.

To assess the accuracy of the method for screening tissue concentrations in non-steady state conditions, oyster interstitial fluid concentrations measured by the biosensor were used to predict tissue concentrations based on the linear regression model reported in Prossner et al. (2022). Briefly, the linear model, $y=47.0x-316.0$ ($R^2=0.88$, df =23), was developed to explain the relationship between biosensor-measured oyster interstitial fluid concentrations and GC–MS-measured tissue concentrations using Elizabeth River field oysters at steady-state.

GC–MS analysis

GC–MS analysis of the oyster tissue and total extractable lipid analysis was conducted by a third-party lab following a standard procedure. Surrogate PAH standards used for analysis included d8-napthalene, d10-phenanthrene, and d12-benzo [a] pyrene. A total of 75 analytes were examined, including parent and alkylated compounds. Results are reported in µg/kg wet weight. Lipid content is reported as percent (%) lipid.

Results and Discussion

Near real-time biosensor monitoring of PAH concentrations over time

Based on biosensor results, the steady state 3-5 ring PAH concentrations following dilution with York River water for Hoops and HFO was estimated to be 2.5 and 15 µg/L in treatment aquaria containing oysters, respectively. For both experiments, the water concentrations measured by the biosensor demonstrated that oysters received a near-constant WAF dose throughout the 3-day uptake period for both the Hoops and HFO experiments (Figure 2). Upon transition to depuration, measured concentrations immediately drop to low or below detection levels.

Biosensor measurement of individual oysters throughout each experiment showed a rapid uptake of PAH in the oyster interstitial fluid, with a final concentration on the last day of uptake that was approximately 10x higher than the estimated total concentrations to which oysters were exposed in test aquaria (Figure 3). Upon transition to depuration during the lower dose Hoops oil experiment, oyster interstitial fluid concentrations decreased to near the detection limit signifying PAH elimination from the oyster. During the depuration period of the higher dose HFO experiment, oyster interstitial fluid concentrations decreased more gradually. By the end of depuration for each experiment, final oyster interstitial fluid concentrations were similar to

concentrations measured at time zero (T0). For both experiments, PAH concentrations were measurable at T0 due to the ubiquity of PAHs in the environment and possible exposure to low ambient concentrations present in York River water used in the experiments. For monitoring of oyster interstitial fluid in near-real time, the biosensor demonstrated its potential value to work over a spatiotemporal scale to quantitatively screen important biota and prioritize samples for additional chemical analysis if needed. Future replications of this study could be enhanced by non-lethal repeated sampling of hemolymph from individual oysters throughout the experiment to further assess individual uptake and depuration kinetics, thereby reducing the potential contribution of inter-organismal variability. Linear regressions comparing biosensor measurements of estimated 3-5 ring PAH concentrations in oyster interstitial fluid to GC–MS-measured tissue concentrations (for all analytes and for the 3-5 ring subset) for each experiment are included in Supplementary Information (Figures S4 and S5).

Comparison of PAH composition measured in oyster tissue

Compound-specific GC–MS data revealed that the composition of PAHs accumulated in oyster tissue between the Hoops oil and HFO test exposures were different (Figure 4). Oysters exposed to Hoops oil accumulated predominately lower molecular weight (2– and 3–ring) PAHs. Nonetheless, oysters in the HFO exposure accumulated a greater concentration of 4–ring PAHs but accumulated lower total concentrations of PAH. The enrichment of lower molecular weight compounds accumulated in oysters exposed to Hoops oil is reflective of the PAH profile of the oil type, Quintana Hoops blend, used to generate the WAF. In contrast, the HFO was enriched in higher molecular weight PAHs relative to Quintana Hoops blend. Although discussed in more detail in the next section, the lower overall tissue concentrations measured in the high dose

exposure suggest that steady-state was not achieved during the 3-day uptake phase for higher molecular weight compounds.

Comparison of biosensor-predicted v. GC–MS-measured tissue concentrations

Biosensor concentrations measured in the oyster interstitial fluid were used to predict tissue concentrations based on the linear regression equation and partition coefficient reported in Prossner et al. 2022 (Figure 5). Considering the 3-5 ring affinity of mAb 2G8 employed in this biosensor analysis, both the total PAH concentrations of PAH (75 analytes) and the total concentrations of 3-5 ring PAH were examined. For the Hoops oil experiment, when the total concentration of 3-5 ring PAH analytes were compared to biosensor-predicted concentrations, estimated concentrations closely followed the measured concentrations during uptake. This finding is corroborated in the regression analysis (Figure 6A). However, during depuration, the association is lost, as confirmed in the regression analysis of depuration concentrations (Figure 6B). During the 12-day depuration period, measured PAH concentrations in the tissue remained significantly higher than our model-derived estimations. Additionally, total PAH concentration in the tissue on the final day of the experiment was still significantly elevated relative to what was measured in the tissue at T0. This deviation in observed trends for the Hoops experiment could be attributed to a few possible explanations. First, tissue concentrations were predicted based on a model that was developed using oyster data collected from a natural system, the Elizabeth River (Virginia, USA) (Prossner et al. 2022), in which legacy pollution due to historic creosote contamination is an important source of PAH to exposed oysters (DiGiulio and Clark 2015). With known differences in PAH composition in pyrogenic relative to petrogenic sources (Abdel-Shafy and Mansour 2016), predicting oyster tissue concentrations based on a model developed from a different system with a differing composition of PAH may be a limitation to

the present study; however, at present, it is the only model available to relate PAH concentrations in the oyster aqueous phase to the tissue phase. In evaluating the utilization of biosensor technology to predict tissue concentration for rapid, low-cost screening of oil-impacted sites, more work is needed to develop a model based off crude oil WAF exposure and compare determined partition coefficients as oyster internal partitioning models may be source-specific. Another important consideration for the deviation in trends observed is that differing kinetic rates of specific organs (e.g. gill relative to. hepatopancreas) from which PAHs are being released may contribute to elevated concentrations retained in the tissues (Widdows et al. 1983; Bustamante et al. 2012). More work is needed to improve association with measured concentrations during the depuration phase and employ the biosensor in non-steady state conditions such as oil spill response.

The observed deviation in association between measured and predicted tissue concentrations throughout the HFO experiment contradicted our hypothesis that an exposure to HFO WAF enriched in 3–ring and higher molecular weight PAHs would yield a higher body burden in the oysters. Overall, we observed that the biosensor significantly overpredicted tissue concentrations during both uptake and depuration (Figure 5B). In addition, throughout the experiment, the measured tissue concentrations were lower than those of the Hoops experiment. Notably, the general trend and peak observed in measured tissue concentrations was also observed in predicted concentrations during the uptake phase at differing concentrations. The association between predicted and measured tissue concentrations in the HFO test was corroborated via linear regression analysis in which an R^2 value of 0.81 is observed (Figure 6C) although the regression equation differs from that derived from Hoops Oil (Figure 6A). The association between predicted and measured concentrations is lost during the depuration phase

(Figure 6D). Possible explanations due to analytical error or experimental variability were investigated and there was no evidence to suggest these sources contributed to the observed differences. GC–MS data show good surrogate recoveries and there was no significant difference in experimental design.

Oyster sizes were found to be significantly different between experiments (Figure S6). For the Hoops test, the average oyster shell height was 91.5 mm, and for the HFO test, the average shell height was 82.7 mm. However, lipid content was not significantly different, suggesting the size differences may not be an important factor (Figure S7). Therefore, the most plausible explanation for the observed difference in concentrations in the HFO test is that steady state was not achieved for higher log K_{ow} PAHs in the acute exposure phase. As indicated, HFO oil was more enriched in higher molecular weight compounds relative to Hoops oil (Figure S1). The length of exposure did not allow enough time for the molecular transfer between the tissue and aqueous phase to reach dynamic equilibrium for the higher molecular weight compounds. Therefore, a higher concentration was still observed in the aqueous phase leading to an overestimation of tissue concentrations based on biosensor measurement. In future studies, the theory that higher molecular weight compounds did not have enough time to come to equilibrium could be further explored through an evaluation of compound-specific tissue half-lives and elimination rates. Faster rates observed for lower molecular weight compounds could support this hypothesis and why a better correlation was observed for Hoops oil during the uptake phase.

Internal partitioning and organ-specific differences in uptake and elimination kinetics may be an important consideration in the differences observed between the aqueous phase and tissue phase. When a dynamic energy budget model was applied to the uptake and depuration kinetics of contaminants, including PAHs, in blue mussels (*Mytilus edulis*), van Haren et al.

(1994) found that accounting for oyster physiology, lipid reserves, and tissue composition played a critical role in evaluating PAH kinetics. Regarding assessments of lipid content in kinetic models, a major assumption in using whole-body lipid contents as study estimates is that all biological lipid possesses a uniform affinity for binding lipophilic chemicals – both lipid content and composition can vary within the same species (McCarty and Mackay 2013). This may impact internal partitioning. Further work should also examine toxic body burdens of individual compounds for possible evidence of narcotic effects. Additionally, the relationship between tissue residue concentrations and aqueous phase concentrations (e.g. hemolymph, serum, or oyster interstitial fluid) within the organism when exposed to narcotic or respiratory-inhibiting chemicals requires further examination to better understand the role of this physiological effect on internal partitioning. This investigation could be facilitated by biosensor analysis as work within a confined spatiotemporal space may be required.

Potential stress responses induced by the oyster, such as disrupting osmoregulation, cell membrane stability, and energy metabolism, may also contribute to a disturbance in the internal partitioning of the chemical and its ability to pass through membranes to dissolve into lipid tissue. In an acute (3d) exposure study examining the tissue specific metabolic responses in the pearl oyster *Pinctada martensii* challenged with two different aqueous doses of benzo [a] pyrene (1µg/L and 10µg/L), Chen et al. (2018) observed significant effects to the gill and digestive gland metabolomes at each dose, particularly in metabolites related to energy metabolism and osmotic regulation. Similar energy metabolism and osmoregulation disturbances were reported in green mussels (*Perna viridis*) in an acute exposure to DDT and benzo [a] pyrene (Song et al. 2016). These findings indicate that inducing a significant change in metabolic response is plausible in short-duration experiments such as our present study. While we did not observe a

significant difference in total lipid content in oysters between experiments nor did we examine stress response parameters as this was beyond our study scope, a more extensive analysis of the lipid profile and toxic effects on regulatory pathways may enhance future iterations of the study by exploring the link between biological response and chemical activity and how these parameters affect measured tissue concentrations.

Conclusions

We conducted a PAH kinetics study in which *C. virginica* oysters were acutely exposed to crude oil WAF in independent experimental iterations. In each experiment, adult oysters were exposed to a dose of 2.5 µg/L of Quintana Hoops oil blend WAF and 15 µg/L HFO distillate WAF, respectively. Our objective was to evaluate antibody-based biosensor technology as a quantitative screening tool to measure total 3-5–ring PAH concentrations in water and oyster interstitial fluid (i.e. aqueous phase) under kinetic conditions. Further, we examined the accuracy of biosensor-derived predictions of tissue concentrations in the kinetic regime to preliminarily assess this role of this technology in oil spill monitoring and response. We found that the biosensor reliably monitored PAH levels in the dosing water for each experiment, confirming oysters received a constant WAF dose during the uptake phase. Therefore, the biosensor shows promise as a tool to rapidly and quantitatively screen for 3-5–ring PAH levels in water, the range of PAHs considered to be most bioavailable, at low-cost for time-sensitive scenarios such as an oil spill.

Overall, the biosensor screening protocol presented in this study requires more work to serve as a reliable PAH screening tool for biota in oil spill response. The biosensor accurately predicted 3-5–ring PAH concentrations during uptake of the Hoops experiment. For the high dose HFO experiment, the biosensor predictions followed the same general trend over time

during the uptake phase, but predicted concentrations were much higher than the measured concentrations. The tissue measurements for the high dose exposure were also lower than those for the low dose exposure. As observed in both exposures, the association between biosensor-predicted and GC–MS-measured tissue concentrations was lost during depuration. The biosensor underpredicted tissue concentrations during depuration. Further assessment of the model used to derive tissue concentration predictions is needed to better understand the possible limitations of this method. While biological factors such as sublethal toxic effects may contribute to the observed differences, the most likely explanation is that a 3-day uptake phase was not enough time for steady-state achievement leading to an overestimation of tissue concentrations based on biosensor measurement. Further refinement of the biosensor screening protocol is necessary to improve tissue predictions in the context of oil spill response. However, with the ability to work within a small spatiotemporal scope, high sensitivity, and low-cost for analysis, this near real-time technology may be valuable in kinetic studies and its utility should be further explored.

References

Abdel-Shafy, H. I., & Mansour, M. S., 2016. A review on polycyclic aromatic hydrocarbons: source, environmental impact, effect on human health and remediation. *Egyptian Journal of Petroleum* 25, 107-123.

ASTM International., 1994. Standard guide for conducting bioconcentration tests with fishes and saltwater bivalve mollusks. In *Annual book of standards* (Vol. 11.04, E1022– 94).

Baeumner, A. J., 2003. Biosensors for environmental pollutants and food contaminants. *Analytical and Bioanalytical Chemistry* 377, 434-445.

Behera, B.K., Das, A., Sarkar, D.J., Weerathunge, P., Parida, P.K., Das, B.K., Thavamani, P., Ramanathan, R. and Bansal, V., 2018. Polycyclic Aromatic Hydrocarbons (PAHs) in inland aquatic ecosystems: Perils and remedies through biosensors and bioremediation. *Environmental Pollution* 241, 212-233.

Bustamante, P., Luna-Acosta, A., Clemens, S., Cassi, R., Thomas-Guyon, H., & Warnau, M. (2012). Bioaccumulation and metabolisation of 14C-pyrene by the Pacific oyster Crassostrea gigas exposed via seawater. *Chemosphere*, 87, 938-944.

Camargo, K., Vogelbein, M.A., Horney, J.A., Dellapenna, T.M., Knap, A.H., Sericano, J.L., Wade, T.L., McDonald, T.J., Chiu, W.A. and Unger, M.A., 2022. Biosensor applications in contaminated estuaries: Implications for disaster research response. *Environmental Research* 204, 111893.

Chen, H., Diao, X. and Zhou, H., 2018. Tissue-specific metabolic responses of the pearl oyster Pinctada martensii exposed to benzo [a] pyrene. *Marine Pollution Bulletin* 131, 17-21.

Christensen, J.H. and Tomasi, G., 2007. Practical aspects of chemometrics for oil spill fingerprinting. *Journal of Chromatography A* 1169, 1-22.

Conder, J., Jalalizadeh, M., Luo, H., Bess, A., Sande, S., Healey, M., & Unger, M. A., 2021. Evaluation of a rapid biosensor tool for measuring PAH availability in petroleum-impacted sediment. *Environmental Advances 3*, 100032.

da Costa Filho, B. M., Duarte, A. C., & Santos, T. A. R., 2022. Environmental monitoring approaches for the detection of organic contaminants in marine environments: a critical review. *Trends in Environmental Analytical Chemistry*, e00154.

Di Nardo, F., Chiarello, M., Cavalera, S., Baggiani, C., & Anfossi, L., 2021. Ten years of lateral flow immunoassay technique applications: Trends, challenges and future perspectives. *Sensors* 21, 5185.

Di Giulio, R. T., & Clark, B. W., 2015. The Elizabeth River story: a case study in evolutionary toxicology. *Journal of Toxicology and Environmental Health, Part B* 18, 259-298.

European Food Safety Authority. Scientific Opinion of the Panel on Contaminants in the Food Chain on a request from the European Commission on Polycyclic Aromatic Hydrocarbons in Food. *EFSA Journal* 724, 1-114

Felemban, S., Vazquez, P. and Moore, E., 2019. Future trends for in situ monitoring of polycyclic aromatic hydrocarbons in water sources: The role of immunosensing techniques. *Biosensors*, *9*, 142.

Gao, Huang, X., Zhu, Y., & Lv, Z., 2018. A brief review of monoclonal antibody technology and its representative applications in immunoassays. *Journal of Immunoassay & Immunochemistry*. 39, 351–364.

Gratz, S.R., Ciolino, L.A., Mohrhaus, A.S., Gamble, B.M., Gracie, J.M., Jackson, D.S., Roetting, J.P., McCauley, H.A., Heitkemper, D.T., Fricke, F.L. and Krol, W.J., 2011. Screening and determination of polycyclic aromatic hydrocarbons in seafoods using QuEChERS-based extraction and high-performance liquid chromatography with fluorescence detection. *Journal of AOAC International* 94, 1601-1616.

Hartzell, S. E., Unger, M. A., McGee, B. L., & Yonkos, L. T. (2017). Effects-based spatial assessment of contaminated estuarine sediments from Bear Creek, Baltimore Harbor, MD, USA. *Environmental Science and Pollution Research* 24, 22158-22172.

James, M.O. (1989). Biotransformation and disposition of PAH in aquatic invertebrates. In *Metabolism of polycyclic aromatic hydrocarbons in the aquatic environment* (pp. 69-91). CRC Press Boca Raton, FL.

Justino, C. I., Duarte, A. C., & Rocha-Santos, T. A. (2017). Recent progress in biosensors for environmental monitoring: A review. *Sensors* 17, 2918.

Kim, M., Yim, U.H., Hong, S.H., Jung, J.H., Choi, H.W., An, J., Won, J. and Shim, W.J. (2010). Hebei Spirit oil spill monitored on site by fluorometric detection of residual oil in coastal waters off Taean, Korea. *Marine Pollution Bulletin* 60, 383-389.

Li, X., Kaattari, S. L., Vogelbein, M. A., Vadas, G. G., & Unger, M. A. (2016). A highly sensitive monoclonal antibody based biosensor for quantifying 3–5 ring polycyclic aromatic hydrocarbons (PAHs) in aqueous environmental samples. *Sensing and Bio-Sensing Research* 7, 115-120.

Mastovska, K., Sorenson, W.R., Hajslova, J. and Collaborators: Betzand J Binkley J Bousova K Cook JM Drabova L Hammack W Jabusch J Keide K Lizak R Lopez-Sanchez P Misunis M Mittendorf K Perez R Perez S Pugh S Pulkrabova J Rosmus J Schmitz J Staples D Stepp J Taffe B Wang J Wenzl T, 2015. Determination of polycyclic aromatic

hydrocarbons (PAHs) in seafood using gas chromatography-mass spectrometry: collaborative study. *Journal of AOAC International* 98, pp.477-505.

Mauseth, G.S., Challenger, G.E., 2001. Trends in rescinding seafood harvest closures following oil spills. In: Proceedings, 2001 International Oil Spill Conference, Tampa, FL, USA, March 26-29, 2001. pp. 679–684.

McCarty, L.S., Arnot, J.A. and Mackay, D., 2013. Evaluation of critical body residue data for acute narcosis in aquatic organisms. *Environmental Toxicology and Chemistry* 32, 2301-2314.

McGrath, J.A. and Di Toro, D.M., 2009. Validation of the target lipid model for toxicity assessment of residual petroleum constituents: monocyclic and polycyclic aromatic hydrocarbons. *Environmental Toxicology and Chemistry* 28, 1130-1148.

Moller, T.H., Dicks, B., Whittle, K.J. and Girin, M., 1999. Fishing and harvesting bans in oil spill response. In *International Oil Spill Conference* (Vol. 1999, No. 1, 693-699). American Petroleum Institute.

National Marine Fisheries Service (NMFS). Annual Commercial Landing Statistics. NOAA, Silver Spring, MD, 2015. www.st.nmfs.noaa.gov/commercial-fisheries/commercial-landings/annual-landings/index. Viewed 20 Dec 2021

Plaza, G., Ulfig, K., & Tien, A. J., 2000. Immunoassays and environmental studies. *Polish Journal of Environmental. Studies* 9, 231-236.

Posthuma-Trumpie, G. A., Korf, J., & van Amerongen, A., 2009. Lateral flow (immuno) assay: its strengths, weaknesses, opportunities and threats. A literature survey. *Analytical and Bioanalytical Chemistry* 393, 569-582.

Prossner, K. M., Vadas, G. G., Harvey, E., & Unger, M. A., 2022. A novel antibody-based biosensor method for the rapid measurement of PAH contamination in oysters. *Environmental Technology & Innovation* 28, 102567.

Song, Q., Chen, H., Li, Y., Zhou, H., Han, Q., & Diao, X., 2016. Toxicological effects of benzo (a) pyrene, DDT and their mixture on the green mussel Perna viridis revealed by proteomic and metabolomic approaches. *Chemosphere* 144, 214-224.

Spier, C. R., Vadas, G. G., Kaattari, S. L., & Unger, M. A., 2011. Near real-time, on-site, quantitative analysis of PAHs in the aqueous environment using an antibody-based biosensor. *Environmental Toxicology and Chemistry* 30, 1557-1563.

Spier, C.R., Unger, M.A. and Kaattari, S.L., 2012. Antibody-based biosensors for small environmental pollutants: Focusing on PAHs. *Biosensors and Environmental Health*, p.273.

US Environmental Protection Agency (EPA)., 1996a. SW-846 Test Method 4000:Immunoassay. https://www.epa.gov/hw-sw846/sw-846-test-method-4000-immunoassay

US Environmental Protection Agency (EPA)., 1996b. SW-846 Test Method 4030: Soil Screening for Petroleum Hydrocarbons by Immunoassay. https://www.epa.gov/hw-sw846/sw-846-test-method-4030-soil-screening-petroleum-hydrocarbons-immunoass

US Food and Drug Administration., 2010. Protocol for interpretation and use of sensory testing and analytical chemistry results for re-opening oil-impacted areas closed to seafood harvesting due to the Deepwater Horizon oil spill. Silver Spring, MD.

Van Haren, R. J. F., Schepers, H. E., & Kooijman, S. A. L. M., 1994. Dynamic energy budgets affect kinetics of xenobiotics in the marine mussel Mytilus edulis. *Chemosphere* 29, 163-189.

Wang, X., Lu, X., & Chen, J., 2014. Development of biosensor technologies for analysis of environmental contaminants. *Trends in Environmental Analytical Chemistry* 2, 25-32.

Widdows, J., Moore, S. L., Clarke, K. R., & Donkin, P., 1983. Uptake, tissue distribution and elimination of [1-14 C] naphthalene in the mussel Mytilus edulis. *Marine Biology 76*, 109-114.

Yender, R., Michel, J.M. and Lord, C., 2002. *Managing seafood safety after an oil spill*. US Department of Commerce, National Oceanic and Atmospheric Administration, National Ocean Service, Office of Response and Restoration.

Yim UH, Kim M, Sung YH, Kim S, Shim WJ., 2012. Oil Spill Environmental Forensics: the Hebei Spirit Oil Spill Case. *Environmental Science and Technology* 46, 6431-6437. DOI: 10.1021/es3004156

Zhang, W., Liu, Q.X., Guo, Z.H. and Lin, J.S., 2018. Practical application of aptamer-based biosensors in detection of low molecular weight pollutants in water sources. *Molecules* 23, 344.

Figures

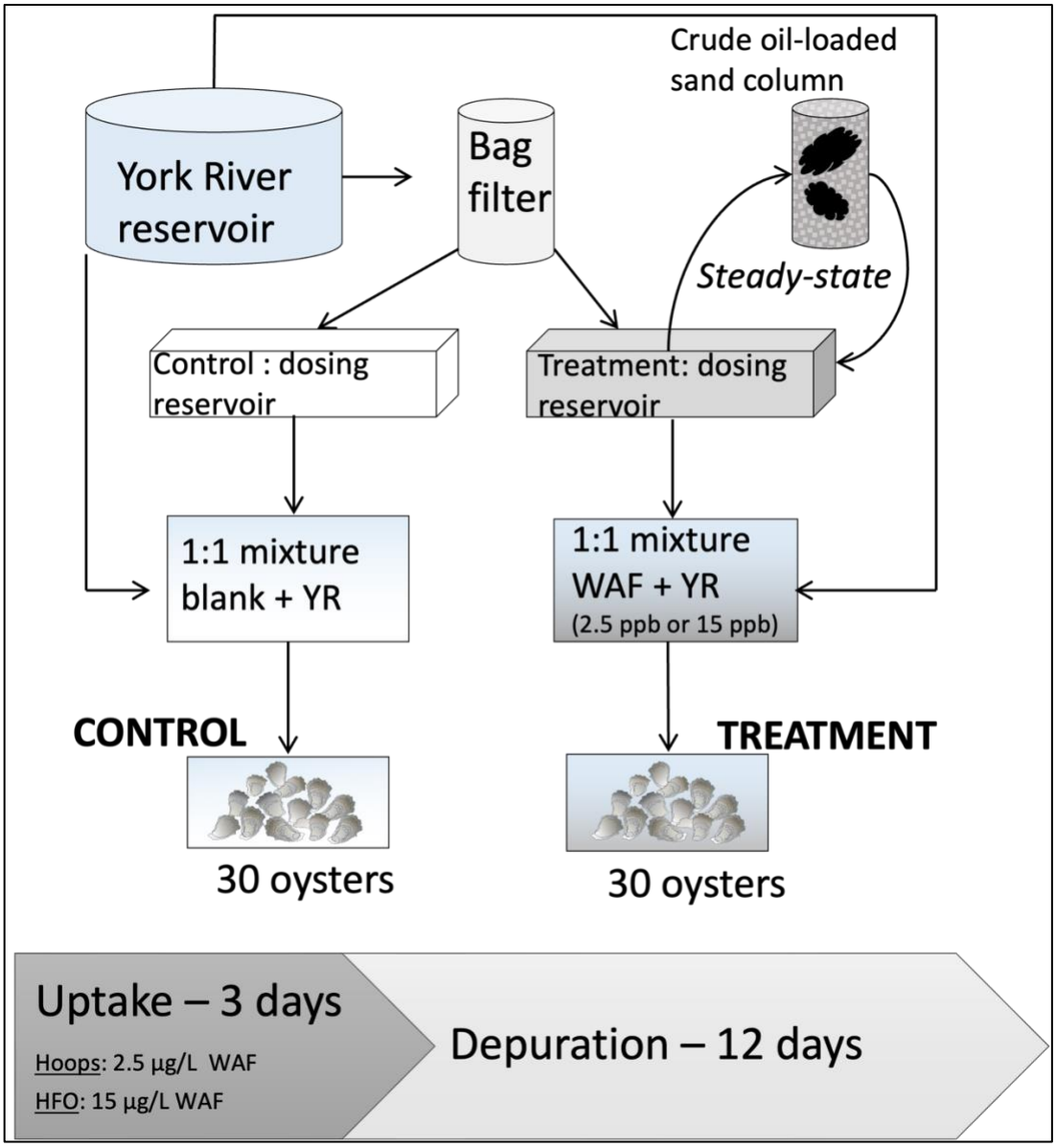

Figure 1. Schematic of experimental design. YR= York River water; WAF= Water accommodated fraction of oil.

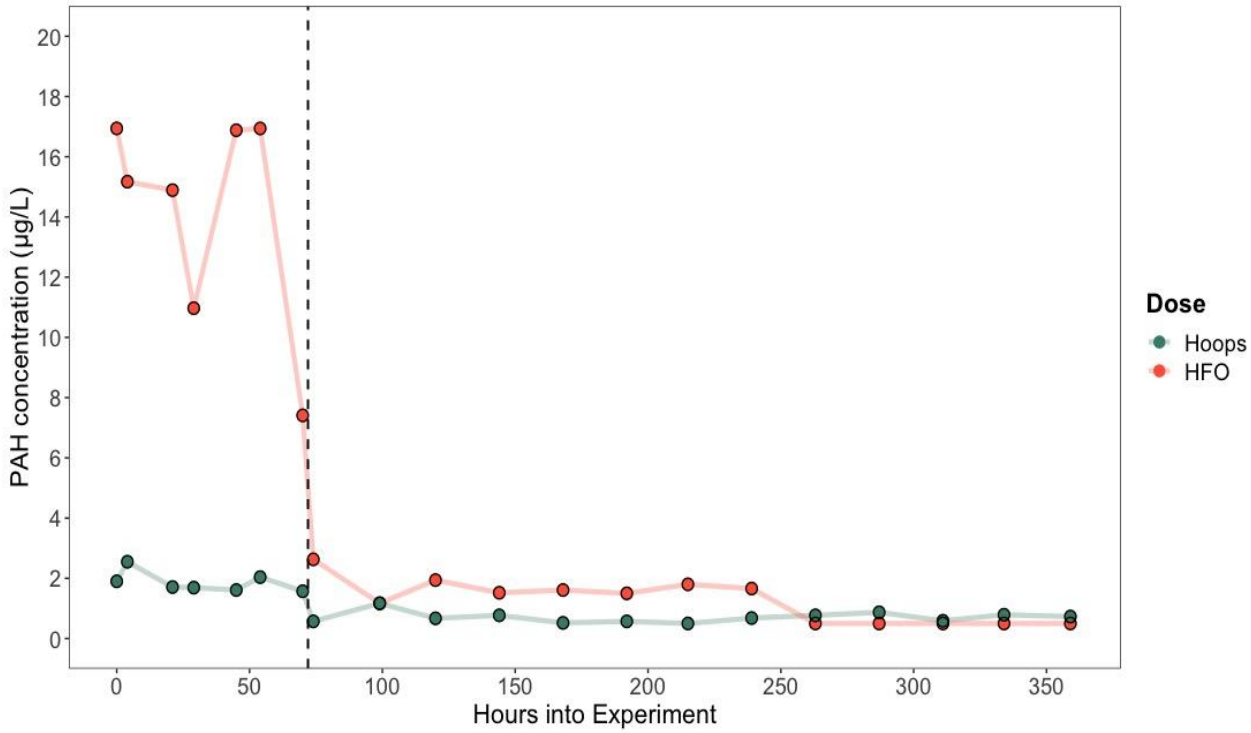

Figure 2. Estimated PAH concentrations measured by biosensor in aquaria media dosed with water accommodated fraction (WAF) for Hoops oil (mean = 2.5 µg/L) and HFO (mean = 15 µg/L) bioconcentration tests. Dashed vertical line indicates the transition from uptake (3-d period) to depuration (12-d period). Starting at 0-hr, samples were collected 2x per day during uptake and 1x per day during depuration.

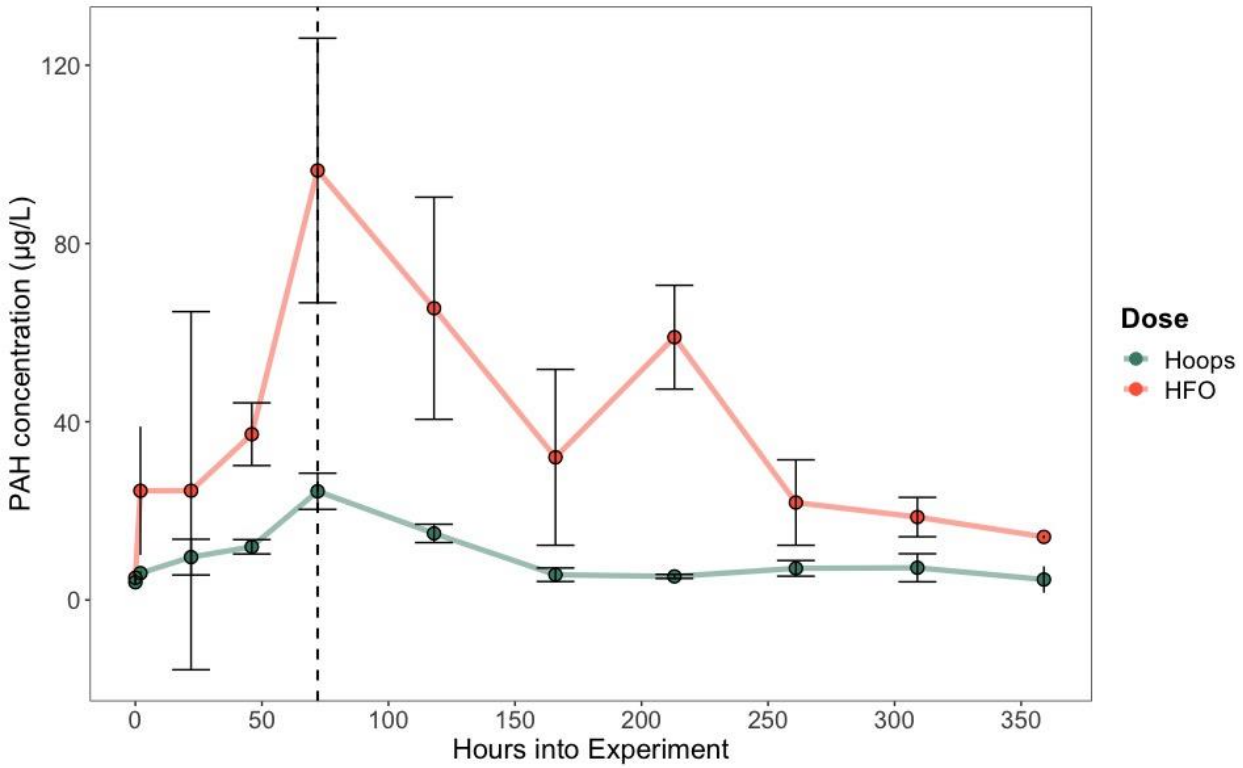

Figure 3. Estimated total PAH concentration in interstitial fluid (i.e. oyster aqueous phase) of individual oysters measured using biosensor through time in bioconcentration studies with two test oils at different exposure levels (Hoops=2.5 µg/L and HFO= 15 µg/L). Dashed vertical line indicates transition from uptake (3 d) to depuration (12 d) phases. Error bars depict standard deviation (n=3). Measurements at 0-hr indicate pre-experiment background concentrations. Samples were collected once per day during the 3-d uptake phase and every other day during the 12-d depuration phase.

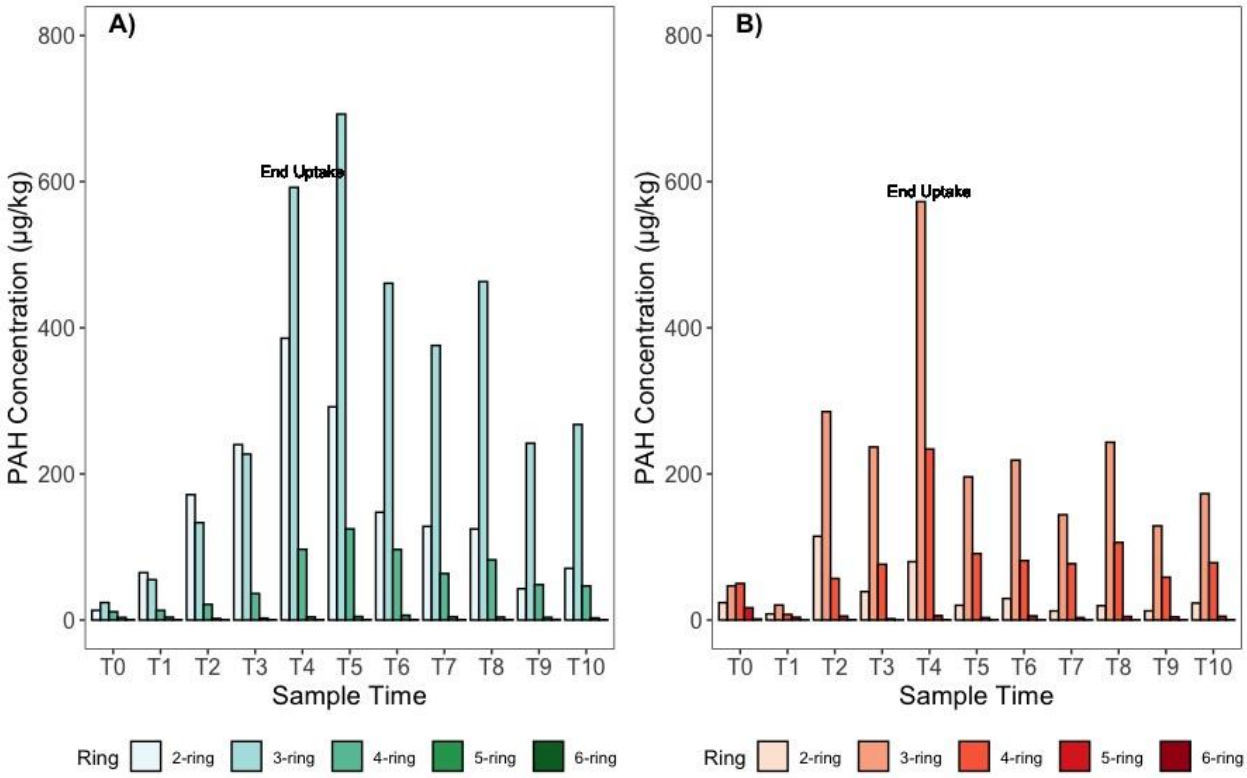

Figure 4. Comparison of PAH composition measured in oyster by GC–MS between **A)** Hoops WAF exposure (2.5 µg/L) and **B)** HFO WAF exposure (15 µg/L). Sample Time=T4 is the last sample collected during the uptake phase as noted above the bar. T0 indicates pre-experiment background concentrations, T1 indicates first sampling during exposure. Samples were collected once per day during the 3-d uptake phase (T1-T4) and every other day during the 12-d depuration phase (T5-T10).

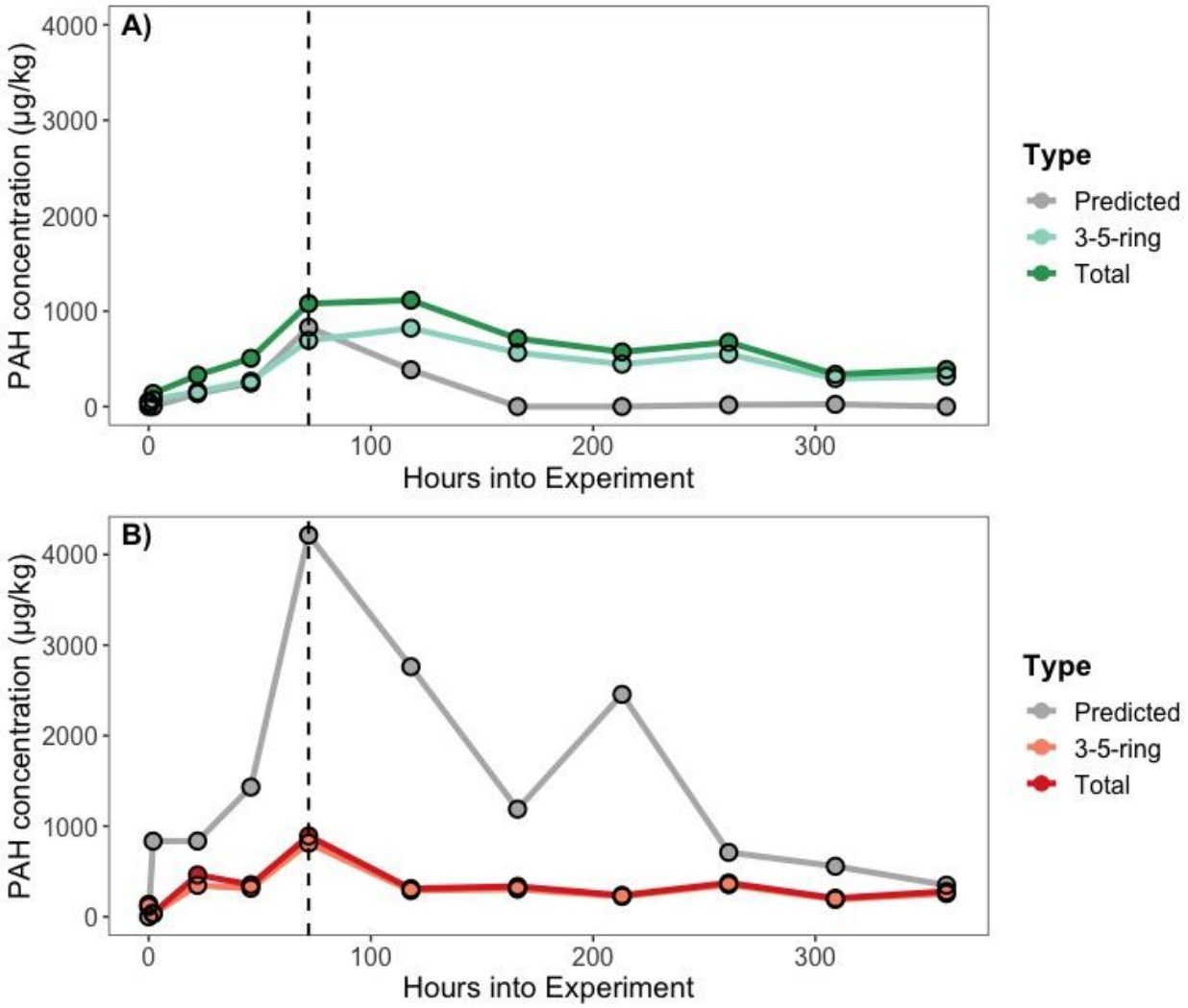

Figure 5. Comparison of uptake and depuration curves of biosensor-predicted PAH concentrations in oyster tissue to GC–MS-measured total tissue concentrations and 3-5–ring subset during a **A)** Hoops oil exposure (2.5 µg/L) and **B)** HFO exposure (15 µg/L). Dashed vertical line depicts the transition from uptake (3 d) to depuration (12 d) phases. Measurements at 0-hr indicate pre-experiment background concentrations. Samples were collected once per day during the 3-d uptake phase and every other day during the 12-d depuration phase.

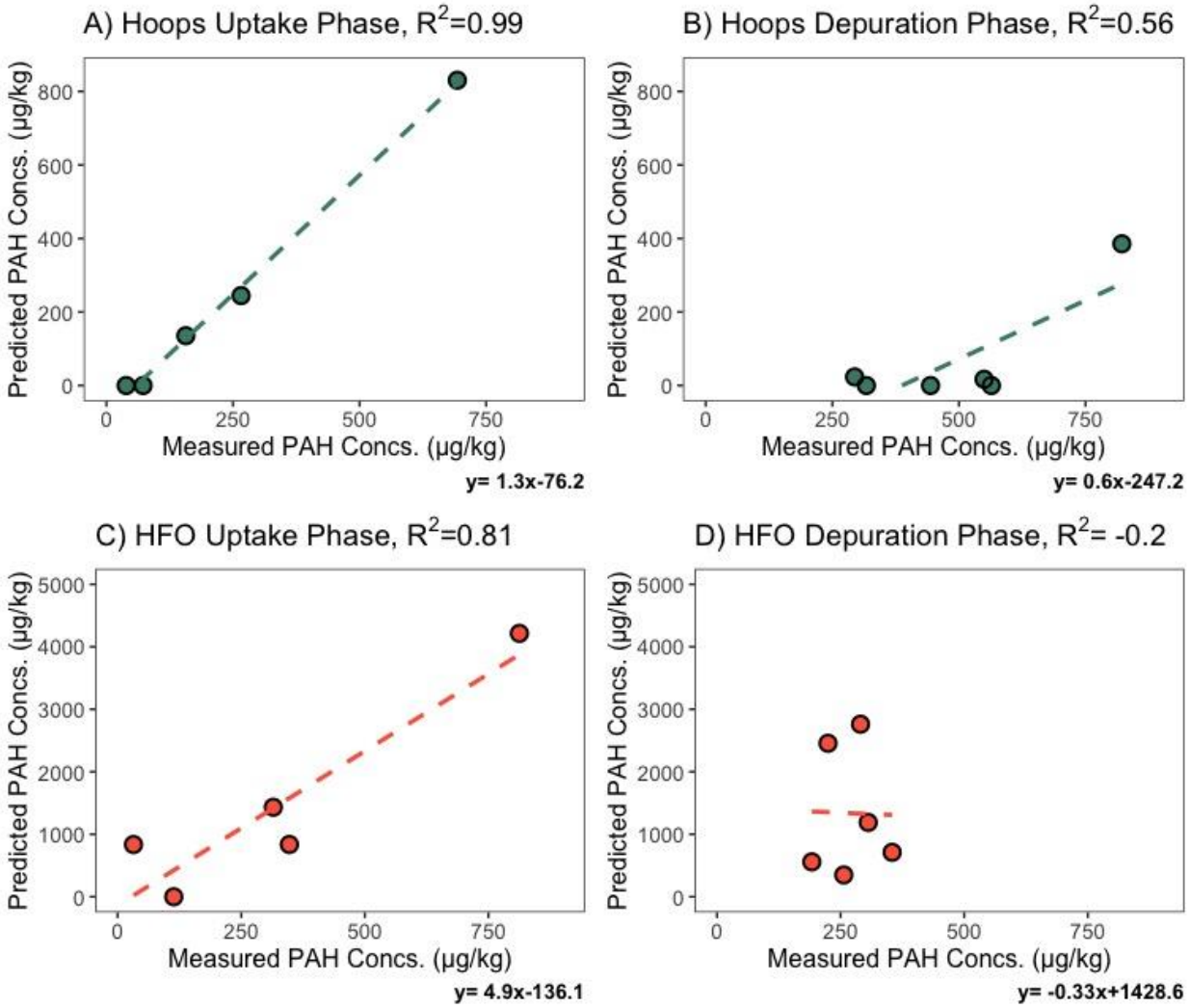

Figure 6. Linear regression comparing GC–MS-measured concentrations (in the 3-5–ring range) in oyster tissue to biosensor-predicted PAH concentrations in oyster tissue. Individual regressions were conducted to compare measurements to predictions during each phase of respective experiments: **A)** uptake phase of the low dose (2.5 µg/L) WAF exposure; **B)** depuration phase of the low dose (2.5 µg/L) WAF exposure; **C)** uptake phase of the high dose (15 µg/L) WAF exposure; **D)** depuration phase of the high dose (15 µg/L) WAF exposure. R^2 values are reported at the top of each regression. Df= 3 for uptake regressions (**A)** and **C)**), and df= 4 for depuration regressions (**B)** and **D)**). Respective regression equations are included in the bottom right below each figure. Note y-axis scale change between 6A-B and 6C-D. Note that the y-axes are different between comparisons.

Chapter 3: Immunofluorescence Visualization of Polycyclic Aromatic Hydrocarbon Mixtures in the Eastern Oyster Crassostrea virginica

Prossner, K.M., Small, H.J., Carnegie, R.B. and Unger, M.A., 2023. Immunofluorescence Visualization of Polycyclic Aromatic Hydrocarbon Mixtures in the Eastern Oyster Crassostrea virginica. *Environmental Toxicology and Chemistry*, *42*, 475-480.

Introduction

A class of hydrophobic organic contaminants known to have toxic and carcinogenic effects in organisms, polycyclic aromatic hydrocarbons (PAHs) exist in the environment as complex mixtures comprised of hundreds of different individual compounds (Latimer & Zheng, 2003; Lawal, 2017). As sessile, benthic fauna with limited metabolic capacity to excrete PAHs, bivalve molluscs such as oysters are highly sensitive to accumulation of this contaminant in their tissues (James, 1989). As an important commercial shellfish, oysters can also represent a potential public health hazard of human PAH exposure via consumption of contaminated oysters (European Food Safety Authority, 2008; National Oceanic and Atmospheric Administration Fisheries Eastern Oyster Biological Review Team, 2007).

The use of immunohistochemistry (IHC) has been a standard practice in medical pathology applications such as assessments of oncological biomarkers, diagnoses of diseases, as well as evaluations of neurodegenerative disorders (Dugger & Dickson, 2017; Hawes et al., 2009). Because of the known impact environmental pollutants like PAHs can have on biological health, there is a growing body of work using novel imaging technologies and IHC approaches, including immunofluorescence, for examining various mechanisms involved in biotic exposure to contaminants (Einsporn & Koehler, 2008; Lobel & Davis, 2002; Sforzini et al., 2014; Strandberg et al., 1998). However, many of these techniques have been limited in their ability to detect only one or a few individual PAH compounds via laboratory exposures (Rodríguez & Bishop, 2005; Sforzini et al., 2014; Speciale et al., 2018; Subashchandrabose et al., 2014; Wang et al., 2012). By targeting a few specific PAHs out of a contaminant class containing hundreds of compounds, such studies do not reflect real-world complex mixtures to which biota are exposed. Further, despite having some of the highest levels of PAHs relative to other food products,

oysters have not served as study organisms in such IHC investigations of PAH bioaccumulation, to the authors' knowledge.

To visualize the accumulation of complex environmental PAH mixtures in eastern oysters (*Crassostrea virginica*), we employed a highly sensitive monoclonal antibody (mAb 2G8) for use in IHC techniques with demonstrated uniform selectivity for a range of three- to five-ring PAHs including both parent compounds and alkylated derivatives (Li et al., 2016). Therefore, PAHs derived from both petrogenic and pyrogenic sources are detected. The mAb 2G8 antibody was initially developed for use on the KinExA Inline Sensor (Sapidyne Instruments), a biosensing instrument that quantifies PAH concentration via the detection of fluorescently tagged antibody bound to PAHs in an aqueous sample (Li et al., 2016). Employing mAb 2G8 conjugated to the far-red fluorescent dye Alexa Fluor 647 (AF647), the biosensor has been successfully used to quantify total three- to five-ring PAH concentrations in environmental samples such as porewater (Camargo et al., 2022; Conder et al., 2021; Hartzell et al., 2017; Li et al., 2016) and oyster interstitial fluid (Prossner et al., 2022). Extending beyond its employment as a quantitative tool, we explore a novel application of AF647-tagged mAb 2G8 to observe PAH localization in oyster gill tissues using IHC techniques coupled with confocal microscopic imaging. For demonstration of this new application for the antibody, we focus our observations of mAb signal to within the water tube and plicae of the gill because we believe these exterior-facing structures to be important regions for accumulation of PAHs dissolved in the aqueous phase. We hypothesize that the incorporation of mAb 2G8 in an IHC approach will allow us to localize PAHs within tissues and that the intensity of observed fluorescent signal will be related to PAH body burden. Bioaccumulation of PAH mixtures from two different examples of oyster exposure was investigated (1) chronic exposure of wild oysters residing in historically

contaminated sites in the Elizabeth River (VA, USA), and (2) acute laboratory-based exposure of oysters to the water accommodated fraction (WAF) of crude oil.

Materials and Methods

Collection of wild Elizabeth River oysters

The Elizabeth River is a tidal urban estuary in southeast Virginia, USA, known for highly elevated levels of PAHs observed in sediment primarily due to historic pollution from several defunct wood treatment and creosote facilities in the area (Di Giulio & Clark, 2015). Six native adult *C. virginica* oysters were collected from Jones Creek, an Elizabeth River site in which elevated PAH levels have been previously observed (Prossner et al., 2022). Collected oysters were placed in coolers and returned to the laboratory, where they were stored whole (in shell) and out of water at 4 °C for 1–2 days prior to processing, to ensure that depuration did not occur.

Collection of WAF-exposed oysters

Adult cultured oysters purchased from an oyster farm on the York River in Gloucester County, Virginia (>80 km away from the Elizabeth River), were exposed to a constant 15-µg/L dose (parts per billion) of crude oil WAF for a period of 4 days, followed by a 12-day depuration period via a flow-through tank system in a PAH kinetics experiment. To dose the oysters during the uptake/depuration kinetics study, a WAF was prepared from heavy fuel oil distillate using a generator column. A large (10 × 70 cm) generator column was packed with ignited filter sand that was coated with 40 ml of heavy fuel oil. The column was pumped at 100 ml/min with York River water in a 310-L closed recirculating system for 260 h until the total PAH concentration in the water reached steady state at 30 µg/L total PAH. This prepared WAF was then diluted 1:1 with clean York River water to maintain an average concentration of 15 µg/L for the duration of the 72-h dosing experiment.

Oysters were held in unfiltered York River water and not provided supplemental food. Background PAH concentration in York River water was monitored consistently throughout the experiment and averaged approximately 1 μg/L. Animal husbandry parameters including temperature, salinity, pH, dissolved oxygen, and ammonia were maintained at appropriate levels, as outlined in ASTM standard guide E1022-94 (ASTM International, 1994). No mortality was observed throughout the experimental period. Three oysters per sampling were collected throughout the experiment at five time points: T0, pre-exposure background; T1, first day of uptake; T2, last day of uptake; T3, day 4 of depuration; T4, day 8 of depuration; and T5, day 12 (last day) of depuration. Oysters were held out of water at 4 °C for 1–2 days prior to processing, to avoid depuration. Interstitial fluid from identical oysters was preserved for biosensor analysis for corresponding PAH concentration measurement (see section Semiquantitative image analysis).

Sample processing

Oysters were scrubbed clean, then shucked using an oyster knife. Gill tissue fragments (~6 mm3) were dissected from each oyster and embedded in optimal cutting temperature (OCT) media within a disposable cryomold (Tissue-Tec). Embedded tissue fragments were subsequently gently frozen over a bath of liquid nitrogen–cooled pentane. Briefly, approximately 300 ml of 100% pentane was poured into a small metal bowl, which was then partially submerged in liquid nitrogen so that the pentane would reach near-freezing temperatures. The bottom of tissue-containing cryomolds was held on the surface of the near-freezing pentane so that the contents of the cryomold would gently freeze (to reduce the risk of a compromised specimen via ice crystal formation). Once frozen, the OCT-tissue blocks were stored at −80 °C. One day prior to cryosectioning, the blocks were transferred to a −20 °C freezer.

Cryosectioning and fluorescent IHC

Components of a protocol for benzo[a]pyrene localization in earthworm (Eisenia andrei) tissue by Sforzini et al. (2014) were adapted for use with oyster tissues and our AF647-tagged mAb 2G8. Individual tissue blocks were initially frozen to an aluminum cryostat chuck using OCT media, and 10-µm frozen sections were cut at −10 °C (for both the cryochamber and object temperature) using a cryostat (Leica CM3050 S). Frozen sections were directly transferred to a glass slide (Superfrost Plus; Fisher Scientific) at ambient room temperature. Tissue sections were fixed in 4% paraformaldehyde in 1× phosphate-buffered saline (PBS) for 20 min at room temperature. Fixed sections were subsequently washed in 1× PBS three times (5 min per wash) before a 1-h incubation at room temperature in a blocking and permeabilization solution containing 0.5% Triton X-100, 2% bovine serum albumin (BSA), and 0.5% rabbit serum in 1× PBS. Sections were then washed three times (as above) and incubated with the AF647-tagged 2G8 mAb (1:100 dilution in 1× PBS containing 1% BSA and 0.05% Triton X-100) overnight at 4 °C in a moist chamber. After overnight incubation, the sections were washed three times (as above), then incubated with 4′,6-diamidino-2-phenylindole (DAPI), a blue fluorescent stain for DNA (to provide histoarchitectural definition to the microscopic images), at a 1:5000 dilution in 1× PBS for 15 min at room temperature. Sections were washed three times (as above) and dried, then a coverslip was mounted using Dako mounting media. On drying, clear nail varnish was applied to seal around the edges of the coverslip prior to fluorescence microscopy. Negative controls (to assess nonspecific fluorescence) consisting of tissue sections from the same individual oyster were processed in an identical manner as above but were not exposed to AF647-tagged 2G8 mAb. Sections were evaluated and images captured using a FLUOVIEW FV1200 confocal laser scanning microscope (Olympus) with filter sets for DAPI and AF647.

Oyster gill tissue fragments were dissected from a separate batch of oysters collected from Jones Creek and then fixed and processed for standard paraffin histology using standard techniques. These were stained with hematoxylin and eosin dye and imaged under a standard light microscope for histoarchitectural comparison with sections processed for confocal microscopy.

Semiquantitative image analysis

Analysis of the change in integrated density of fluorescent signal in gill tissue sections of WAF-exposed oysters was conducted using FIJI software (Schindelin et al., 2012). Integrated density is the product of total selected area and mean gray value (i.e., amount of signal in the selected image area). Because imaged gill sections varied in terms of extracellular space and intercellular cavities, three representative gill plicae per image were selected to provide standardization in measurement based on uniform scaling of the image. Measurements were repeated in triplicate to reduce random error. Analysis of variance followed by a Tukey post hoc test was conducted to compare means across different sampling time periods (T0–T5) during the WAF exposure experiment. Integrated density of the fluorescent signal was then compared with PAH concentration measured in the corresponding oyster interstitial fluid via KinExA Inline Sensor methodology (Prossner et al., 2022) to observe if a signal–concentration trend existed throughout the experiment.

Results and Discussion

IHC in wild C. virginica

No fluorescent signal was detected in gill tissues from control sections that were processed without the inclusion of the AF647-tagged 2G8 mAb (Figure 1A). Immunofluorescence signal indicative of the presence of select three- to five-ring PAHs was observed in gill sections exposed to mAb 2G8 (Figure 1B). Specifically, intense fluorescent

signal was observed in a key gill structure involved in water filtration and transportation—the water tube (Eble & Scro, 1996). Localization in the water tube was confirmed through comparison with a hematoxylin and eosin–stained gill tissue section, which provides a more refined image of the target gill structures (Figure 1C). The accumulation of PAHs and thus intense mAb 2G8 signal primarily along the lipid membrane of these gill structures is reasonable because the lipid in this region serves as a first point of contact for these lipophilic molecules on entering the oyster gill. Although fluorescence is observed mainly within the external regions of the gill, due in part to the focus of our study, we still interpret this as localization of PAH distributed within tissue, not solely bound to the tissue surface. Observation of fluorescence in 1-µm slices of the images through the z-axis via z-stack analysis on the confocal microscope, with maximum fluorescence observed in the middle slice, supports our interpretation. In addition, the use Triton X-100 in the described IHC protocol permeabilizes eukaryotic cell membranes and facilitates mAb 2G8 binding to intracellular PAH.

IHC and PAH quantification in WAF-exposed C. virginica

Exposing oysters to WAF in a PAH kinetics study provided an ideal opportunity to examine time-dependent dose and its effect on tissue concentrations and imaging. Imaging of gill tissue collected from WAF-exposed oysters allowed for comparison of mAb 2G8 fluorescent signal to accumulated PAH concentrations through time (Figures 2 and 3). Overall, IHC staining of gill structures in laboratory-exposed oysters (Figure 2A–F) was similar to that in chronically exposed native oysters (Figure 1A–C); however, a stronger signal was observed in the plicae of the laboratory-exposed oysters, another important gill structure for water filtration and transportation (Eble & Scro, 1996). Due to the ubiquity of PAHs in the environment, the susceptibility of oysters to accumulation, and the sensitivity of mAb 2G8, fluorescent signal

indicative of low levels of PAHs was observed in preexposure background oysters (Figure 2A). On the first day of exposure, T1 (Figure 2B), a stronger signal relative to T0 (Figure 2A) was observed, which can be attributed to the capacity of oysters to filter large volumes of water (0.12 m3 g−1 dry wt/day or ∼50 gallons or ∼190 L of water per day for an individual oyster; Newell, 1988). Thus, oysters can rapidly concentrate environmental contaminants such as PAHs. The highest PAH signal intensity was observed on the final day of uptake (T2; Figure 2C) and steadily decreased throughout the depuration period (Figure 2D,E). By the last day of depuration, T5 (Figure 2F), fluorescent signal for PAH had returned to nearly the same levels observed at T0 (Figure 2A). Notably, the two PAH mixtures employed as sources of exposure for the present study vary greatly in PAH composition: Creosote, the predominant source of PAH pollution in the Elizabeth River, is comprised primarily of pyrogenic PAHs, whereas the heavy fuel oil WAF consists of mostly petrogenic PAHs (Neff et al., 2005). Through successful imaging of fluorescent signal in oysters exposed to different PAH sources via a mAb uniformly selective for a wide range of PAH compounds, we demonstrate the versatility of mAb 2G8 for future imaging applications.

Overall, the level of integrated density of specific fluorescent signal for PAHs (AF647-tagged 2G8 mAb; Figure 3A) measured in gill tissue images (Figure 2A–F) followed a similar trend as the PAH concentration measured in the interstitial fluid of the identical oyster (Figure 3B). An analysis of variance yielded a significant difference ($F = 40.0$, $df = 5$, $p < 0.05$) in integrated density of signal across the different time points of the experiment. Through Tukey post hoc testing, it was determined that T2, the final day of uptake and the highest PAH concentration, was significantly different from all other sampling periods. Periods T1, T3, and T4 were not significantly different from each other but were significantly different from T0 and

T5, the final day of depuration. Periods T0 and T5 were also not significantly different from each other. Groupings of specific significant differences across sampling periods are reported in Figure 3A. Through semiquantitative analysis, we found that the change in intensity of fluorescent signal observed throughout the experiment is related to PAH body burden measured at corresponding time points. This suggests that mAb 2G8 can be used not only as a visualization tool to localize where PAHs accumulate in tissue but also to observe the relative distribution of PAHs within the tissues. We determined that a similar general trend between signal and tissue concentration exists, supporting the future direction of the technique to compare relative concentration gradients within biological tissues (e.g., PAH distribution in gills relative to digestive gland) as well as providing additional evidence of PAH selectivity of the antibody. To describe a more specific correlative relationship between signal and tissue concentration, more in-depth quantitative analysis is needed, which is neither within the scope of this initial study nor an intended objective. We do not intend for this new application of mAb 2G8 to serve as a quantitative tool to predict tissue concentrations but, instead, to allow for a more in-depth understanding of accumulation and distribution of complex PAH mixtures in tissue via immunofluorescence.

Conclusions

In the present study, we demonstrate the application of a PAH mAb for use in IHC techniques to detect and localize accumulation of two complex PAH mixtures with differing PAH compositions in biotic tissue. To our knowledge, this is the first IHC study of PAH accumulation in oysters—a potentially important source of PAH exposure for humans via consumption following contamination events such as oil spills. Although gill tissue was the focus of the present study, we plan to explore PAH accumulation in other tissues using this technique.

The signal detected using the AF647-tagged mAb 2G8 reflects more realistic levels of exposure experienced by organisms than what can be analyzed using current techniques for visualizing exposure of one or a few individual PAHs. In addition, as known carcinogens, the ability to localize and visualize exposure to PAH mixtures in tissue may have important medical or veterinary applications. Demonstrating that the PAH signal intensity via image analysis is related to PAH body burden, we also predict that mAb 2G8 can help evaluate important environmental and biological partitioning mechanisms, which will be a target for future research.

References

ASTM International, 1994. Standard guide for conducting bioconcentration tests with fishes and saltwater bivalve mollusks. In Annual book of standards (Vol. 11.04, E1022– 94).

Camargo, K., Vogelbein, M. A., Horney, J. A., Dellapenna, T. M., Knap, A. H., Sericano, J. L., Wade, T. L., McDonald, T. J., Chiu, W. A., & Unger, M. A., 2022. Biosensor applications in contaminated estuaries: Implications for disaster research response. *Environmental Research*, 204, 111893.

Conder, J., Jalalizadeh, M., Luo, H., Bess, A., Sande, S., Healey, M., & Unger, M. A., 2021. Evaluation of a rapid biosensor tool for measuring PAH availability in petroleum-impacted sediment. *Environmental Advances* 3, 100032.

Di Giulio, R. T., & Clark, B. W., 2015. The Elizabeth River story: A case study in evolutionary toxicology. *Journal of Toxicology and Environmental Health, Part B* 18, 259– 298.

Dugger, B. N., & Dickson, D. W., 2017. Pathology of neurodegenerative diseases. *Cold Spring Harbor Perspectives in Biology*, 9, a028035.

Eble, A. F., & Scro, R., 1996. General anatomy. In V. S. Kennedy, R. I. E. Newell, & A. F. Eble (Eds.), The eastern oyster: Crassostrea virginica (pp. 19– 30). Maryland Sea Grant College.

Einsporn, S., & Koehler, A., 2008. Immuno-localisations (GSSP) of subcellular accumulation sites of phenanthrene, aroclor 1254 and lead (Pb) in relation to cytopathologies in the gills and digestive gland of the mussel Mytilus edulis. *Marine Environmental Research* 66, 185– 186.

European Food Safety Authority, 2008. Scientific opinion of the panel on contaminants in the food chain on a request from the European Commission on polycyclic aromatic hydrocarbons in food. The EFSA Journal, 724, 1– 114.

Hartzell, S. E., Unger, M. A., McGee, B. L., & Yonkos, L. T., 2017. Effects-based spatial assessment of contaminated estuarine sediments from Bear Creek, Baltimore Harbor, MD, USA. *Environmental Science and Pollution Research*, 24, 22158– 22172.

Hawes, D., Shi, S. R., Dabbs, D. J., Taylor, C. R., & Cote, R. J., 2009. Immunohistochemistry. In N. Weidner, R. J. Cote, S. Suster, & L. M. Weiss (Eds.), Modern surgical pathology (Vol. 1, pp. 48– 70). Elsevier.

James, M., 1989. Biotransformation and disposition of PAH in aquatic invertebrates. In U. Varanasi (Ed.), Metabolism of polycyclic aromatic hydrocarbons in the aquatic environment (pp. 69– 92). CRC.

Lobel, L. M. K., & Davis, E. A., 2002. Immunohistochemical detection of polychlorinated biphenyls in field collected damselfish (Abudefduf sordidus; Pomacentridae) embryos and larvae. *Environmental Pollution*, 120, 529– 532.

Latimer, J., & Zheng, J., 2003. The sources, transport, and fate of PAHs in the marine environment. In P. E. T. Douben (Ed.), PAHs: An ecotoxicological perspective (pp. 7– 33). Wiley.

Lawal, A. T., 2017. Polycyclic aromatic hydrocarbons. A review. *Cogent Environmental Science* 3, Article 1339841.

Li, X., Kaattari, S. L., Vogelbein, M. A., Vadas, G. G., & Unger, M. A., 2016. A highly sensitive monoclonal antibody based biosensor for quantifying 3–5 ring polycyclic aromatic hydrocarbons (PAHs) in aqueous environmental samples. *Sensing and Bio-Sensing Research* 7, 115– 120.

National Oceanic and Atmospheric Administration Fisheries Eastern Oyster Biological Review Team., 2007. Status review of the eastern oyster (Crassostrea virginica). Report to the National Marine Fisheries Service (NOAA Technical Memo NMFS F/SPO-88). National Marine Fisheries Service.

Neff, J. M., Stout, S. A., & Gunster, D. G., 2005. Ecological risk assessment of polycyclic aromatic hydrocarbons in sediments: Identifying sources and ecological hazard. *Integrated Environmental Assessment and Management* 1, 22– 33.

Newell, R. (1988, August). Ecological changes in Chesapeake Bay: Are they the result of over-harvesting the American oyster, Crassostrea virginica? In M. P. Lynch & E. C. Krome (Eds.), Understanding the estuary: Advances in Chesapeake Bay research (pp. 536– 546). Chesapeake Bay Consortium.

Prossner, K. M., Vadas, G. G., Harvey, E., & Unger, M. A., 2022. A novel antibody-based biosensor method for the rapid measurement of PAH contamination in oysters. *Environmental Technology and Innovation* 28, 102567.

Rodríguez, S. J., & Bishop, P. L., 2005. Competitive metabolism of polycyclic aromatic hydrocarbon (PAH) mixtures in porous media biofilms. *Water Science and Technology* 52, 27– 34.

Schindelin, J., Arganda-Carreras, I., Frise, E., Kaynig, V., Longair, M., Pietzsch, T., & Cardona, A., 2012. Fiji: An open-source platform for biological-image analysis. *Nature Methods*, 9, 676– 682. https://doi.org/10.1038/nmeth.2019

Sforzini, S., Moore, M. N., Boeri, M., Benfenati, E., Colombo, A., & Viarengo, A., 2014. Immunofluorescence detection and localization of B[a]P and TCDD in earthworm tissues. *Chemosphere* 107, 282– 289.

Speciale, A., Zena, R., Calabrò, C., Bertuccio, C., Aragona, M., Saija, A., & Cascio, P. L., 2018. Experimental exposure of blue mussels (Mytilus galloprovincialis) to high levels of benzo[a]pyrene and possible implications for human health. *Ecotoxicology and Environmental Safety* 150, 96– 103.

Strandberg, J. D., Rosenfield, J., Berzins, I. K., & Reinisch, C. L., 1998. Specific localization of polychlorinated biphenyls in clams (Mya arenaria) from environmentally impacted sites. *Aquatic Toxicology*, 41, 343– 354.

Subashchandrabose, S. R., Krishnan, K., Gratton, E., Megharaj, M., & Naidu, R., 2014. Potential of fluorescence imaging techniques to monitor mutagenic PAH uptake by microalga. *Environmental Science & Technology* 48, 9152– 9160.

Wang, P., Wu, T. H., & Zhang, Y., 2012. Monitoring and visualizing of PAHs into mangrove plant by two-photon laser confocal scanning microscopy. *Marine Pollution Bulletin* 64, 1654– 1658.

Figures

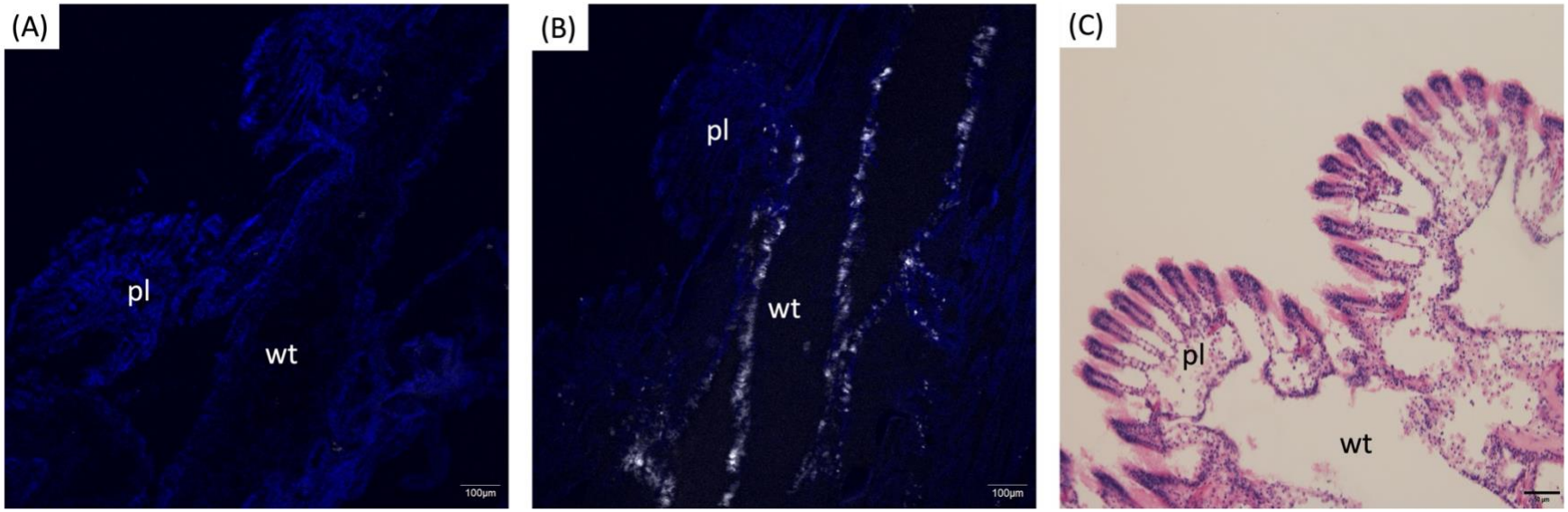

Figure 1. Representative images of immunofluorescence detection of 3-5 ring PAHs in gill tissue of a wild Elizabeth River oyster. **A)** negative control not exposed to 2G8 mAb; **B)** immunofluorescence detection of PAHs (white signal) in gill structures; **C)** hematoxylin and eosin-stained gill section from native Elizabeth River oyster from the same site with more refined histoarchitecture for comparison (note scale change). Gill structure abbreviations: pl = plica, wt = water tube. Figs. 1A and 1B were stained with DAPI for cell nuclei (blue signal).

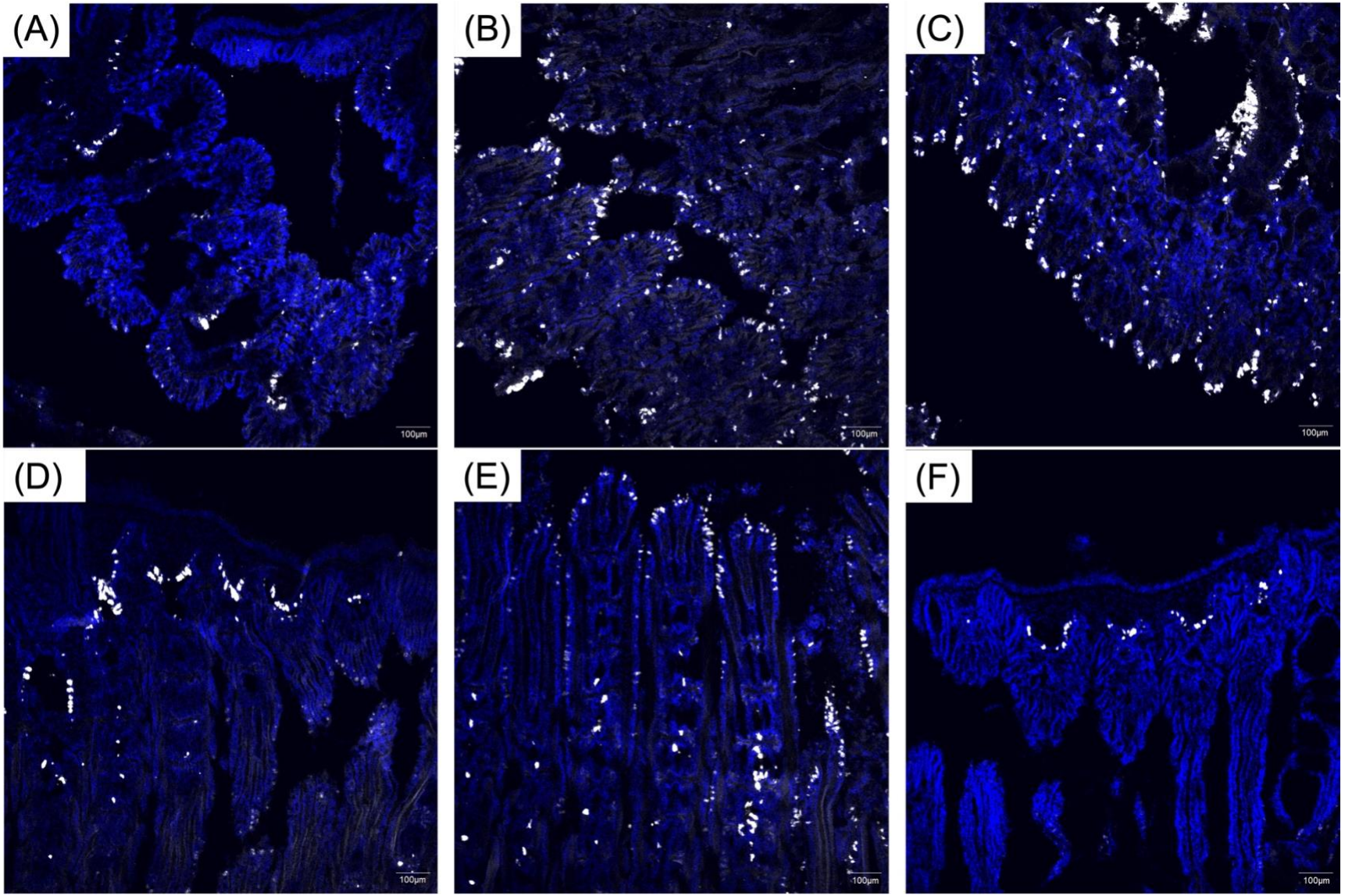
(A)
(B)
(C)
(D)
(E)
(F)
100μm

Figure 2. Representative images of immunofluorescence detection of PAH by mAb 2G8 in gill sections from oysters sampled at different time points throughout a 16-day laboratory oil-WAF exposure: **A)** = T0, background (pre-exposure); **B)** = T1, first day uptake; **C)** = T2, last day uptake; **D)** = T3, day 4 depuration; **E)** = T4, day 8 depuration; and **F)** = T5, final day of depuration. Sections were also stained with DAPI (blue signal).

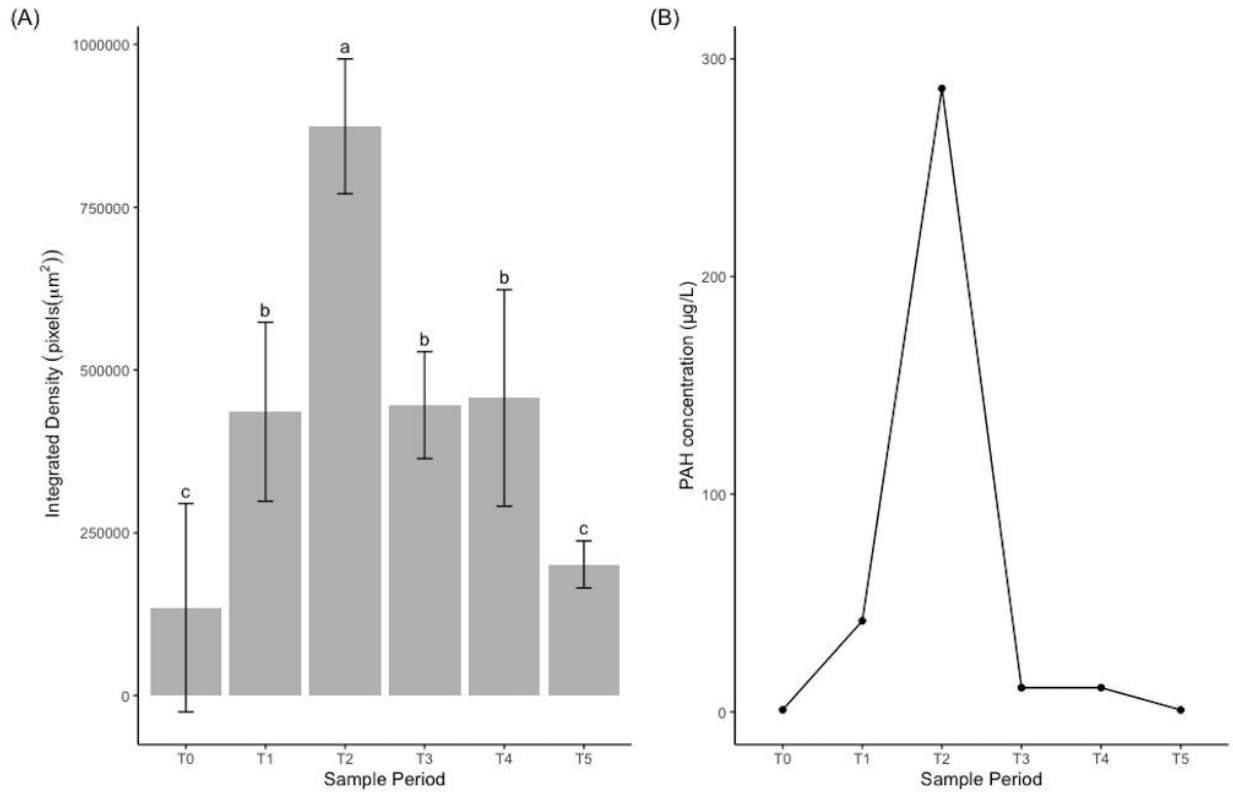

Figure 3. Comparison of **A)** image-integrated density in representative oyster gill tissue images (Fig. 2) across sampling periods during crude oil WAF exposure experiment to **B)** corresponding PAH concentrations measured in interstitial fluid of identical oysters (Prossner et al., 2022). Error bars depict standard deviations. Letters depict groupings of specific significant differences across sampling periods determined via Tukey post hoc testing. Sample periods with the same letter are not significantly different from each other but are different from groups with a different letter.

Chapter 4: Exploring PAH Kinetics in Transplanted Triploid and Diploid vs. Wild Oysters at an Impacted Field Site Using Immunological Techniques

Introduction

As sessile, benthic filter-feeders, bivalves such as *Crassostrea virginica* are susceptible to the accumulation of lipophilic contaminants such as polycyclic aromatic hydrocarbons (PAH) and have limited capacity for biotransformation of these compounds (James, 1989). Accordingly, *C. virginica* are a well-established biomonitoring species for persistent organic pollutants such as PAHs. They have served as key sentinel species to determine the bioavailability of PAHs in aquatic ecosystems in large-scale monitoring programs such as NOAA Mussel Watch since its establishment in 1976 and global programs such as the UNESCO-IOC International Mussel Watch Project (Goldberg et al. 1978; Farrington et al. 1983; Wade et al. 1998; Farrington et al. 2016). Two methods for biomonitoring exist. Passive biomonitoring involves the collection of wild bivalves inhabiting sites of for pollution monitoring and has been historically employed in long-term monitoring efforts such as NOAA Mussel Watch (Farrington et al. 1983; Sericano et al. 1995). Further, they can be immediately sampled since it can be assumed that wild oysters have equilibrated with the environment. Active biomonitoring involves the deployment of caged bivalves, either collected from a pristine site and relocated or purchased from an aquaculture. This method can overcome the heterogenous distribution of wild bivalves or complete absence of bivalves in sites of interest (Lacroix et al. 2015). The stock, origin, and biological parameters of the species used in active biomonitoring can also be more easily controlled, reducing variability and enhancing replication of the study (Besse et al. 2012). However, bivalves must be deployed at sites of interest for an extended time to reach steady-state with the environment (Sericano et al. 1996). Further, the reported optimal length of time required for equilibration is highly variable, ranging from 3 weeks to up to 2 years (Bodin et al. 2004; Marigomez et al. 2013; Beyer et al. 2017).

Although both techniques are employed, differences in total concentrations have been observed in PAH uptake and depuration when two oyster populations are compared (Kazour and Amara, 2020). In a cross-transplantation study, Sericano et al. (1996) foud that on the final day of a 48-day uptake phase, *C. virginica* oysters transplanted from a pristine to an impacted site in the Houston Ship Channel accumulated PAHs to levels comparable to those detected in oysters native to the impacted site. On the final day of a 50-day depuration period at the pristine site, the transplanted oyster (returned to their original location) concentrations were lower than concentrations measured in oysters native to the PAH-impacted site (transplanted to the pristine site). The authors proposed that newly exposed oysters can eliminate contaminants at a much faster rate than those chronically exposed. In a 6-month PAH accumulation study, Schøyen et al. (2017) found that transplanted *M. edulis* mussels never accumulated PAHs to levels observed in the native population at an impacted site. Lacroix et al. (2015), found that transplanted *Mytilus spp.* mussels accumulated higher levels of PAH in the digestive gland relative to that of native oysters at an impacted site in the Brest Harbor (France). Not only are there inconsistencies in which group (native relative to transplant) assimilates the highest PAH concentrations, but there is also a lack of consensus as to why these differences are observed. Some studies attribute differences between groups as being driven by chemical kinetic rates and lack of sufficient time for reaching steady state (Sericano et al. 1996; Greenfield et al. 2014; Schøyen et al. 2017). Others suggest that biological response drives the observed differences and that chronically exposed oysters native to contaminated sites may have set up metabolic adaptations to reduce stress response (Faria et al. 2010; Marigomez et al. 2013; Lacroix et al. 2015). Therefore, the questions of why differences are observed, and which strategy is a more appropriate evaluation of changes in environmental quality due to contamination warrant further scrutiny to enhance the

precision of future biomonitoring efforts. Addressing these differences is especially important when these approaches are employed for the assessment of potential risk to human health against safety thresholds (Beyer et al. 2017).

Oysters for active biomonitoring can be sourced from pristine sites or purchased from aquaculture farms (Beyer et al. 2017). There has been an increasing incentive for farms to produce triploid oysters due to their faster growth rates and ability to reach market-size earlier than diploid counterparts. This results in maintaining a desirable meat quality year-round for consumers (Nell 2002; Cheney 2010). In the Chesapeake Bay (USA), triploid *C. virginica* have been widely adopted in aquaculture and account for the majority of oysters brought to market (Callam et al. 2016; Wadsworth et al. 2019). The commercial advantages are attributed to energy reallocation from gametogenesis to somatic growth seen in triploids (Allen and Downing, 1986). Triploid oysters are partially sterile, induced through chemical or physical methods of manipulation (Stanley et al. 1984; Allen et al. 1989; Guo et al. 1996; Nell et al. 2002). Therefore, spawning and subsequent emaciation due to depleted energy reserves does not occur to the same extent as seen in diploid counterparts (Nell et al. 2002). Multiple studies have assessed the effect of ploidy as it relates to oyster health and performance in commercial aquaculture production, such as disease susceptibility (Meyers et al. 1991; Barber and Mann 1991; Dégremont et al. 2015) and growth (Garnier-Géré et al. 2002; Walton et al. 2013). However, the effect of contaminant stress as well as the differences in chemical kinetics in triploids relative to diploids exposed to environmental contaminants such as PAH is vastly understudied. Studies evaluating the bioaccumulation differences in triploids and diploids for environmental contaminants are generally scarce; however, only one other study has been documented examining the effect of ploidy on PAH accumulation (Miles et al. 2014). To date, the difference in PAH uptake and

depuration in transplanted triploid and transplanted diploid oysters relative to wild oysters inhabiting impacted sites has not been investigated. Given the increased growth rate of triploid strains of oysters, further investigation into the role for this popular commercial product in the accumulation of PAHs is necessary.

Antibody-based biosensor technology, specifically the KinExA Inline Sensor coupled with a monoclonal antibody uniformly selective for 3-5–ring PAHs, mAb 2G8, has previously demonstrated its value as a quantitative screening technique for environmental monitoring of contaminants (Camargo et al. 2022; Conder et al. 2021; Li et al. 2016; Hartzell et al. 2017). With near real-time data turnaround and higher sample throughput due to limited expense and minimal preparation requirements, the biosensor has also been successfully employed in a river watershed scale monitoring survey (Prossner et al. 2022). PAH levels were screened in wild oysters to prioritize future remediation efforts throughout the river. In addition, due to the high sensitivity and uniform selectivity of mAb 2G8 and a low-volume sample requirement for analysis, biosensor technology can work within a more refined spatiotemporal scope compared to conventional methods for chemical analysis. For measuring PAH concentrations in biota, gas chromatography coupled with mass spectrometry (GC–MS) is typically employed. GC–MS provides reliable compound-specific concentration measurements for a more extensive quantitative analysis. However, due to time-intensive steps involved in sample preparation including extraction, separation, and cleaning using expensive organic solvents, this approach is not as easily employed for widescale monitoring efforts.

The antibody mAb 2G8, covalently bonded to a fluorescent tag, AlexaFluor 647 (AF647), has also been previously employed in immunohistochemical investigation of the accumulation of environmental PAH mixtures in specific oyster tissues (Prossner et al. 2023). In

a crude oil water-accommodated fraction (WAF) exposure study, oysters were collected throughout a 3-day uptake period and 12-day depuration period. When signal response observed in the plicae of the oyster gill tissue was compared as a time series throughout the exposure, integrated density (i.e. amount of signal in selected image area) was found to increase throughout the uptake phase and decrease throughout the depuration phase. A similar trend was observed in the change in oyster interstitial fluid concentration throughout the experiment, suggesting the amount of signal response of mAb 2G8 bound to PAHs in the tissue is related to PAH body burden at corresponding time points.

In this study, we explore the difference in PAH concentration between wild and transplanted triploid and diploid oysters at the start and end of a 30-day uptake phase and at the end of a 2-week depuration phase. We compare PAH concentration measurements in the oyster interstitial fluid (aqueous phase) measured by biosensor to measurements in the tissue phase measured by GC–MS. Further, we investigated differences in internal PAH partitioning between wild oysters and transplanted triploid oysters, specifically the differences in partitioning between digestive gland (i.e. hepatopancreas) and gill, to gain insight into possible mechanisms driving the observed differences in biomonitoring approaches. The uptake phase took place at an unremediated field site in the Elizabeth River (Virginia, USA) at the historic Republic creosote plant site, a known PAH hotspot. Oysters were then relocated to the York River (Virginia, USA) for a 14-day depuration period. This is the first-documented study comparing these three populations in a PAH exposure study.

Methods and Materials

Experimental design

The uptake phase of the study took place in early summer conditions (late May to early July) at the Republic field site in the Elizabeth River (Virginia, USA), a sub-tributary located near the mouth of the Chesapeake Bay. Republic is the site of a former creosote wood treatment plant and known PAH hotspot. Oysters were held in cages secured to a dolphin piling centrally located at the site in subtidal conditions. The uptake phase lasted for a 30-day period. On the final day of uptake, oysters were relocated to the York River in Gloucester Point, VA to depurate for 14 days. Oyster cages were secured to concrete pier pilings and held in subtidal conditions. Oyster were sampled at the start of uptake (T0), end of uptake (T4), and at the end of depuration (T6). Three replicate cages, each containing one bag of wild oysters and diploid oysters and two bags of triploid oysters (one bag for total concentration comparison and internal partitioning, respectively), were employed to avoid overcrowding of oysters and for protection against predation and loss due to vessel traffic and large wakes.

Wild oysters were collected from pilings and shoreline at the Republic site as samples of convenience. Farmed diploid oysters were reared in the Rappahannock River from seed in Middlesex County, Virginia, USA (~112 km from study site). Farmed triploid oysters were reared in Gloucester County, Virginia, USA in the York River (~80km from study site). Oyster shell heights from the umbo to the bill edge were measured using calipers prior to experimentation.

Sample Preparation for biosensor analysis

For biosensor analysis of transplanted triploid and diploid oysters total PAH concentrations, whole, (i.e. in-shell) oysters were collected, immediately placed in plastic bags

and transported in coolers on ice to the laboratory (~65 km away). Upon arrival, the animals were immediately stored whole at -20°C until further preparation. For processing, oysters were thawed, opened with a shucking knife, and an aliquot of oyster interstitial fluid pooled within the shell was collected using a disposable glass Pasteur pipet. The aliquot of fluid was transferred to a glass 20mL scintillation vial. The oyster interstitial fluid was then filtered through a 0.45 µm PTFE syringe filter, the filtrate transferred to a clean scintillation vial, and stored at -20°C until analysis. Three individual oysters were sampled per group per time point. Due to constraints on the availability of diploid oysters for transplantation, the total concentration was the sole measurement collected for this group by biosensor. Remaining soft tissue of the three individual oysters per group per cage at each time point were pooled (i.e. triplicate pooled samples per group per time point), and transferred to a glass screw-top jar for further preparation for GC–MS analysis.

For biosensor analysis of transplanted triploids for internal partitioning, sample collection, transport from the field, and storage prior to preparation were described above. Separate groups of triploid oysters were used for the comparisons of total concentrations and internal partitioning to ensure adequate sample volumes. The gill and digestive gland were dissected from 5 individual oysters and pooled. Based on a preliminary experiment, a minimum of 5 oysters is required to achieve sufficient volume for biosensor analysis (~1 mL). A small section of each tissue type from one of the 5 oysters per group per cage was collected for further cryopreservation and IHC preparation described in the below section. The pooled samples were homogenized via manual maceration to create one homogenized gill sample and one homogenized digestive gland sample. One sample of each tissue was collected per group per cage at each time point (i.e. the gill and digestive gland was removed from 5 individual oysters

per group per time point for 3 replicate cages). Homogenized gill and digestive gland samples were then centrifuged, and the supernatant was collected using a glass disposable Pasteur pipet and transferred to a glass scintillation vial. Gill and digestive gland fluid was then filtered through a 0.45µm PTFE syringe filter and transferred to a clean scintillation vial. Samples were stored at -20°C until analysis.

Sample preparation for wild oysters proceeded as described above; however, due to the constraint of limited abundance of wild oysters at the Republic site, oyster interstitial fluid for total concentration comparison, gill and digestive gland fluid for internal partitioning, and individual tissue sections for IHC were collected from the same individual oysters. Therefore, an aliquot of oyster interstitial fluid from 5 oysters per cage per time point were sampled for total concentration comparison. Then, respective gill and digestive glands were dissected, pooled, and homogenized to generate digestive gland fluid and gill fluid. The remaining tissue following centrifugation was reserved and combined with the remaining soft tissue of the 5 oysters per cage per time point. The soft tissue was then pooled to generate triplicate samples per time point for further preparation for GC–MS analysis. This constraint led to an unequal sample size between groups so that the minimum sample size requirement for generating gill and digestive gland fluid could also be achieved. This was accounted for in subsequent statistical analyses, as described in the corresponding section. Figure 1 describes the sampling regime throughout the experiment and experimental set-up.

Biosensor Analysis

The procedure for analysis with the KinExA Inline Sensor (Sapidyne Instruments) as well as the selection and screening of mAb 2G8 have been described previously (Spier et al. 2011; Spier et al., 2012; Li et al. 2016; Prossner et al. 2022). Briefly, the sensor functions as a kinetic

assay in which AF647-tagged mAb 2G8 mixes with an aqueous sample and binds PAH. The sample-antibody solution is passed over antigen (1-pyrene-butyric acid), held stationary in a glass flow cell in front of the detector, and remaining free antibody will bind to the antigen and a signal response (dV) is measured. Prior to sample analysis, a 5-point calibration curve is generated using series of phenanthrene standards (0.5 to 2.5 µg/L) and laboratory blank (double deionized water; ddH2O) to establish the linear range of the detector's response. To stay within the range of the calibration curve, samples are diluted with ddH20, if necessary. The measured signal response and required dilution factor are then used to calculate a total 3-5 ring PAH concentration (µg/L).

GC–MS analysis

Preparation of oyster tissue for GC–MS analysis has been described previously (Prossner et al. 2022). Composite tissue samples were thawed and homogenized using a Virtis Homogenizer. All components for homogenization (stainless steel blades, glass reservoir, and lid) were cleaned prior to each sample. The liquified sample was then poured into a pre-cleaned glass trough and freeze-dried along with a laboratory blank. Samples and blanks were spiked with a deuterated PAH surrogate standard and solvent extracted using an accelerated solvent extractor. Samples were then reduced under a gentle stream of nitrogen held in a 40°C bath in a TurboVap evaporator. For size exclusion separation, a standard protocol was followed using a high-performance liquid chromatograph (HPLC) coupled with a gel permeation column (GPC). Fractionation and polar compound removal was achieved via open column chromatography containing deactivated silica gel through a series of elutions. The tissue extracts were then solvent exchanged to 100% dichloromethane and concentrated to a final volume. A set of calibration standards was spiked with an internal standard, p-terphenyl, and used to generate a

calibration curve for analysis. Both parent and methylated compounds were analyzed for a total of 64 analytes. Concentrations are reported in µg/kg dry weight.

Tissue specimen preparation and IHC processing for imaging

Section preparation and IHC processing for oyster tissue have been described previously (Prossner et al. 2023). Gill and digestive gland tissue fragments (~6mm^3) were dissected from each oyster and embedded in optimal cutting temperature (OCT) media in a disposable cryo-mold. Approximately 300mL of pentane was held in a small stainless-steel bowl within a bath of liquid nitrogen. The mold was then partially submerged in the cooled pentane until entirely frozen. Frozen blocks were stored at -80°C. Twenty-four hours prior to cryosectioning, blocks were warmed to -20°C. Upon cryosectioning, blocks were removed from their mold and frozen to an aluminum chuck and 10µm sections were cut at -10°C on a cryostat (Leica CM3050 S). Sections were pressed onto a positively-charged glass slide (Superfrost Plus; Fisher Scientific) at room temperature. Once mounted, sections were fixed in 4% paraformaldehyde in 1X phosphate buffered saline (PBS) for 20 mins, then immersed in a blocking and permeabilization solution for a 1hr incubation period. Sections were then incubated in an AF647-tagged mAb 2G8 coating solution overnight in a moist chamber at 4°C. The next day, sections were incubated with 4′,6-diamidino-2-phenylindole (DAPI) in 1X PBS for 15 minutes. Between each step, sections were thoroughly washed via three five-minute baths in 1X PBS. Upon carefully wiping off excess moisture, a coverslip was mounted using Dako mounting media. After drying, the edges around the cover slip were sealed with clear nail varnish. Preparation of negative controls followed the same procedure but were incubated in a blank antibody solution overnight. Images were captured using a FLUOVIEW FV1200 confocal laser scanning microscope (Olympus) with filter sets for DAPI and AF647.

Image analysis

The procedure for image analysis has been described previously (Prossner et al. 2023). Integrated density was measured using FIJI image analysis software (Schindelin et al. 2012). Integrated density is the product of total selected measurement area and mean gray value within the area. Upon analysis, a uniform scale and intensity threshold was set across images for comparison. In gill tissue, measurements in triplicate were made on three plicae per image. For subsequent comparison between groups, individual Welch two-sample t-tests were performed at each time point to determine if a significant difference in group means was present.

Statistical Analyses

The assumptions of homoscedasticity and normality were not met to conduct an analysis of variance (ANOVA), based on results on a Shapiro-Wilke test for normality, Bartlett's test for homogeneity of variance, and plotting of residuals. Therefore, the response factor, PAH concentration (µg/L), was $\log_{10}$-transformed to better meet or approximate these assumptions. In addition, the experimental set-up did not allow for the assumption of independent data to be met when means are compared across all time points. Because different individual oysters were sampled at each time point, a repeated measures ANOVA is inappropriate. In addition, comparing the rate of change in PAH concentration over time between groups was not a research objective. Therefore, separate ANOVAs were conducted at each time point to meet all assumptions for ANOVA which was sufficient for testing our hypotheses. For determining a significance difference in mean total PAH concentrations between groups, a one-way ANOVA was conducted in R using the pipeline-friendly 'rstatix' package for streamlined incorporation of statistical results into figures when data were plotted using package 'ggplot2'. If results of the ANOVA indicated that the true difference between means was not equal to zero, a Games-

Howell *post hoc* test was used to account for unequal sample size. For determining significant difference in mean gill fluid and digestive gland fluid between groups, individual two-way ANOVAs were conducted at each time point. A 0.05 significance level was selected for all analyses.

Results and Discussion

Total concentration comparison

Oysters exhibited significant differences in their uptake and depuration of 3-5–ring PAH concentrations in the oyster interstitial fluid based on their origin of location: wild oysters inhabiting a PAH-impacted field site in the Elizabeth River (the former site of Republic creosote plant), transplanted diploid oysters, and transplanted triploid oysters. At the start of uptake (Figure 2A), wild oysters had significantly higher concentrations measured in oyster interstitial fluid relative to the transplanted groups. There was no significant difference between transplant concentrations in diploid and triploid cultured oysters. Notably, concentrations above the detection limit were present in both transplanted groups, even though they were originally acquired from aquaculture facilities. At the end of uptake (Figure 2B), both transplanted groups had accumulated concentrations that were significantly higher than what was measured in the wild oysters. There was no significant difference observed between the two transplanted groups. By the end of depuration in the York River (Figure 2C), the concentration of residual PAH in oyster interstitial fluid was significantly different between the wild Republic oysters and transplanted triploids. In addition, the variance was much wider in the concentrations found in wild oysters from the contaminated site.

PAH concentrations measured in wild oysters were similar between the start of uptake and end of uptake, supporting the assumption that wild oysters are at steady-state with the

environment at Republic. The similar levels of PAH accumulated by the end of uptake observed in the transplanted oyster groups aligns with the results observed in Miles et al. (2014). When transplanted triploid oysters were compared to transplanted diploid oysters that had not yet spawned, similar PAH concentrations were observed. We also found that concentrations were similar between transplanted triploids and diploids suggesting the diploids were in a pre-spawning state during this experiment. However, Miles and colleagues found significant differences were observed during spawning season in which triploids had overall higher levels relative to diploids. A higher triploid body burden was also observed in a study comparing trace metal bioaccumulation between groups when deployed in an estuary (Robinson et al. 2005).

At the end of depuration, the observation of elevated, though highly variable, concentrations in the wild Republic oysters relative to the transplanted groups supports findings by Sericano et al. (1996) in which newly exposed transplanted oysters were compared to chronically exposed native oysters inhabiting a PAH-impacted site in the Houston Ship Channel. By the end of depuration, native oysters retained higher levels of PAH relative to the transplanted oysters. Notably, the matrices used for analysis are different between studies so only a general trend comparison can be made. The variability in concentrations measured in wild oysters may be attributed to limitations of passive sampling approaches: an inability to control for biological parameters in wild populations and the requirement of convenience sampling due to the heterogenous distribution of oysters at a site (Beyer et al. 2017).

Mean shell height of the transplanted diploid oysters was significantly longer than both the wild and transplanted triploid groups (Supplemental Figure S1). However, when total extractable lipid on a dry weight basis was compared across groups, transplanted triploids had a significantly higher percentage of lipid relative to the wild oysters (Supplemental Figure S2).

The size difference observed between oysters may be a confounding factor in this study; however, based on the comparison of the lipid per dry weight, diploid size difference may not be an influential factor. A limitation for this study was the availability of wild oysters and diploid cultured oysters for transplantation. Future iterations of this study should control for size to avoid this potential source of variability.

When mean PAH concentrations in oyster tissue were compared between groups at each time point, different trends were observed relative to the oyster interstitial fluid. A significant difference was only observed between wild and transplanted triploids at the start of uptake (Figure 3A). The wild and transplanted diploids comparison was on the margin of significance ($p=0.053$). Concentrations were not significantly different between groups at the end of uptake (Figure 3B) and at the end of depuration (Figure 3C). Total concentrations per cage were also compared at each time point and no significant difference was detected, suggesting cage assignment did not contribute additional variability (Supplemental Figure S3).

The difference in trends observed in tissue concentrations relative to those of oyster interstitial fluid concentrations supports the hypothesis that 30 days was not enough time for the transplanted oysters to achieve steady state with the environment, as has been suggested previously (Sericano et al. 1996, Shoyen et al. 2017). And as an extension, revealed through biosensor analysis of the oyster interstitial fluid, the observed differences in trends between the aqueous (oyster interstitial fluid) and tissue phase within an oyster reflect non-steady state conditions within the oyster as well. The biosensor demonstrates value in facilitating further scrutiny of mechanistic differences in contaminant between transplanted and native groups with its ability to work within small spatiotemporal scales.

Future replication of this study should incorporate seasonal variation into experimental design to further investigate the effect of ploidy and differences in dynamic energy budgeting on PAH kinetics. Dynamic energy budgeting models have been previously employed to account for biological factors, such as physiology, energy storage, and reproductive status, that can influence contaminant uptake (van Haren et al. 1994; van Haren and Koojman 1993; Grech et al. 2017; Beyer et al. 2017). More work is needed to better understand how a difference in energy budgeting and reproductive status in triploids could impact overall contaminant body burden. This is important not only for evaluating triploid oysters as a novel biomonitoring tool, but for understanding potential adverse health risks associated with consuming this popular seafood product.

Internal partitioning

Digestive gland and gill fluid comparison via biosensor

Overall, differences in PAH concentrations were observed between groups and between fluid types throughout the experiment. At the start of the uptake period (Figure 4A), wild Republic oysters had an overall higher level of PAH relative to the transplanted triploid for both fluid types. By the end of uptake (Figure 4B), transplanted triploids had accumulated an overall higher concentration of PAH for both fluid types relative to the wild oysters. In addition, when the overall concentrations between tissue types were compared, a significantly higher level of PAH was measured in the digestive gland fluid relative to gill fluid. At the end of depuration (Figure 4C), the overall concentrations between groups were similar; however, the digestive gland fluid had an overall higher level of residual PAH relative to the gill fluid.

The differences observed in PAH concentrations between groups and between overall fluid types at each time point suggest that internal partitioning is important in driving the overall

PAH concentrations observed in wild and transplanted oysters. At the start of uptake, the concentrations measured in each fluid type for each group are similar, which indicates that internal compartments are at steady state for each oyster group at the start of the experiment. By the end of uptake, a higher level of PAH was measured in the digestive gland. This trend is maintained through the end of the experiment where the digestive gland fluid still retains a significantly higher PAH concentration relative to the gill. These findings provide further evidence that elimination of PAH from this lipid-rich organ is rate-limiting, also supporting previous hypotheses that mechanisms controlling uptake and depuration in bivalves are complex, and that simple one-compartment kinetic models ascribed to these organisms for simplicity may be inappropriate (Beyer et al. 2012; Grech et al. 2017; van Haren et al. 1994; van Haren and Koojman 1993). Higher PAH concentrations in bivalve digestive gland tissue relative to other tissue types and slower elimination rates have been measured in previous PAH kinetic studies exploring internal partitioning, indicating that this organ is an important storage site for PAH accumulation (Widdows et al.1983; Bustamante et al. 2012; Wang et al. 2020). Further Lacroix et al. (2015) observed higher PAH concentrations in the digestive gland tissue of transplanted mussels relative to wild mussels at an impacted site in a study comparing active and passive biomonitoring methods.

The results from this preliminary internal partitioning study warrant further investigation in a larger-scale study with increased sample size. Using the results from this study to determine an effect size for a power analysis, an estimated sample size of n=18-20 fluid per group would be needed to have a higher probability of detecting a significant difference between fluid types of respective groups. With a low-volume sample requirement, antibody-based biosensor technology demonstrates its value in exploring internal partitioning as final digestive gland and gill fluid

volumes successfully collected for analysis were typically less than 1mL. This technology shows promise in facilitating future investigations of mechanisms driving internal partitioning within different compartments in an individual oyster and calibrating ascribed kinetic models. An improved understanding internal chemical dynamics may lead to a better understanding of the differences observed between transplanted and wild groups.

IHC-facilitated visualization of PAH in tissue and comparative analysis

IHC analysis provided further visual evidence of differences in internal partitioning between wild and transplanted triploids and these findings were confirmed via a comparative analysis of integrated signal density. The level of signal observed in wild gill tissue did not appear to significantly change between the start and end of the uptake phase at Republic, further confirming steady state conditions within these oysters (Figures 5A-B). When transferred to the York River, the level of signal observed in the wild Republic gill was reduced (Figure 5C). Comparing the intensity of signal observed in wild Republic gill to transplant triploid gill, the signal appears less intense in the transplanted triploids at the start of the uptake phase (Figure 5D). However, by the end of uptake the transplanted triploid gill had accumulated a PAH level that far surpassed the level observed in wild Republic gill collected at the same time point as evidenced by the significantly more intense signal (Figure 5E). By the end of depuration, a higher signal is observed in the transplant triploid gill relative to the wild Republic oyster suggesting higher levels of PAH were retained (Figure 5F). Negative controls were prepared and autofluorescence was not observed in gill images, confirming that our observed signal is attributed to mAb 2G8 binding to PAH (Supplemental Figure S4). Our visual observations at each time point were confirmed when integrated density was measured for three plicae per image and means were compared at each time point (Welch Two-Sample T-test) (Figure 6).

Interference due to suspected autofluorescence prevented adequate visualization of PAH binding and further analysis of digestive gland images. Through visual comparison to positive control gill images, there appears to be a distinct size, shape, and location associated with the signal association with PAH-bound mAb 2G8. Granular particles generally uniform in size and intensity are observed along the plicae edges throughout all gill image sections. In the positive control digestive gland images, structures of similar shape and size are observed along the interior edges of digestive tubules (Figure S5) and are not observed in the negative control images (Figure S6). Further work is needed to identify these structures associated with PAH signal and to differentiate this signal from autofluorescence in the digestive gland or reduce autofluorescence altogether.

At the start of uptake, the results of our gill plicae image analysis align with visual observations in Figure 4A: wild Republic oysters had higher PAH level in gill fluid relative to the transplanted triploids (although not found to be statistically significant). In addition, at the end of uptake, the results of gill image analysis aligns with our visual comparisons in Figure 4B, that transplanted triploids had accumulated PAH in gill fluid that surpassed the levels measured in wild oyster gill fluid (although, again, determined to be statistically insignificant). The trend observed at the end of depuration in image analysis differed from our findings in gill fluid concentration comparison at the same time point Figure 4C in which concentrations were similar. It is important to note the small sample size for tissue fluid comparison and immunohistochemical comparison further extrapolation of our findings. However, our preliminary findings suggest the incorporation of immunohistochemical visualization in analysis could be valuable in understanding PAH kinetics in organisms and possible mechanistic differences between wild and transplanted groups. Immunohistochemical visualization utilizing

mAb 2G8 could be coupled with biomarker studies investigating potential metabolic adaptations in chronically exposed wild population that may reduce stress response. Further work should also investigate differences between transplanted diploid and triploid groups.

Conclusions

Using novel immunological techniques and conventional GC–MS analysis, we explored differences in PAH concentrations between wild oysters inhabiting a PAH-impacted field site in the Elizabeth River, Republic, and cultured triploid and diploid oysters. We also preliminarily investigated differences in internal partitioning between wild Republic oysters and transplanted triploid oysters. Transplanted oysters were deployed at Republic for 30 days, and then all oysters were relocated to the York River for a 14-day depuration period. When oyster interstitial fluid concentrations were compared between groups, wild oysters had higher levels at the start of the 30-day uptake period, but levels measured in transplanted groups by the end of uptake surpassed those observed in the wild oysters. By the end of depuration, wild oysters retained higher levels of PAH relative to the transplanted triploids. Concentrations were not significantly different between transplanted groups at each time point. Interestingly, a different trend was observed at the end of uptake and depuration when tissue concentrations were compared: all three groups had similar concentrations at these time points. These findings support the hypothesis that kinetic rates and insufficient equilibration time (both with the environment and within internal phases of the oyster) may significantly contribute to observed differences in wild and transplanted groups. Future work should also incorporate seasonal variability to observe differences in PAH body burden and energy budgeting between triploid and diploid oysters post-spawning.

To explore the differences in internal partitioning within an oyster, digestive gland homogenate fluid and gill homogenate fluid were compared between wild Republic oysters and

transplanted triploids. Although a significant difference in concentration was not detected between the different tissue-specific fluids of respective groups, overall differences were observed between tissue types and between treatment groups. At the start of uptake, the wild Republic oysters had higher concentration overall relative to transplanted triploids At the end of uptake, transplanted triploids had accumulated a higher overall concertation relative to what was measured in the wild oysters. This aligns with the trends observed in the oyster interstitial fluid at this time point. Overall, the digestive gland fluid concentrations were significantly higher than gill fluid concentrations at the end of uptake and end of depuration, suggesting the importance of the digestive gland in sequestering PAH. Overall our findings suggest that internal partitioning may be an important factor in total concentrations measured in an oyster. Visualization of PAH accumulation in oyster gill tissue and subsequent image analysis supports our observed trends at the start and end of uptake in overall concentration differences between groups.

Overall, the decision of which biomonitoring method to use may depend on the research question and objectives. Passive biomonitoring may be more valuable for long-term monitoring of impacted sites and remediation progress. To evaluate an acute exposure, active biomonitoring may be the better approach. However, it is still necessary to have a better understanding of why differences in total PAH concentrations are observed between methods. By applying of sensitive analytical approaches such as antibody-based biosensor instrumentation and immunohistochemistry, we demonstrate their value in investigating mechanisms driving PAH kinetics in oysters. The low-volume sample requirement of biosensor technology allows for the analysis of individual oysters and fluid samples from individual organs. These features make investigating small-scope mechanistic questions much more feasible. With the employment of mAb 2G8, selective for a range of 3-5 PAH compounds, in an immunohistochemical application,

we are able to visualize bioaccumulation of a PAH mixtures to which oysters were exposed in the environment. Although our exploration into internal partitioning differences between transplanted triploids and wild oysters is preliminary in nature, nevertheless, we further demonstrate the value of incorporating a novel approach for addressing environmental chemistry-related questions that cannot be as sufficiently answered by conventional methods. This includes understanding the differences between active and passive biomonitoring methods.

References

Allen Jr, S. K., & Downing, S. L., 1986. Performance of triploid Pacific oysters, Crassostrea gigas (Thunberg). I. Survival, growth, glycogen content, and sexual maturation in yearlings. *Journal of Experimental Marine Biology and Ecology* 102, 197-208.

Allen, S.K., Downing, S. L., & Chew, K. K.,1989. *Hatchery manual for producing triploid oysters*. Washington Sea Grant Program.

Barber, B. J., & Mann, R. L., 1991. Sterile triploid Crassostrea virginica (Gmelin, 1791) grow faster than diploids but are equally susceptible to Perkinsus marinus. *Journal of Shellfish Research* 10, 445.

Besse, J. P., Geffard, O., & Coquery, M., 2012. Relevance and applicability of active biomonitoring in continental waters under the Water Framework Directive. *TrAC Trends in Analytical Chemistry* 36, 113-127.

Beyer, J., Green, N.W., Brooks, S., Allan, I.J., Ruus, A., Gomes, T., Bråte, I.L.N. and Schøyen, M., 2017. Blue mussels (Mytilus edulis spp.) as sentinel organisms in coastal pollution monitoring: a review. *Marine Environmental Research* 130, 338-365.

Bodin, N., Burgeot, T., Stanisiere, J.Y., Bocquené, G., Menard, D., Minier, C., Boutet, I., Amat, A., Cherel, Y. and Budzinski, H., 2004. Seasonal variations of a battery of biomarkers and physiological indices for the mussel Mytilus galloprovincialis transplanted into the northwest Mediterranean Sea. *Comparative Biochemistry and Physiology Part C: Toxicology & Pharmacology* 138, 411-427.

Bustamante, P., Luna-Acosta, A., Clemens, S., Cassi, R., Thomas-Guyon, H., & Warnau, M., 2012. Bioaccumulation and metabolisation of 14C-pyrene by the Pacific oyster Crassostrea gigas exposed via seawater. *Chemosphere* 87, 938-944.

Callam, B. R., Allen Jr, S. K., & Frank-Lawale, A., 2016. Genetic and environmental influence on triploid Crassostrea virginica grown in Chesapeake Bay: growth. *Aquaculture* 452, 97-106.

Camargo, K., Vogelbein, M.A., Horney, J.A., Dellapenna, T.M., Knap, A.H., Sericano, J.L., Wade, T.L., McDonald, T.J., Chiu, W.A. and Unger, M.A., 2022. Biosensor applications in contaminated estuaries: Implications for disaster research response. *Environmental Research* 204, 111893.

Cheney, D.P., 2010. Bivalve shellfish quality in the USA: from the hatchery to the consumer. *Journal of the World Aquaculture Society* 41, 192-206.

Conder, J., Jalalizadeh, M., Luo, H., Bess, A., Sande, S., Healey, M., & Unger, M. A., 2021. Evaluation of a rapid biosensor tool for measuring PAH availability in petroleum-impacted sediment. *Environmental Advances* 3, 100032.

Dégremont, L., Garcia, C., & Allen Jr, S. K., 2015. Genetic improvement for disease resistance in oysters: a review. *Journal of Invertebrate Pathology* 131, 226-241.

Faria, M., López, M. A., Díez, S., & Barata, C., 2010. Are native naiads more tolerant to pollution than exotic freshwater bivalve species? An hypothesis tested using physiological responses of three species transplanted to mercury contaminated sites in the Ebro River (NE, Spain). *Chemosphere* 81, 1218-1226.

Farrington, J. W., Goldberg, E. D., Risebrough, R. W., Martin, J. H., & Bowen, V. T., 1983. US" Mussel Watch" 1976-1978: an overview of the trace-metal, DDE, PCB, hydrocarbon and artificial radionuclide data. *Environmental Science & Technology* 17, 490-496.

Farrington, J. W., Tripp, B. W., Tanabe, S., Subramanian, A., Sericano, J. L., Wade, T. L., & Knap, A. H., 2016. Edward D. Goldberg's proposal of "The Mussel Watch": Reflections after 40 years. *Marine Pollution Bulletin* 110, 501-510.

Garnier-Géré, P.H., Naciri-Graven, Y., Bougrier, S., Magoulas, A., Héral, M., Kotoulas, G., Hawkins, A. and Gérard, A., 2002. Influences of triploidy, parentage and genetic diversity on growth of the Pacific oyster Crassostrea gigas reared in contrasting natural environments. *Molecular Ecology* 11, 1499-1514.

Goldberg, E.D., Bowen, V.T., Farrington, J.W., Harvey, G., Martin, J.H., Parker, P.L., Risebrough, R.W., Robertson, W., Schneider, E. and Gamble, E., 1978. The mussel watch. *Environmental conservation* 5, 101-125.

Greenfield, R., Brink, K., Degger, N., & Wepener, V., 2014. The usefulness of transplantation studies in monitoring of metals in the marine environment: South African experience. *Marine pollution bulletin* 85, 566-573.

Grech, A., Brochot, C., Dorne, J. L., Quignot, N., Bois, F. Y., & Beaudouin, R., 2017. Toxicokinetic models and related tools in environmental risk assessment of chemicals. *Science of the Total Environment* 578, 1-15.

Guo, X., DeBrosse, G. A., & Allen Jr, S. K., 1996. All-triploid Pacific oysters (Crassostrea gigas Thunberg) produced by mating tetraploids and diploids. *Aquaculture* 142, 149-161.

Hartzell, S. E., Unger, M. A., McGee, B. L., & Yonkos, L. T., 2017. Effects-based spatial assessment of contaminated estuarine sediments from Bear Creek, Baltimore Harbor, MD, USA. *Environmental Science and Pollution Research* 24, 22158-22172.

James, M., 1989. Biotransformation and disposition of PAH in aquatic invertebrates. In: Varanasi, U. (Ed.), Metabolism of Polycyclic Aromatic Hydrocarbons in the Aquatic Environment. CRC Press, Boca Raton, FL, USA, pp. 69–92.

Kazour, M. and Amara, R., 2020. Is blue mussel caging an efficient method for monitoring environmental microplastics pollution?. *Science of The Total Environment* 710, 135649.

Lacroix, C., Richard, G., Seguineau, C., Guyomarch, J., Moraga, D., & Auffret, M., 2015. Active and passive biomonitoring suggest metabolic adaptation in blue mussels (Mytilus spp.) chronically exposed to a moderate contamination in Brest harbor (France). *Aquatic Toxicology* 162, 126-137.

Li, X., Kaattari, S. L., Vogelbein, M. A., Vadas, G. G., & Unger, M. A., 2016. A highly sensitive monoclonal antibody-based biosensor for quantifying 3–5 ring polycyclic aromatic hydrocarbons (PAHs) in aqueous environmental samples. *Sensing and Bio-Sensing Research* 7, 115-120.

Marigómez, I., Zorita, I., Izagirre, U., Ortiz-Zarragoitia, M., Navarro, P., Etxebarria, N., Orbea, A., Soto, M. and Cajaraville, M.P., 2013. Combined use of native and caged mussels to assess biological effects of pollution through the integrative biomarker approach. *Aquatic toxicology* 136, 32-48.

Meyers, Judith A., Eugene M. Burreson, Bruce J. Barber, and Roger L. Mann., 1991. "Susceptibility of diploid and triploid Pacific oysters, Crassostrea gigas (Thunberg, 1793) and eastern oysters, Crassostrea virginica (Gmelin, 1791), to Perkinsus marinus." *Journal of Shellfish Research* 10, 433.

Miles, M. S., Malone, R. F., & Supan, J. E., 2014. Evaluation of Triploid Oysters as a Tool to assess Short-and Long-term Seafood Contamination of Oil Spill-impacted Areas. In *International Oil Spill Conference Proceedings* (Vol. 2014, No. 1, pp. 1958-1971). American Petroleum Institute.

Nell, J. A., 2002. Farming triploid oysters. *Aquaculture* 210, 69-88.

Prossner, K. M., Vadas, G. G., Harvey, E., & Unger, M. A., 2022. A novel antibody-based biosensor method for the rapid measurement of PAH contamination in oysters. *Environmental Technology and Innovation* 28, 102567.

Prossner, K.M., Small, H.J., Carnegie, R.B. and Unger, M.A., 2023. Immunofluorescence Visualization of Polycyclic Aromatic Hydrocarbon Mixtures in the Eastern Oyster Crassostrea virginica. *Environmental Toxicology and Chemistry* 42, 475-480.

Robinson, W. A., Maher, W. A., Krikowa, F., Nell, J. A., & Hand, R., 2005. The use of the oyster Saccostrea glomerata as a biomonitor of trace metal contamination: intra-sample, local scale and temporal variability and its implications for biomonitoring. *Journal of Environmental Monitoring* 7, 208-223.

Schindelin, J., Arganda-Carreras, I., Frise, E., Kaynig, V., Longair, M., Pietzsch, T., Preibisch, S., Rueden, C., Saalfeld, S., Schmid, B. and Tinevez, J.Y., 2012. Fiji: an open-source platform for biological-image analysis. *Nature Methods* 9, 676-682.

Schøyen, M., Allan, I.J., Ruus, A., Håvardstun, J., Hjermann, D.Ø. and Beyer, J., 2017. Comparison of caged and native blue mussels (Mytilus edulis spp.) for environmental monitoring of PAH, PCB and trace metals. *Marine Environmental Research* 130, 221-232.

Sericano, J.L., Wade, T.L., Jackson, T.J., Brooks, J.M., Tripp, B.W., Farrington, J.W., Mee, L.D., Readmann, J.W., Villeneuve, J.P. and Goldberg, E.D., 1995. Trace organic contamination in the Americas: an overview of the US National Status & Trends and the International 'Mussel Watch' programmes. *Marine Pollution Bulletin* 31, 214-225.

Sericano, J. L., Wade, T. L., & Brooks, J. M., 1996. Accumulation and depuration of organic contaminants by the American oyster (Crassostrea virginica). *Science of the Total Environment* 179, 149-160.

Spier, C. R., Vadas, G. G., Kaattari, S. L., & Unger, M. A., 2011. Near real-time, on-site, quantitative analysis of PAHs in the aqueous environment using an antibody-based biosensor. *Environmental Toxicology and Chemistry* 30, 1557-1563.

Spier, C.R., Unger, M.A. and Kaattari, S.L., 2012. Antibody-based biosensors for small environmental pollutants: Focusing on PAHs. *Biosensors and Environmental Health*, p.273.

Stanley, J. G., Hidu, H., & Allen Jr, S. K., 1984. Growth of American oysters increased by polyploidy induced by blocking meiosis I but not meiosis II. *Aquaculture*, *37*, 147-155.

Van Haren, R. J. F., & Kooijman, S. A. L. M., 1993. Application of a dynamic energy budget model to Mytilus edulis (L.). *Netherlands Journal of Sea Research* 31, 119-133.

Van Haren, R. J. F., Schepers, H. E., & Kooijman, S. A. L. M., 1994. Dynamic energy budgets affect kinetics of xenobiotics in the marine mussel Mytilus edulis. *Chemosphere* 29, 163-189.

Wade, T. L., Sericano, J., Gardinali, P. R., Wolff, G., & Chambers, L., 1998. NOAA's 'Mussel Watch'project: Current use organic compounds in bivalves. *Marine Pollution Bulletin* 37, 20-26.

Wadsworth, P., Wilson, A. E., & Walton, W. C., 2019. A meta-analysis of growth rate in diploid and triploid oysters. *Aquaculture* 499, 9-16.

Walton, W. C., Rikard, F. S., Chaplin, G. I., Davis, J. E., Arias, C. R., & Supan, J. E., 2013. Effects of ploidy and gear on the performance of cultured oysters, Crassostrea virginica:

survival, growth, shape, condition index and Vibrio abundances. *Aquaculture* 414, 260-266.

Wang, H., Huang, W., Gong, Y., Chen, C., Zhang, T. and Diao, X., 2020. Occurrence and potential health risks assessment of polycyclic aromatic hydrocarbons (PAHs) in different tissues of bivalves from Hainan Island, China. *Food and Chemical Toxicology* 136, 111108.

Widdows, J., Moore, S. L., Clarke, K. R., & Donkin, P., 1983. Uptake, tissue distribution and elimination of [1-14 C] naphthalene in the mussel Mytilus edulis. *Marine Biology* 76, 109-114.

Figures

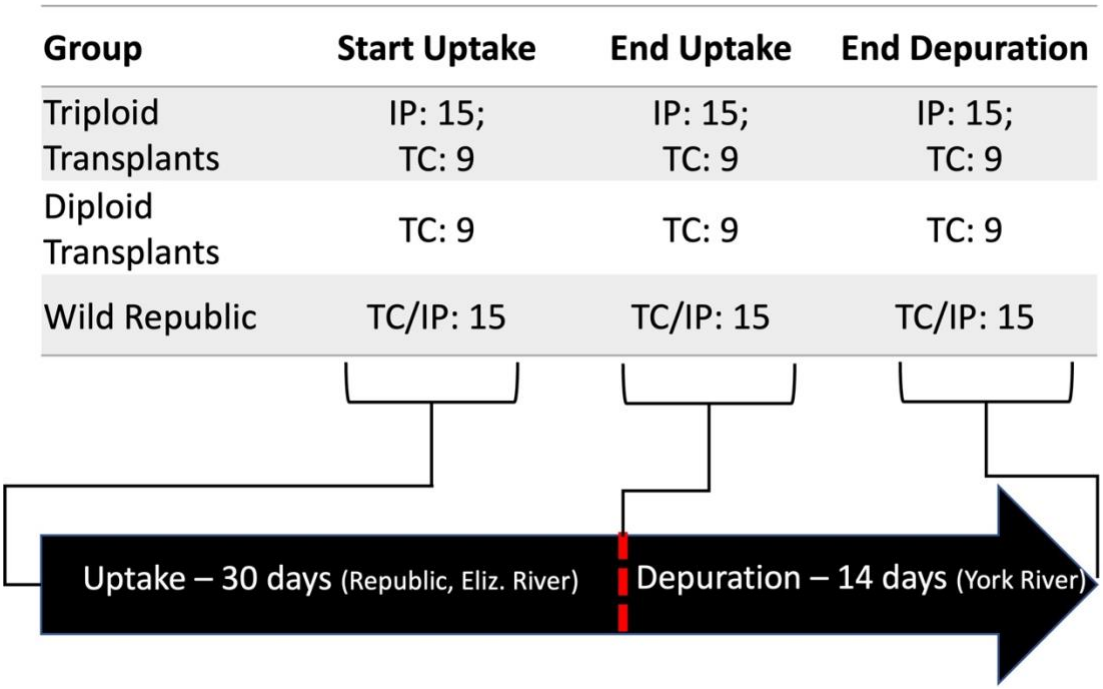

Figure 4. Schematic of experimental design and sampling regime at each time point as described in text. IP = number of oysters collected for analysis of digestive gland fluid and gill fluid to evaluate internal partitioning. TC= number of oysters collected for analysis of oyster interstitial fluid to compare mean PAH concentrations across oyster groups. IP/TC= samples collected for both analyses of respective objectives that were conducted on the same set of oysters. Number of samples collected at each time point (15 or 9) depict the total number of oysters collected across 3 cages (i.e. 5 oysters per cage or 3 oysters per cage for each time point). Not depicted in schematic: a gill and digestive gland tissue fragment was collected from one IP oyster per group per time for IHC.

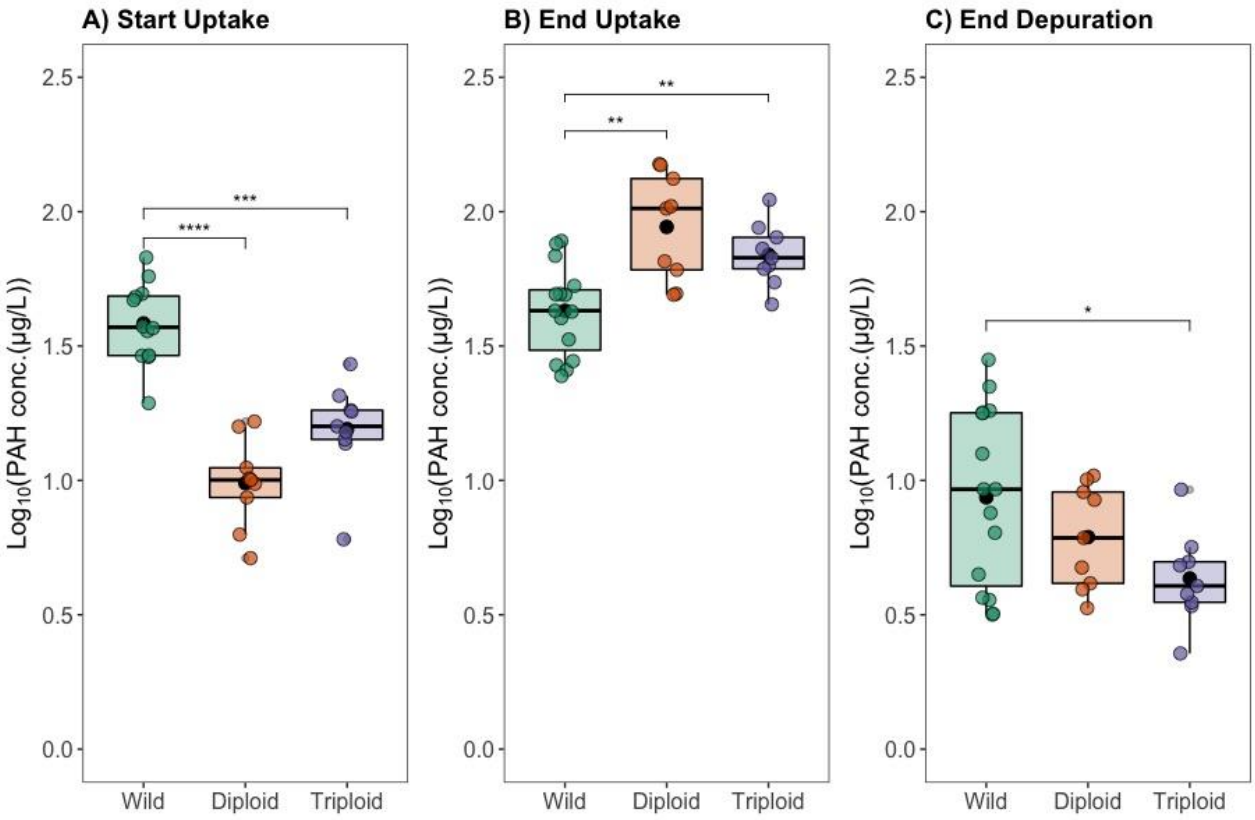

Figure 5. Mean total PAH concentrations in oyster interstitial fluid as measured by antibody-based biosensor technology compared between wild oysters from the Republic site, transplanted diploid oysters, and transplanted triploid oysters at each time point: **A)** start of uptake phase (Day 0); **B)** end of uptake phase (Day 30); and **C)** end of depuration phase (Day 44). During a 30-day uptake period, all oysters were held in cages at a PAH-impacted field site, Republic, in the Elizabeth River (Virginia, USA). During a 14-day depuration period, oysters were held in the York River (Virginia, USA). Results were not compared across time points due to an inability to meet the independent data assumption across time for analysis of variance (ANOVA). Brackets with asterisks depict significant results of Games-Howell post hoc comparison, conducted following a significant one-way ANOVA at each respective time point. The ends of each bracket depict which groups were compared and found to be significantly different (e.g. wild vs. triploid in 2C). The number of asterisks above each bracket depicts the cut-off value for each level of significance and is coded as follows: ****=0.0001; ***=0.001; **=0.01, *=0.05. Non-significant results (i.e. p-value > 0.05) are not shown. For interpretation of the boxplot: The black point depicts the mean, the filled area of the boxplot depicts the interquartile range, with the solid black line depicting the median. Vertical lines (i.e. whiskers) extending from the box depict the upper and lower quartiles.

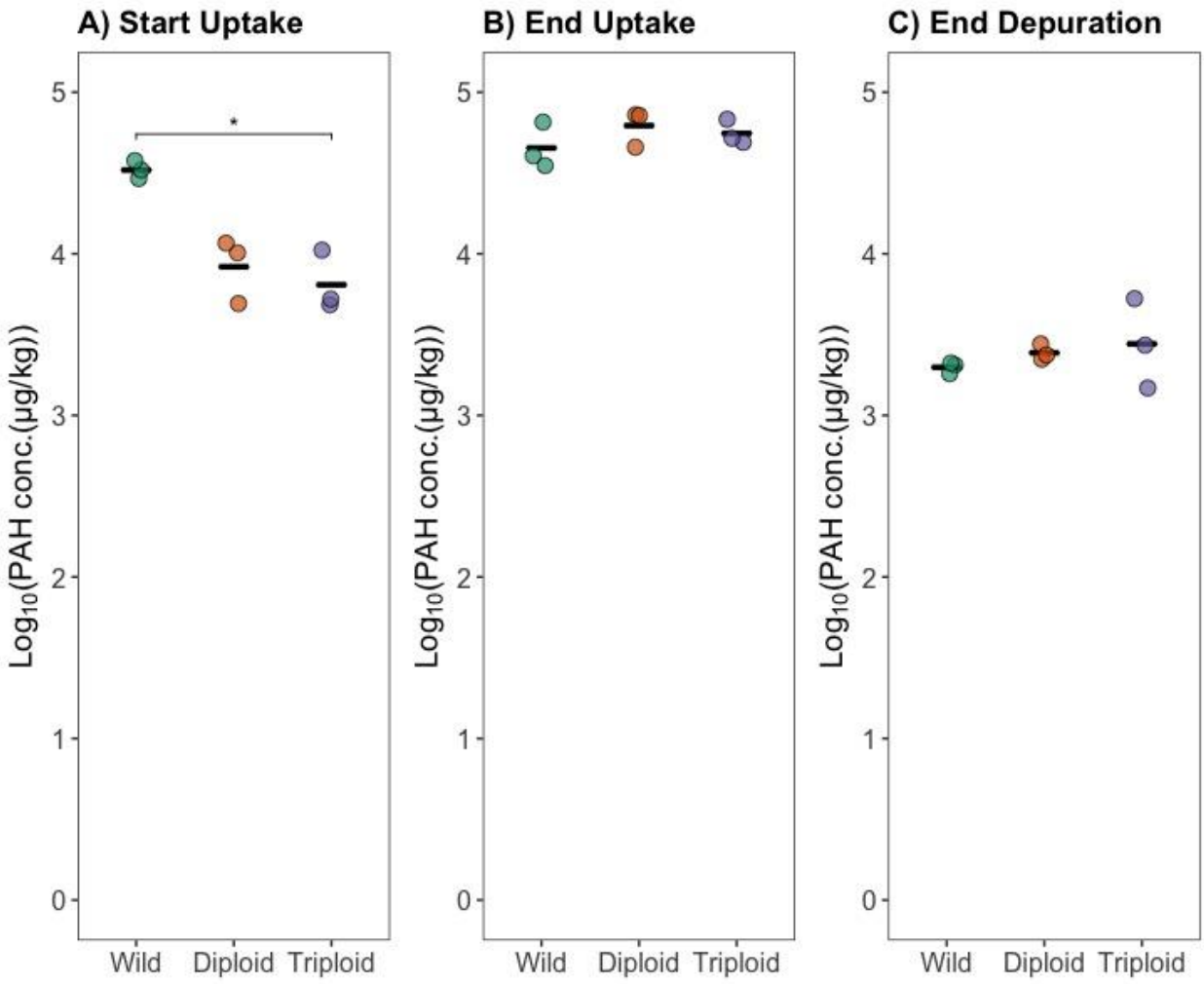

Figure 6. Mean total PAH concentrations in oyster interstitial fluid measured by antibody-based biosensor technology were compared between wild oysters inhabiting Republic, transplanted diploid oysters, and transplanted triploid oysters at each time point: **A)** start of uptake phase (Day 0); **B)** end of uptake phase (Day 30); and **C)** end of depuration phase (Day 44). During a 30-day uptake period, all oysters were held in cages at a PAH-impacted field site, Republic, in the Elizabeth River (Virginia, USA). During a 14-day depuration period, oysters were held in the York River (Virginia, USA). Results were not compared across time point due to an inability to meet the independent data assumption across time for analysis of variance (ANOVA). The black crossbar depicts the mean. Brackets with asterisks depict significant results of Games-Howell post hoc comparison, conducted following a significant one-way ANOVA at each respective time point. The ends of each bracket depict which groups were compared and found to be significantly different (e.g. wild vs. triploid in 3.C). The number of asterisks above each bracket depicts the cut-off value for each level of significance and is coded as follows: *=0.05. Non-significant results (i.e. p-value > 0.05) are not shown.

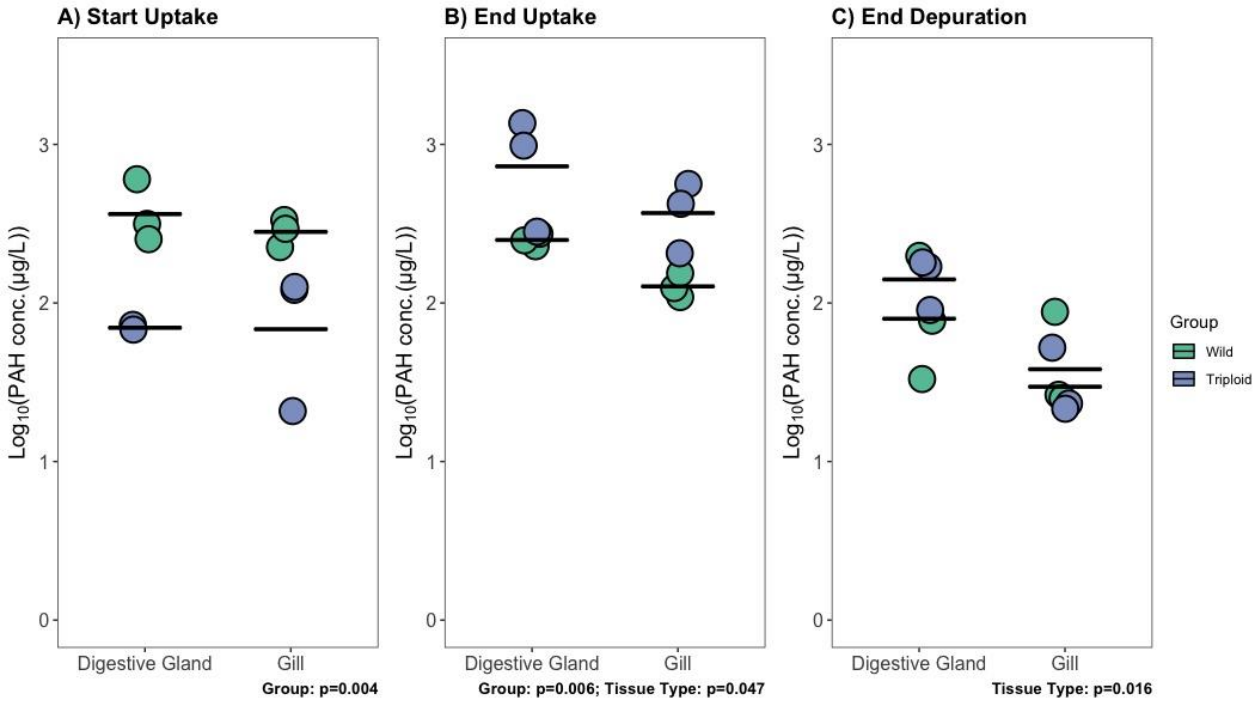

Figure 4. Total 3-5–ring PAH concentrations measured in the digestive gland fluid and gill fluid. Concentrations measured in respective fluid of wild oysters inhabiting a PAH-impacted field site, Republic, in the Elizabeth River (Virginia, USA) are compared to those of transplanted culture triploid oysters at each sampling point: **A)** start of uptake phase (Day 0); **B)** end of uptake phase (Day 30); **C)** end of depuration (Day 44). During the uptake phase, oysters were held at Republic for a 30-day period. At the end of uptake, all oysters were relocated to the York River (Virginia, USA) for a 14-day depuration period. Log_{10}-transformed individual measurements are shown. The black crossbar depicts the mean for each tissue type for respective groups. Independent two-way ANOVAs were conducted at each time point. Significant P-value results are reported below each figure. A 0.05 significance level was selected for analysis. No significant difference between tissue types as a function of oyster group was observed.

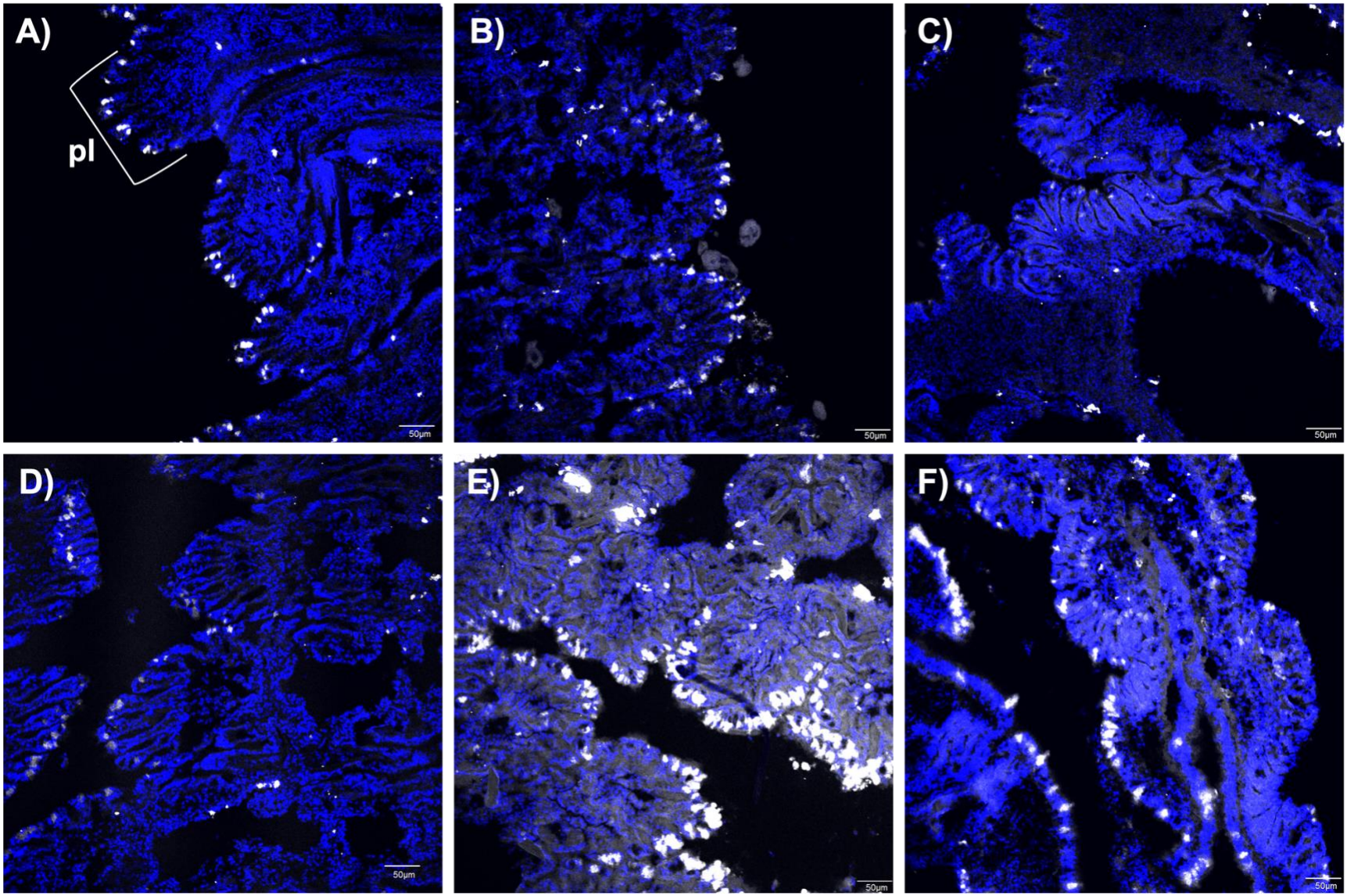
A)
pl
50µm
B)
50µm
C)
50µm
D)
50µm
E)
50µm
F)
50µm

Figure 5. Positive control confocal microscope images of oyster gill tissue collected at each timepoint of the study. Oysters were held at PAH-impacted site in the Elizabeth River for uptake (30 days) and relocated to the York River for 14-day depuration period. **5.A-C)** wild Republic oyster gill at **5.A)** start of uptake (Day 0); **5.B)** end of uptake (Day 30); **5.C)** end of depuration (Day 44). **5.D-F)** transplanted triploid oyster gill at **5.D)** start of uptake; **5.E)** end of uptake; **5.F)** end of depuration. AF647-tagged anti-PAH antibody (mAb 2G8) is depicted in white; 4′,6-diamidino-2-phenylindole (DAPI) stain for cell nuclei depicted in blue; pl=gill plica, the target gill structure for analysis, shown in 5.A as reference.

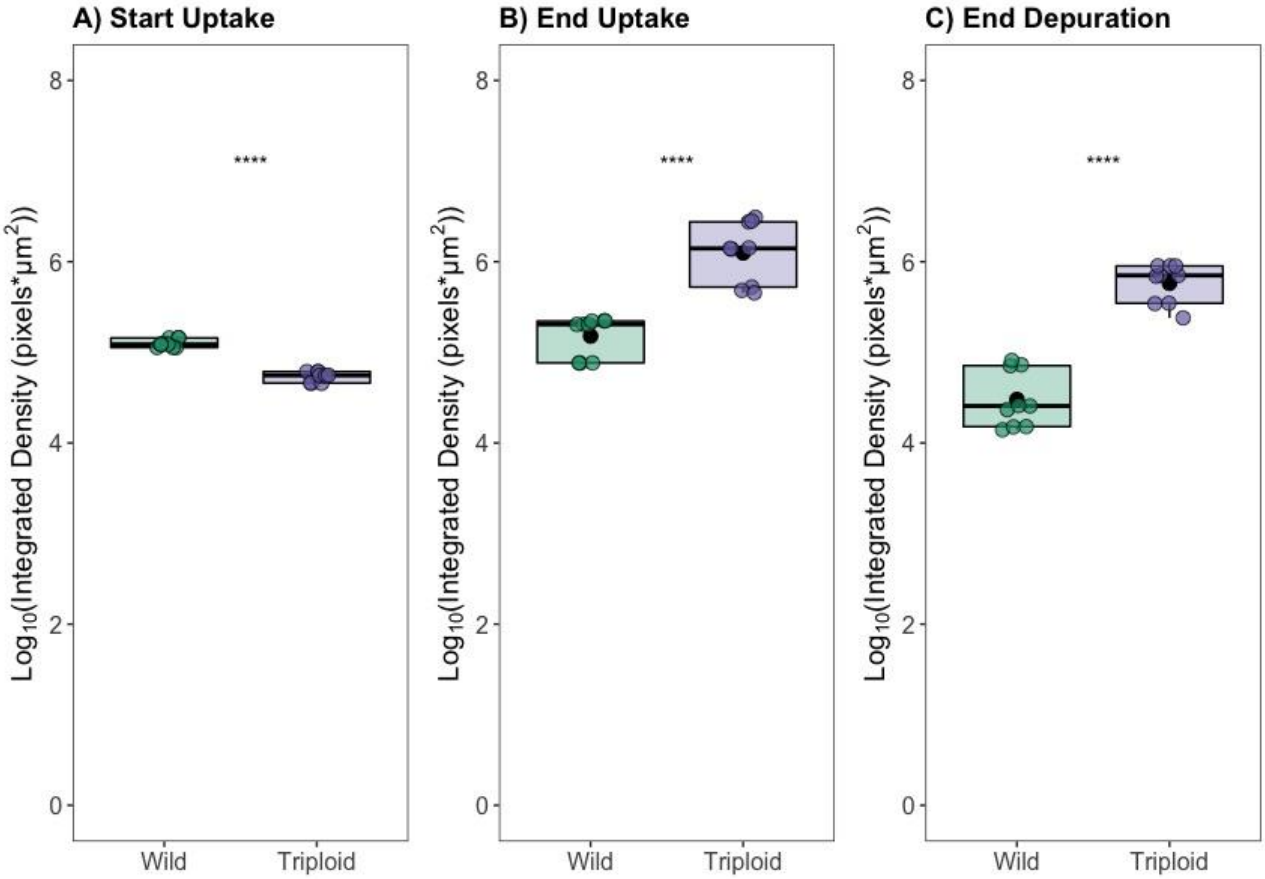

Figure 6. Analysis of the integrated density of mAb 2G8 signal measured in the gill plicae of wild and transplanted triploid oyster as measured from confocal images (Figure 5). Three plicae per image were measured in triplicate. To satisfy assumptions for statistical analysis, measurements were $\log_{10}$-transformed and individual Welch Two-Sample t-tests were performed at each time point: **A)** start of uptake phase (Day 0); **B)** end of uptake phase (Day 30); **C)** end of depuration (Day 44). During the uptake phase, oysters were held at Republic for a 30-day period. At the end of uptake, all oysters were relocated to the York River (Virginia, USA) for a 14-day depuration period. Asterisks denote a significant difference (p-value < 0.05) between group means.

Conclusions

Polycyclic aromatic hydrocarbons (PAHs) are not new or emerging contaminants. They have a long history as target analytes in environmental health and monitoring studies. Nevertheless, as a suite of ubiquitous and persistent environmental contaminants with a known ability to induce toxic, carcinogenic, and mutagenic effects, PAHs remain a top pollutant on the ATSDR substance priority list. Although PAHs have been included in numerous environmental contamination studies, our understanding of the fate and distribution of these contaminants and their associated health risks is limited by the ability of existing instrumentation to adequately measure contaminants in a complex organic matrix.

The work presented in this dissertation demonstrates that by developing and testing sensitive unconventional techniques, a new scope of questions about well-studied compounds can be explored that cannot be sufficiently addressed through standard methods in environmental analytical chemistry. Legacy contaminants such as PAHs are still important and by reaching developing new techniques, we can gain new insight into contaminant partitioning and accumulation in organisms to better address complexities in environmental monitoring and management. The idea of an immunoassay, the backbone of the immunological techniques discussed in this body of work, serving as a rapid, inexpensive, on-site screening tool is not new to the biomedical field (i.e., home pregnancy tests and COVID-19 rapid antigen tests). However, through its manipulation to fit the needs for environment analysis, the applicability of this biochemical test can be expanded into an entirely new field. The development and use of new immunological techniques may not be limited to PAHs because they can be adapted to other contaminants for which an antibody has been developed.

The purpose of this work is not to replace conventional analytical methods, as there are certainly limitations in utilizing such immunological approaches as discussed throughout this

dissertation. However, the exploration of novel applications for immunological technologies provides evidence that creative problem-solving to achieve sensitive detection limit and the ability to work within a confined spatiotemporal space is valuable for evaluating environmental contamination. Novel methodologies will be required to grapple with the impact of new, unstudied contaminants on the environment and human health. Future work should continue to prioritize the development of sensitive, inexpensive analyses that can evaluate a class of environmental pollutants, not just a few individual compounds.

Appendices

Appendix A: Chapter 1 Supplementary Data

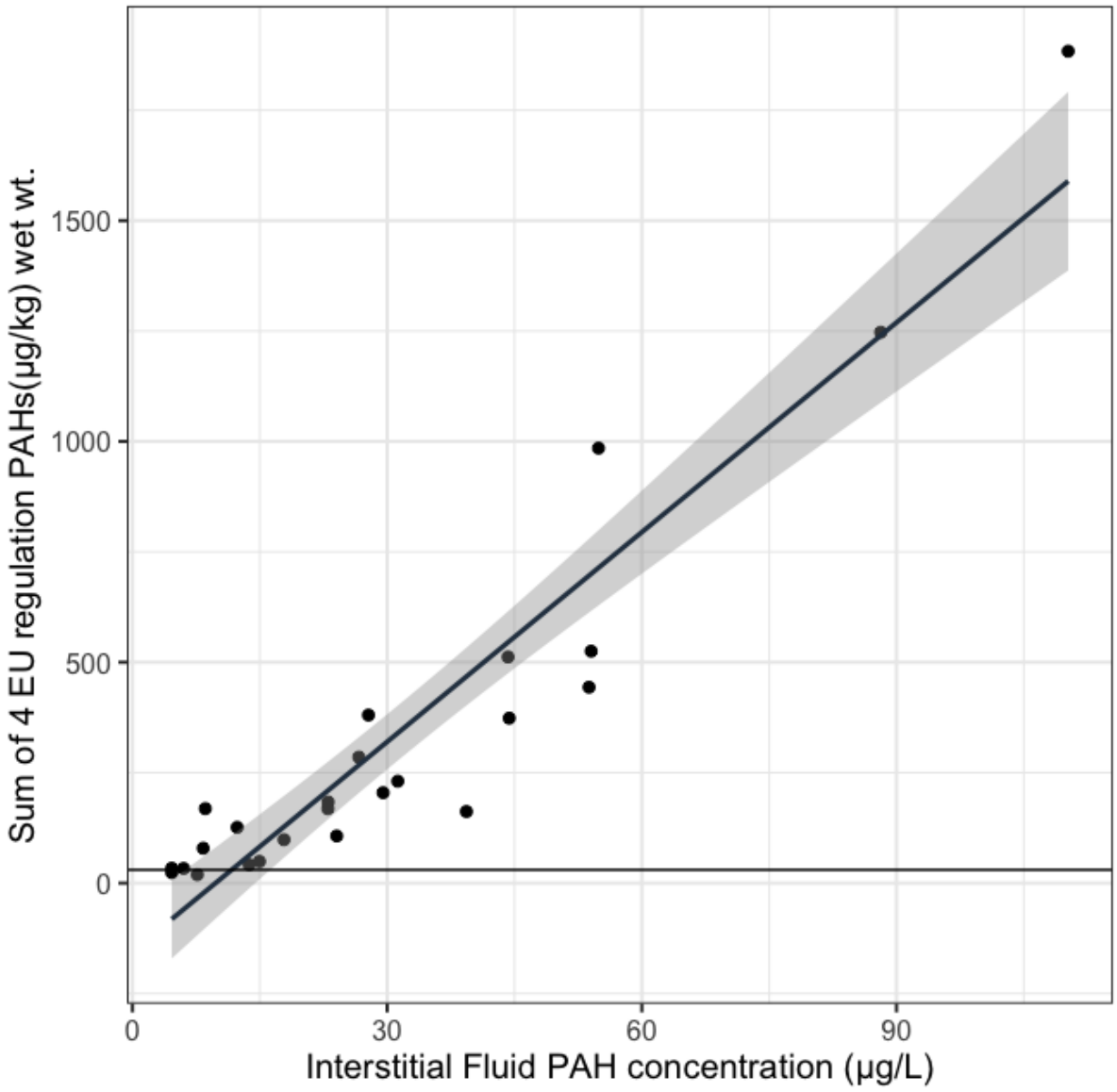

Figure S1. Regression model calibrated for PAH4 of EU regulation (Eqn: y=15.82x-154.79; r^2 =0.89, df=23). Most oysters from the Elizabeth River sites had PAH levels that were orders of magnitude above maximum limits for human consumption (30µg/kg wet wt.

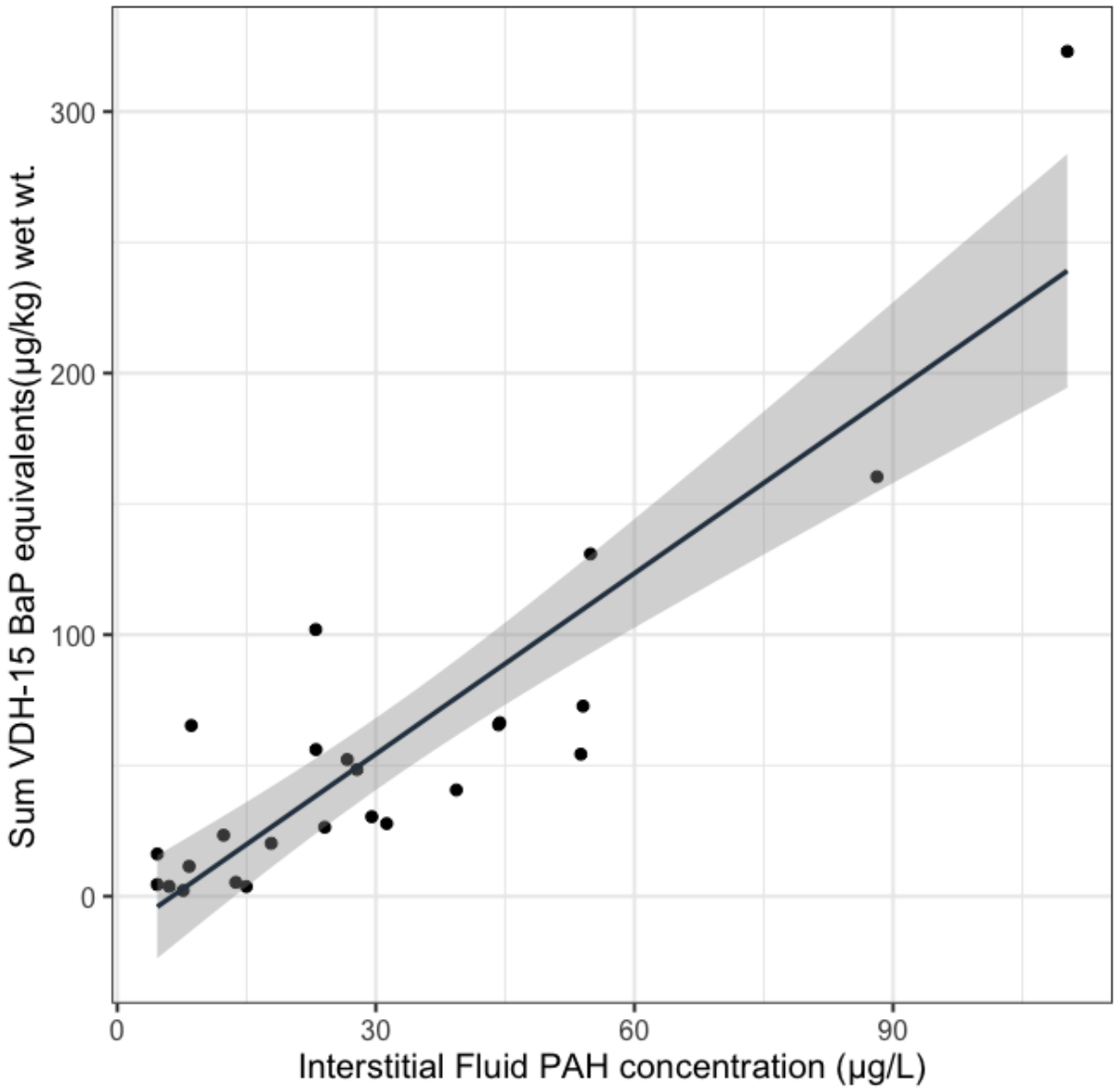

Figure S2. Regression model calibrated for 15 BaP equivalent concentrations of VDH health advisory (Eqn: y=2.3x-14.67; r^2 =0.77, df=23). Oysters from sites throughout the Elizabeth River fell within all 4 tiers of the VDH multi-tier advisory approach.

Table S1. List of PAH analytes, internal standard, and surrogate standards for GC-MS analysis

Name	CAS no.	Name	CAS no.
p-terphenyl (internal standard)	92-94-4	phenanthridine	229-87-8
d8-naphthalene (surrogate std)	1146-65-2	carbazole	86-74-8
naphthalene	91-20-3	4-methyl dibenzothiophene	7372-88-5
benzo{b}thiophene	95-15-8	1-phenyl naphthalene	605-02-7
isoquinoline	119-65-3	2-methyl phenanthrene	2531-84-2
quinoline	91-22-5	2-methyl anthracene	613-12-7
2-methyl naphthalene	91-57-6	benzo(c)cinnoline	230-17-1
1-methyl naphthalene	90-12-0	4,5-methylene phenanthrene	203-64-5
biphenyl	92-52-4	1-methylanthracene	610-48-0
2-ethylnaphthalene	939-27-5	4-methylphenanthrene	832-64-4
1-ethylnaphthalene	1127-76-0	1-methylphenanthrene	832-69-9
2-methyl biphenyl (2-phenyl toluene)	643-58-3	4,6-dimethyldibenzothiophene	1207-12-1
diphenyl ether	101-84-8	9-methyl anthracene	779-02-2
2,6&2,7 dimethyl naphthalene	581-42-0	2-phenyl naphthalene	612-94-2
1,3&1,7 -dimethyl naphthalene	575-41-7	3,6-dimethyl phenanthrene	1576-67-6
1,6-dimethyl naphthalene	575-43-9	2-ethyl anthracene	52251-71-5
1,4&2,3 dimethyl naphthalene	571-58-4	fluoranthene	206-44-0
1,5-dimethyl naphthalene	571-61-9	pyrene	129-00-0
acenaphthylene	208-96-8	9,10-dimethyl anthracene	781-43-1
1,2-dimethyl naphthalene	573-98-8	2,3-benzofluorene	243-17-4
1,8-dimethyl naphthalene	569-41-5	1-methylpyrene	2381-21-7
d10-acenaphthene (surrogate std)	15067-26-2	1,1' binaphthyl (surrogate std)	604-53-5
3-methyl biphenyl	643-93-6	9-phenyl anthracene	602-55-1
acenaphthene	83-32-9	benz(a)anthracene	56-55-3
dibenzofuran	132-64-9	d12-chrsyene (surrogate std)	1719-03-5
2,3,6 trimethyl naphthalene	829-26-5	chrysene	218-01-9
2,3,5-trimethyl naphthalene	2245-38-7	benzo(b)fluoranthene	205-99-2
fluorene	86-73-7	benzo(k)fluoranthene	207-08-9
3,3'-dimethyl biphenyl	612-75-9	benzo(j)fluoranthene	205-82-3
1,4,5-trimethyl naphthalene	2131-41-1	benzo(e)pyrene	192-97-2
1-methylfluorene	1730-37-6	benzo(a)pyrene	50-32-8
dibenzo[b]thiophene	132-65-0	d12-perylene (surrogate std)	1520-96-3
d10-phenathrene (surrogate std)	1517-22-2	perylene	198-55-0
phenanthrene	85-01-8	indeno (1,2,3-cd) pyrene	193-39-5
anthracene	120-12-7	dibenzo (a,h) anthracene	53-70-3
acridine	260-94-6	benzo (g,h,i) perylene	191-24-2

Table S2. List of toxic equivalent factors (TEF) and converted benzo [a] pyrene equivalent concentrations (BaPEs) for VDH's 15 priority PAHs across Elizabeth River Sites. BaPEs were calculated by multiplying their respective TEF (first column) by original analyte concentration. Concentrations listed in the table have already been converted to a BaPE concentration. Total BaPE concentrations at each site were then converted to a wet weight concentration via wet to dry weight ratio for each sample.

PAH compound	TEF	MP2	JRWS	PARCR	JCBH	JCBR	RS	GR	CLY	HB	HR	PB	GLM	264	HS	NSC	CMP	BK	MPB	PCR	164	JB	CB-001	CB-002	CB-004	CB-005
acenanapthylene	0.001	0.1	0.0	0.0	0.0	0.0	0.0	0.0	0.0	0.0	0.1	0.0	0.0	0.0	0.0	0.0	0.0	0.0	0.0	0.0	0.0	0.0	0.2	0.0	0.0	0.1
acenapthene	0.001	0.0	0.0	0.0	0.0	0.0	0.0	0.0	0.0	0.0	0.0	0.0	0.0	0.0	0.0	0.0	0.0	0.0	0.0	0.0	0.0	0.0	0.0	0.0	0.0	0.0
fluorene	0.001	0.0	0.0	0.0	0.0	0.1	0.0	0.0	0.0	0.0	0.0	0.0	0.0	0.0	0.0	0.0	0.0	0.0	0.0	0.0	0.0	0.0	0.0	0.0	0.0	0.0
phenathrene	0.001	0.1	0.1	0.0	0.1	0.6	0.1	0.1	0.0	0.0	0.0	0.0	0.1	0.1	0.3	0.2	0.2	0.2	0.1	0.2	0.1	0.2	0.1	0.1	0.1	0.2
anthracene	0.01	0.7	0.0	0.3	0.4	1.4	1.1	0.1	0.1	0.1	0.2	0.2	0.2	0.1	0.1	0.1	0.2	0.2	0.2	0.2	0.2	0.3	0.5	0.9	1.1	1.0
fluoranthene	0.001	0.6	0.3	0.7	0.9	3.2	9.3	0.2	0.2	0.2	0.4	0.3	0.6	0.5	1.2	0.8	1.4	1.4	1.4	1.8	1.0	1.8	1.0	1.4	2.2	3.3
pyrene	0.001	0.5	0.3	0.5	0.5	2.2	6.3	0.2	0.1	0.1	0.3	0.2	0.4	0.3	1.0	0.6	0.9	0.8	0.9	1.2	0.6	1.1	0.5	0.7	1.1	1.8
benz (a) anthracene	0.1	22.4	3.5	17.2	22.9	67.3	149.2	7.6	4.9	3.1	11.9	6.6	14.5	5.0	33.5	21.9	29.1	38.4	45.5	58.5	15.8	46.8	16.9	25.1	30.4	36.8
chrysene	0.01	3.7	0.6	2.4	3.3	16.7	39.7	0.9	0.8	0.6	1.7	1.0	2.6	1.5	3.6	2.3	4.9	5.5	6.4	8.3	6.6	14.9	5.7	8.5	15.2	19.1
benzo(b) fluoranthene	0.1	114.7	4.0	40.0	66.2	125.0	785.3	8.2	8.5	4.7	19.3	9.3	24.6	10.8	29.0	13.0	39.2	46.8	69.9	83.1	50.1	128.3	134.9	201.8	390.3	472.6
benzo(k)fluoranthene	0.1	90.4	6.6	26.8	35.2	65.7	522.5	5.6	6.2	3.5	11.0	6.2	12.2	1.6	26.9	9.6	23.6	21.5	35.8	40.0	18.9	48.1	74.2	87.4	118.3	184.3
benzo(a)pyrene	1	550.2	179.0	101.1	206.1	144.6	810.3	0.0	6.4	2.5	24.5	0.0	13.0	2.7	197.5	63.2	75.7	48.6	76.2	90.4	65.0	115.0	100.8	80.9	147.5	123.8
ideno(1,2,3,cd)pyrene	0.1	47.4	21.3	0.0	13.6	11.7	49.3	2.1	0.0	0.0	1.7	4.7	2.2	0.0	21.4	8.0	12.3	4.3	5.7	6.9	4.1	4.4	17.3	15.7	22.9	28.5
dibenz(a,h)anthracene	5	0.0	0.0	0.0	0.0	0.0	0.0	0.0	0.0	0.0	0.0	0.0	50.2	0.0	376.2	30.9	182.9	41.9	95.0	0.0	0.0	62.3	0.0	0.0	0.0	0.0
benzo(g,h,i)perylene	0.1	51.2	0.0	0.0	10.2	21.6	55.5	2.9	2.0	1.5	2.9	4.7	3.0	0.6	22.4	8.5	11.0	5.9	7.0	6.6	4.1	5.5	36.9	21.1	51.0	44.8
SUM VDH-15 (dry wt.)		882.0	215.8	189.0	359.7	460.4	2428.7	27.9	29.2	16.3	73.9	33.3	123.6	23.2	713.2	159.0	381.5	215.6	344.2	297.3	166.5	428.6	389.1	443.7	780.2	916.2
wet to dry wt. ratio		0.24	0.57	0.11	0.14	0.04	0.06	0.00	0.03	0.02	0.05	0.00	0.02	0.01	0.17	0.10	0.06	0.03	0.04	0.04	0.05	0.03	0.05	0.03	0.03	0.02
SUM VDH-15 (wet wt.)		**65.3**	**16.2**	**20.2**	**40.6**	**54.3**	**323.0**	**3.8**	**4.5**	**2.2**	**11.5**	**5.3**	**23.4**	**3.7**	**102.0**	**26.4**	**56.1**	**30.4**	**52.3**	**48.5**	**27.8**	**65.6**	**17.9**	**11.2**	**19.6**	**15.9**

Table S3. List of EFSA-4 PAH concentrations across Elizabeth River Sites. Total dry weight concentrations converted to wet weight through multiplying by wet to dry weight ratio for each sample.

PAH compound	MP2	JRWS	PARCR	JCBH	JCBR	RS	GR	CLY	HB	HR	PB	GLM	264	HS	NSC	CMP	BK	MPB	PCR	164	JB	CB-001	CB-002	CB-004	CB-005
benz(a)anthracene	224.1	34.7	171.8	229.2	673.5	1491.6	75.8	48.8	30.6	119.2	66.5	145.4	50.5	335.2	218.8	290.7	384.3	454.6	585.4	157.8	467.9	168.9	251.1	303.9	368.4
chrysene	369.6	61.8	241.9	333.2	1673.8	3967.8	85.8	78.6	60.5	173.6	100.5	264.6	147.1	356.7	231.7	493.3	551.7	642.9	826.8	655.9	1486.7	570.6	853.9	1515.4	1907.1
benzo(b)fluoranthene	1147.4	40.5	400.2	661.6	1250.4	7853.5	82.4	84.9	46.9	192.8	93.0	245.7	107.6	289.8	129.9	392.4	467.9	698.8	830.6	501.2	1283.5	1349.0	2018.4	3903.1	4725.6
benzo(a)pyrene	550.2	179.0	101.1	206.1	144.6	810.3	0.0	6.4	2.5	24.5	0.0	13.0	2.7	197.5	63.2	75.7	48.6	76.2	90.4	65.0	115.0	100.8	80.9	147.5	123.8
SUM EFSA-4 (dry wt.)	2291.3	316.1	915.0	1430.1	3742.4	14123.1	244.0	218.7	140.5	510.1	260.0	668.7	307.8	1179.3	643.5	1252.1	1452.5	1872.5	2333.2	1379.9	3353.1	2189.4	3204.3	5869.9	7124.9
wet to dry wt. ratio	0.24	0.57	0.11	0.14	0.04	0.06	0.00	0.03	0.02	0.05	0.00	0.02	0.01	0.17	0.10	0.06	0.03	0.04	0.04	0.05	0.03	0.05	0.03	0.03	0.02
SUM EFSA-4 (wet wt.)	**168.7**	**23.6**	**98.3**	**162.1**	**443.5**	**1883.6**	**33.2**	**33.7**	**19.1**	**79.0**	**41.6**	**126.2**	**49.2**	**168.5**	**106.7**	**183.5**	**204.6**	**285.1**	**380.4**	**230.7**	**512.1**	**373.5**	**525.2**	**984.8**	**1247.2**

Table S4. List of EPA-16 PAH concentrations across Elizabeth River Sites. Total dry weight concentrations converted to wet weight through multiplying by wet to dry weight ratio for each sample.

PAH compound	MP2	JRWS	PARCR	JCBH	JCBR	RS	GR	CLY	HB	HR	PB	GLM	264	HS	NSC	CMP	BK	MPB	PCR	164	JB	CB-001	CB-002	CB-004	CB-005
naphthalene	0.0	28.3	22.1	12.2	18.7	74.6	21.5	0.0	9.5	26.5	51.1	14.6	16.3	28.7	27.6	37.6	24.9	21.3	13.8	23.8	15.6	111.8	42.7	113.9	36.5
acenaphthylene	55.2	0.0	0.0	36.7	25.0	46.6	0.0	0.0	0.0	52.9	0.0	14.6	0.0	21.6	0.0	0.0	8.3	21.3	20.8	7.9	23.4	167.7	34.2	46.9	116.8
acenaphthene	32.0	0.0	20.9	23.5	49.6	22.8	38.1	22.4	11.2	15.9	42.2	15.1	17.3	17.0	19.0	23.5	23.4	25.7	21.2	18.0	26.0	8.8	23.4	29.3	0.0
fluorene	0.0	0.0	0.0	44.7	101.7	31.4	32.7	22.4	22.4	15.9	35.2	15.1	17.3	22.7	19.0	11.8	23.4	15.4	21.2	18.0	15.6	0.0	20.8	0.0	0.0
phenanthrene	104.9	103.7	44.6	82.9	610.2	148.8	60.0	30.8	30.3	23.8	43.4	88.8	117.2	344.4	158.9	203.0	173.0	122.4	154.8	148.1	153.5	111.4	133.6	145.3	158.2
anthracene	69.9	0.0	27.2	39.3	141.8	113.0	10.7	8.8	9.3	15.9	15.3	21.1	14.3	12.7	10.2	19.8	20.1	24.0	24.7	17.4	26.7	53.4	86.4	106.7	97.7
fluoranthene	624.4	282.2	684.1	928.8	3212.5	9289.9	233.5	206.7	184.0	394.2	319.3	553.8	459.1	1231.8	784.1	1411.1	1376.7	1370.5	1843.5	972.7	1762.3	1016.5	1414.2	2187.0	3262.3
pyrene	524.6	250.2	529.6	538.2	2191.7	6317.0	162.8	149.5	118.8	259.3	214.6	355.1	286.9	1012.1	556.0	911.0	840.0	912.1	1238.0	583.6	1110.4	545.4	693.4	1105.5	1840.2
benz(a)anthracene	224.1	34.7	171.8	229.2	673.5	1491.6	75.8	48.8	30.6	119.2	66.5	145.4	50.5	335.2	218.8	290.7	384.3	454.6	585.4	157.8	467.9	168.9	251.1	303.9	368.4
chrysene	369.6	61.8	241.9	333.2	1673.8	3967.8	85.8	78.6	60.5	173.6	100.5	264.6	147.1	356.7	231.7	493.3	551.7	642.9	826.8	655.9	1486.7	570.6	853.9	1515.4	1907.1
benzo(b)fluoranthene	1147.4	40.5	400.2	661.6	1250.4	7853.5	82.4	84.9	46.9	192.8	93.0	245.7	107.6	289.8	129.9	392.4	467.9	698.8	830.6	501.2	1283.5	1349.0	2018.4	3903.1	4725.6
benzo(k)fluoranthene	903.8	66.1	267.6	352.4	656.7	5225.0	56.4	61.6	34.6	109.7	61.6	121.7	16.3	268.6	95.9	236.3	215.1	358.3	400.0	188.7	481.3	742.0	873.7	1183.4	1842.7
benzo(a)pyrene	550.2	179.0	101.1	206.1	144.6	810.3	0.0	6.4	2.5	24.5	0.0	13.0	2.7	197.5	63.2	75.7	48.6	76.2	90.4	65.0	115.0	100.8	80.9	147.5	123.8
indeno(1,2,3-cd)pyrene	473.7	213.4	0.0	136.2	117.0	492.6	21.0	0.0	0.0	16.6	47.0	22.1	0.0	214.2	80.4	122.8	43.3	57.0	68.7	41.3	43.6	172.7	156.5	228.8	284.7
dibenzo(a,h)anthracene	0.0	0.0	0.0	0.0	0.0	0.0	0.0	0.0	0.0	0.0	0.0	10.0	0.0	75.2	6.2	36.6	8.4	19.0	0.0	0.0	12.5	0.0	0.0	0.0	0.0
benzo(g,h,i)perylene	512.1	0.0	0.0	102.5	216.5	554.8	28.5	19.9	15.4	29.0	47.0	30.1	5.7	224.4	85.0	109.8	58.7	69.7	65.6	41.3	54.5	369.0	210.8	510.2	448.2
SUM EPA-16 (dry wt.)	5592.0	1259.9	2511.2	3727.5	11083.7	36439.7	909.2	740.7	576.1	1469.6	1136.7	1930.7	1258.4	4652.8	2485.8	4375.4	4267.9	4889.0	6205.5	3440.7	7078.5	5488.1	6894.1	11526.9	15212.1
wet to dry wt. ratio	0.1	0.1	0.1	0.1	0.1	0.1	0.1	0.2	0.1	0.2	0.2	0.2	0.2	0.1	0.2	0.1	0.1	0.2	0.2	0.2	0.2	0.2	0.2	0.2	0.2
SUM EPA-16 (wet wt.)	**411.6**	**94.2**	**269.7**	**422.4**	**1313.4**	**4860.0**	**123.8**	**114.2**	**78.4**	**227.7**	**181.9**	**364.5**	**200.9**	**664.7**	**412.2**	**641.3**	**601.3**	**744.3**	**1011.7**	**575.3**	**1081.0**	**936.2**	**1129.9**	**1933.8**	**2662.8**

Appendix B: Chapter 2 Supplementary Data

Table S3. Chemical composition of test oils, Heavy Fuel oil (HFO) and Hoops oil

Chemical	HFO C oil mg/kg	Hoops C oil mg/kg
Benzene	0	793
Toluene	0	3590
Ethylbenzene	0	961
p/m-Xylene	0	4540
o-Xylene	0	1950
Naphthalene	636	253
C1-Naphthalene	2140	671
C2-Naphthalenes	3920	1160
C3-Naphthalenes	3540	1170
C4-Naphthalenes	2220	677
Biphenyl	59.3	53.8
Dibenzofuran	125	19.6
Acenaphthylene	4	4.92
Acenaphthene	233	17.4
Fluorene	372	46.7
C1-Fluorenes	1030	135
C2-Fluorenes	2310	252
C3-Fluorenes	2980	267
Anthracene	443	6.86
Phenanthrene	2330	94.3
C1-Phenanthrenes/Anthracenes	10000	247
C2-Phenanthrenes/Anthracenes	16900	324
C3-Phenanthrenes/Anthracenes	14700	238
C4-Phenanthrenes/Anthracenes	7720	125
Retene	0	50.2
Dibenzothiophene	690	81.5
C1-Dibenzothiophenes	2920	355
C2-Dibenzothiophenes	5660	807
C3-Dibenzothiophenes	6480	964
C4-Dibenzothiophenes	4080	595
Benzo(b)fluorene	841	6.67
Fluoranthene	396	3.71
Pyrene	2480	9.62
C1-Fluoranthenes/Pyrenes	8360	43

C2-Fluoranthenes/Pyrenes	9210	69.8
C3-Fluoranthenes/Pyrenes	6060	94.2
C4-Fluoranthenes/Pyrenes	2830	104
Naphthobenzothiophenes	1470	22.4
C1-Naphthobenzothiophenes	3000	97.8
C2-Naphthobenzothiophenes	2730	225
C3-Naphthobenzothiophenes	1570	266
C4-Naphthobenzothiophenes	722	221
Benz[a]anthracene	943	2.25
Chrysene/Triphenylene	1450	12
C1-Chrysenes	3610	33.2
C2-Chrysenes	3890	56
C3-Chrysenes	2550	68.9
C4-Chrysenes	1090	52.3
Benzo[b]fluoranthene	106	1.92
Benzo[k]fluoranthene	11.6	0
Benzo[a]fluoranthene	36.3	0
Benzo[e]pyrene	156	3.71
Benzo[a]pyrene	183	1.69
Perylene	56	14
Indeno[1,2,3-cd] pyrene	10.5	0
Dibenz[ah]anthracene/Dibenz[ac]anthracene	13.5	0
Benzo[g,h,i]perylene	24.4	1.51
n-Nonane (C9)	0	9840
n-Decane (C10)	0	8120
n-Undecane (C11)	0	7570
n-Dodecane (C12)	0	6660
n-Tridecane (C13)	0	6330
2,6,10 Trimethyldodecane (1380)	0	1360
n-Tetradecane (C14)	0	5560
2,6,10 Trimethyltridecane (1470)	0	1960
n-Pentadecane (C15)	0	5190
n-Hexadecane (C16)	0	4340
Norpristane (1650)	0	1240
n-Heptadecane (C17)	0	3610
Pristane	0	2000

n-Octadecane (C18)	0	3230
Phytane	0	1650
n-Nonadecane (C19)	0	2650
n-Eicosane (C20)	0	2650
n-Heneicosane (C21)	0	1950
n-Docosane (C22)	0	1720
n-Tricosane (C23)	0	1440
n-Tetracosane (C24)	0	1300
n-Pentacosane (C25)	0	1370
n-Hexacosane (C26)	0	985
n-Heptacosane (C27)	0	775
n-Octacosane (C28)	0	644
n-Nonacosane (C29)	0	597
n-Triacontane (C30)	0	516
n-Hentriacontane (C31)	0	416
n-Dotriacontane (C32)	0	536
n-Tritriacontane (C33)	0	387
n-Tetratriacontane (C34)	0	294
n-Pentatriacontane (C35)	0	222
n-Hexatriacontane (C36)	0	194
n-Heptatriacontane (C37)	0	160
n-Octatriacontane (C38)	0	155
n-Nonatriacontane (C39)	0	116
n-Tetracontane (C40)	0	108

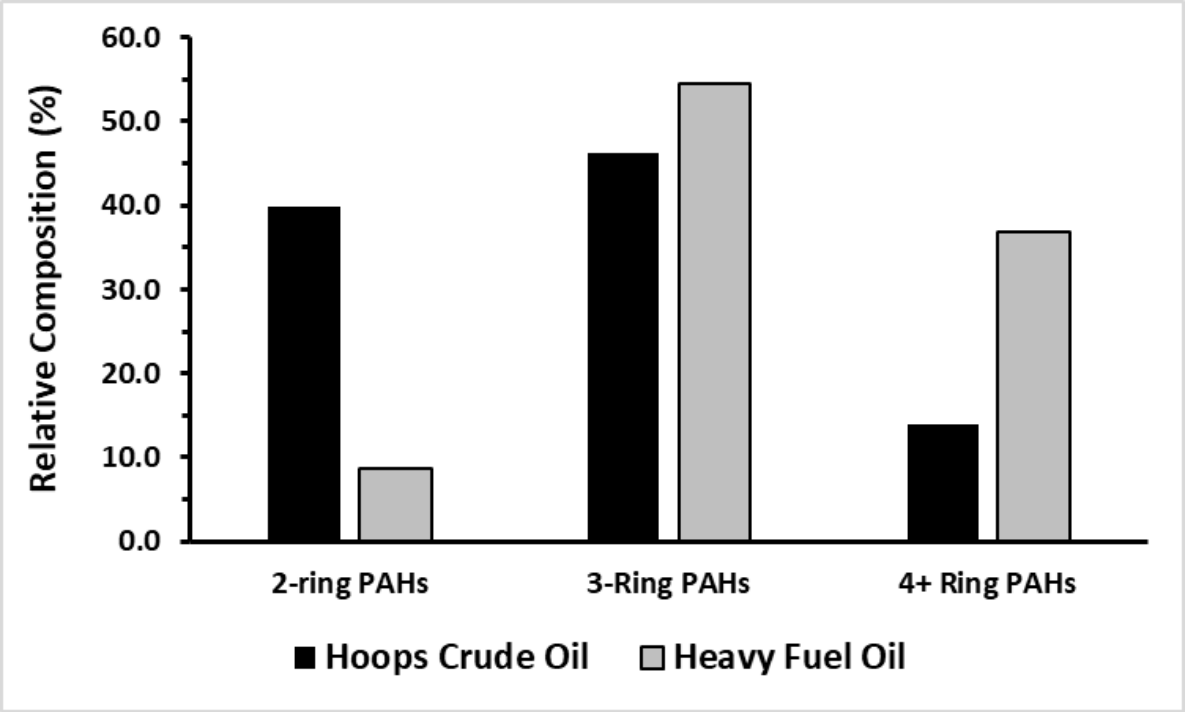

Figure S1. Comparison of relative percentages of 2, 3, and >4–ring PAHs between test oils, Hoops and Heavy Fuel Oil (HFO)

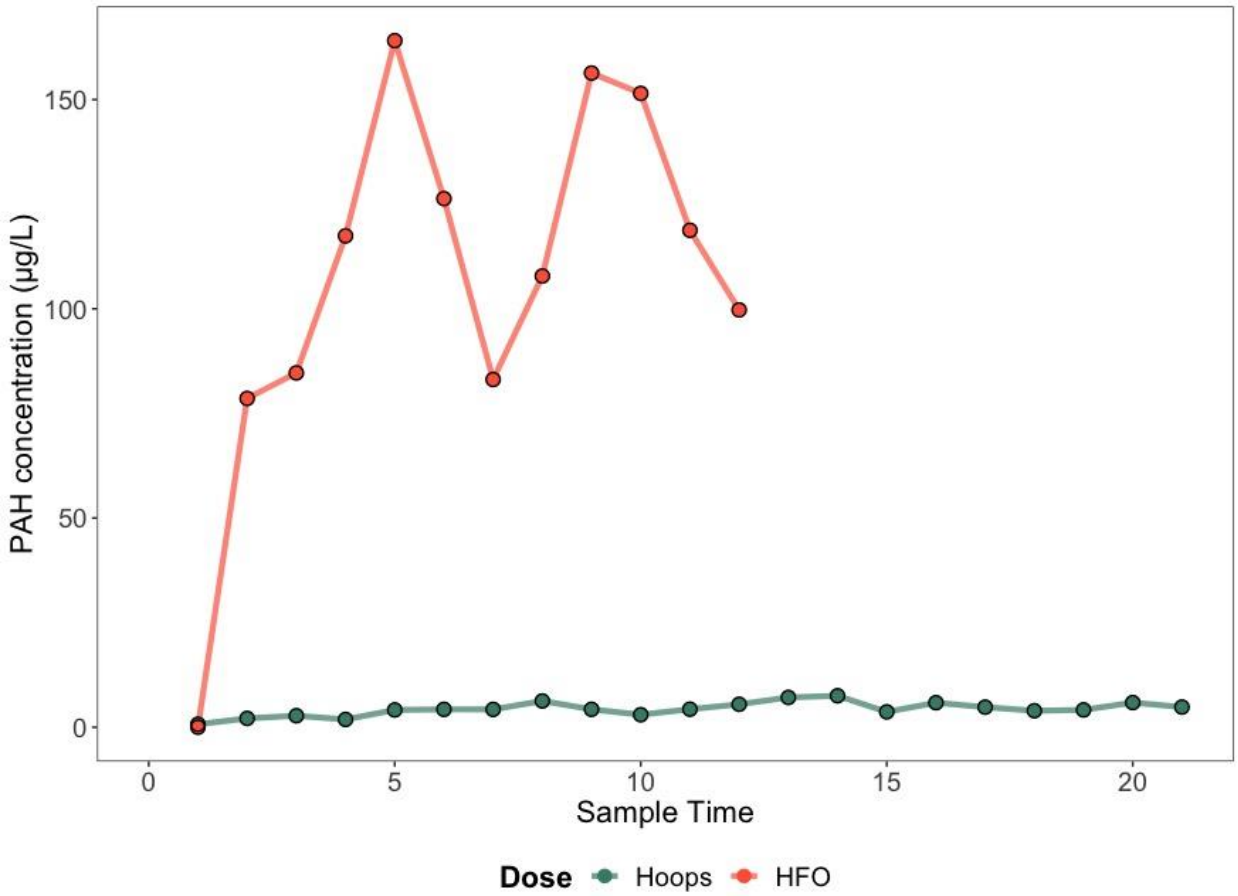

Figure S2. Biosensor measurement of effluent from the sand generator column loaded with either Quintana Hoops oil (low dose) or HFO distillate (high dose) for each experiment. The dosing reservoir was monitored to ensure steady-state achievement with the generator column prior to experiment. Final WAF concentrations measured were ~5 µg/L for the low dose experiment and ~30µg/L for the high dose experiment prior to 1:1 mixing with unfiltered York River to achieve a final dose concentration of 2.5µg/L and 15µg/L, respectively, measured by biosensor technology. Hoops samples were collected 2x per day for ~12 days and HFO samples were collected 1x per day for ~12 days.

Table S2. Water Quality Measurements for Hoops exposure (2.5 µg/L) control oyster tank

Day of Experiment	Phase	Temp (°C)	Salinity	pH	Diss. Oxygen (ppm)	Ammonia (ppm)
1	Uptake	15	15	7.5	6	0
2	Uptake	16.2	16			
3	Uptake	16.2	17	7.5	7	0
4	Uptake	15.6	17	7.5	6.8	0
5	Depuration	15.6	NA	NA	NA	NA
6	Depuration	14.7	17	NA	NA	NA
7	Depuration	13.3	17	NA	NA	NA
8	Depuration	14.4	18	NA	NA	NA
9	Depuration	13.9	18	NA	NA	NA
10	Depuration	14.2	18	NA	NA	NA
11	Depuration	14.9	17	NA	NA	NA
12	Depuration	15.3	18	NA	NA	NA
13	Depuration	13.6	17	NA	NA	NA
14	Depuration	13.8	17	NA	NA	NA
15	Depuration	13.8	17	NA	NA	NA
16	Depuration	15	17	7.5	7.4	0

Table S3. Water Quality Measurements for Hoops exposure (2.5 µg/L) treatment oyster tank

Day of Experiment	Phase	Temp (°C)	Salinity	pH	Diss. Oxygen (ppm)	Ammonia (ppm)
1	Uptake	16.6	15	7.5	6.6	0
2	Uptake	17.8	16	NA	NA	NA
3	Uptake	17.9	17	7.5	6.4	0
4	Uptake	12.9	18	7.5	8.3	0
5	Depuration	15.9	NA	NA	NA	NA
6	Depuration	15.1	17	NA	NA	NA
7	Depuration	13.9	18	NA	NA	NA
8	Depuration	15	18	NA	NA	NA
9	Depuration	13.9	19	NA	NA	NA
10	Depuration	15.2	18	NA	NA	NA
11	Depuration	14.5	17	NA	NA	NA
12	Depuration	14.5	18	NA	NA	NA
13	Depuration	14.2	18	NA	NA	NA
14	Depuration	14.8	18	NA	NA	NA
15	Depuration	15.3	18	NA	NA	NA
16	Depuration	16.1	18	7.8	7.2	0

Table S4. Water Quality Measurements for HFO exposure (15 µg/L) control oyster tank

Day of Experiment	Phase	Temp (°C)	Salinity	pH	Diss. Oxygen (ppm)	Ammonia (ppm)
1	Uptake	16.1	20	7.5	6.2	0.1
2	Uptake	17.2	20	NA	NA	NA
3	Uptake	17.4	20	7.5	6.2	0.05
4	Uptake	17.9	20	7.5	6	0.05
5	Depuration	NA	NA	NA	NA	NA
6	Depuration	16.8	NA	NA	NA	NA
7	Depuration	16	20	NA	NA	NA
8	Depuration	16	20	NA	NA	NA
9	Depuration	NA	NA	NA	NA	NA
10	Depuration	16.9	20	NA	NA	NA
11	Depuration	17.7	20	NA	NA	NA
12	Depuration	16.9	20	NA	NA	NA
13	Depuration	NA	NA	NA	NA	NA
14	Depuration	15.9	20	NA	NA	NA
15	Depuration	NA	NA	NA	NA	NA
16	Depuration	15.1	20	7.5	6.7	0.05

Table S5. Water Quality Measurements for HFO exposure (15 µg/L) treatment oyster tank

Day of Experiment	Phase	Temp (°C)	Salinity	pH	Diss. Oxygen (ppm)	Ammonia (ppm)
1	Uptake	16.6	20	7.5	6.8	0.1
2	Uptake	17.6	20	NA	NA	NA
3	Uptake	17.9	20	7.5	6.5	0.05
4	Uptake	18.2	20	7.5	6.8	0.05
5	Depuration	NA	NA	NA	NA	NA
6	Depuration	17.2	NA	NA	NA	NA
7	Depuration	16.5	20	NA	NA	NA
8	Depuration	16.6	20	NA	NA	NA
9	Depuration	NA	NA	NA	NA	NA
10	Depuration	17.3	20	NA	NA	NA
11	Depuration	18.6	20	NA	NA	NA
12	Depuration	17.2	20	NA	NA	NA
13	Depuration	NA	NA	NA	NA	NA
14	Depuration	15.8	20	NA	NA	NA
15	Depuration	NA	NA	NA	NA	NA
16	Depuration	15	20	7.5	6.6	0.05

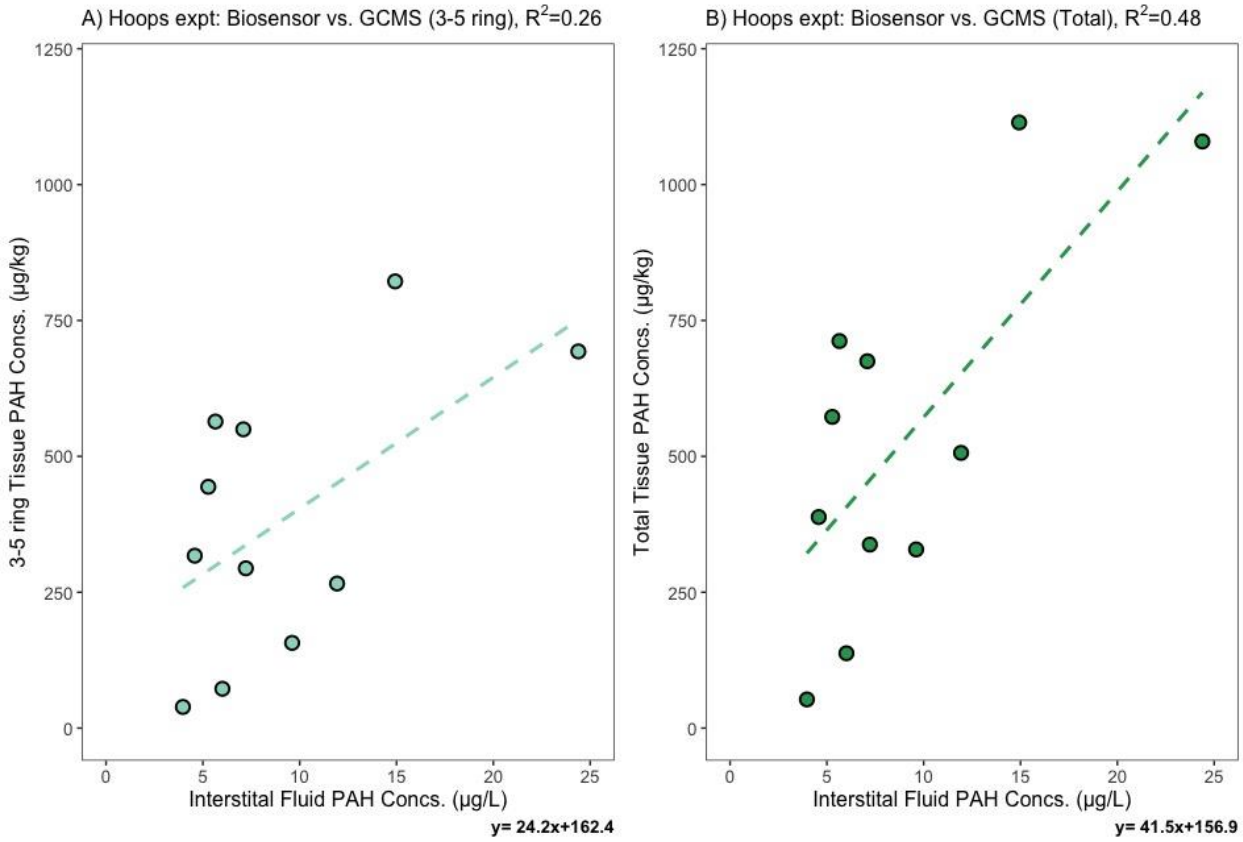

Figure S4. Linear regression between oyster interstitial fluid estimate 3-5 ring PAH concentrations measured by biosensor and **A)** 3-5 ring PAH concentrations in oyster tissue measured by GC–MS and **B)** Total PAH concentrations in oyster tissue measured by GC–MS for all analytes during the Hoops oil WAF exposure experiment.

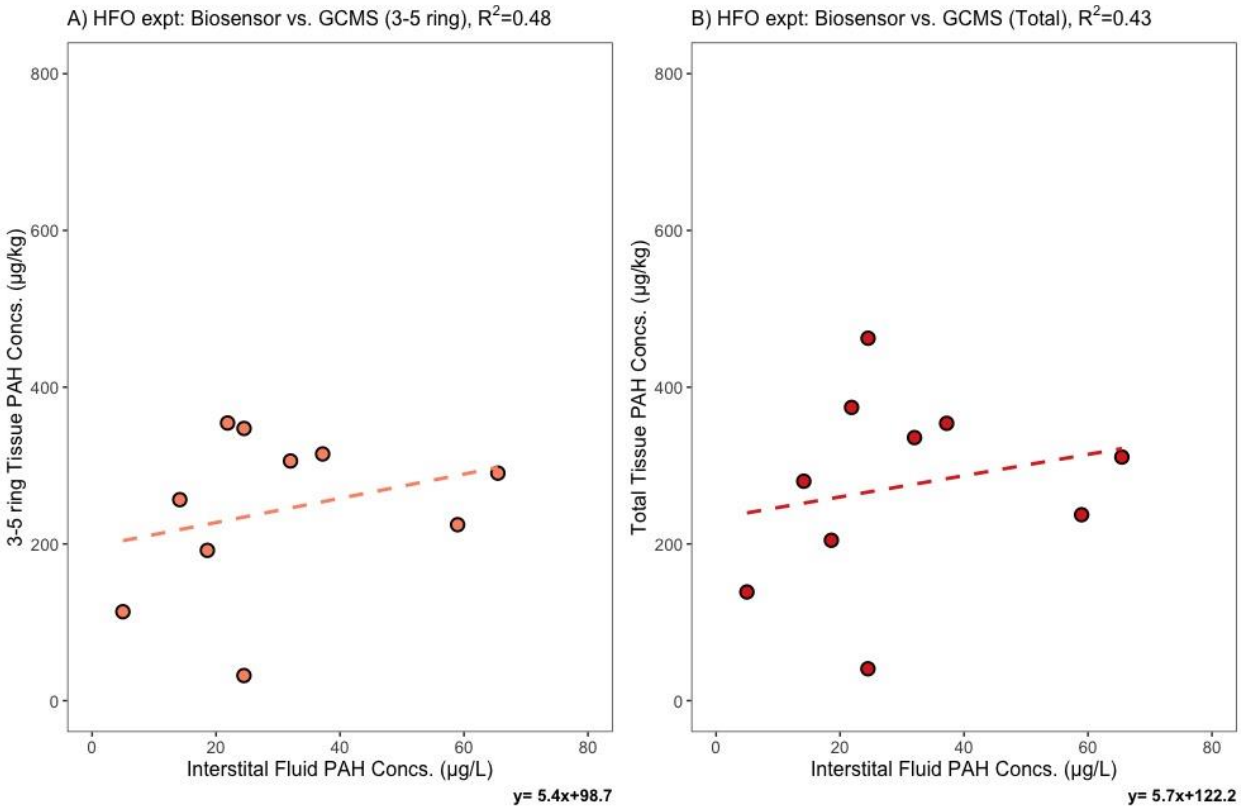

Figure S5. Linear regression between oyster interstitial fluid estimate 3-5 ring PAH concentrations measured by biosensor and **A)** 3-5 ring PAH concentrations in oyster tissue measured by GC–MS and **B)** Total PAH concentrations in oyster tissue measured by GC–MS for all analytes during the HFO oil WAF exposure experiment.

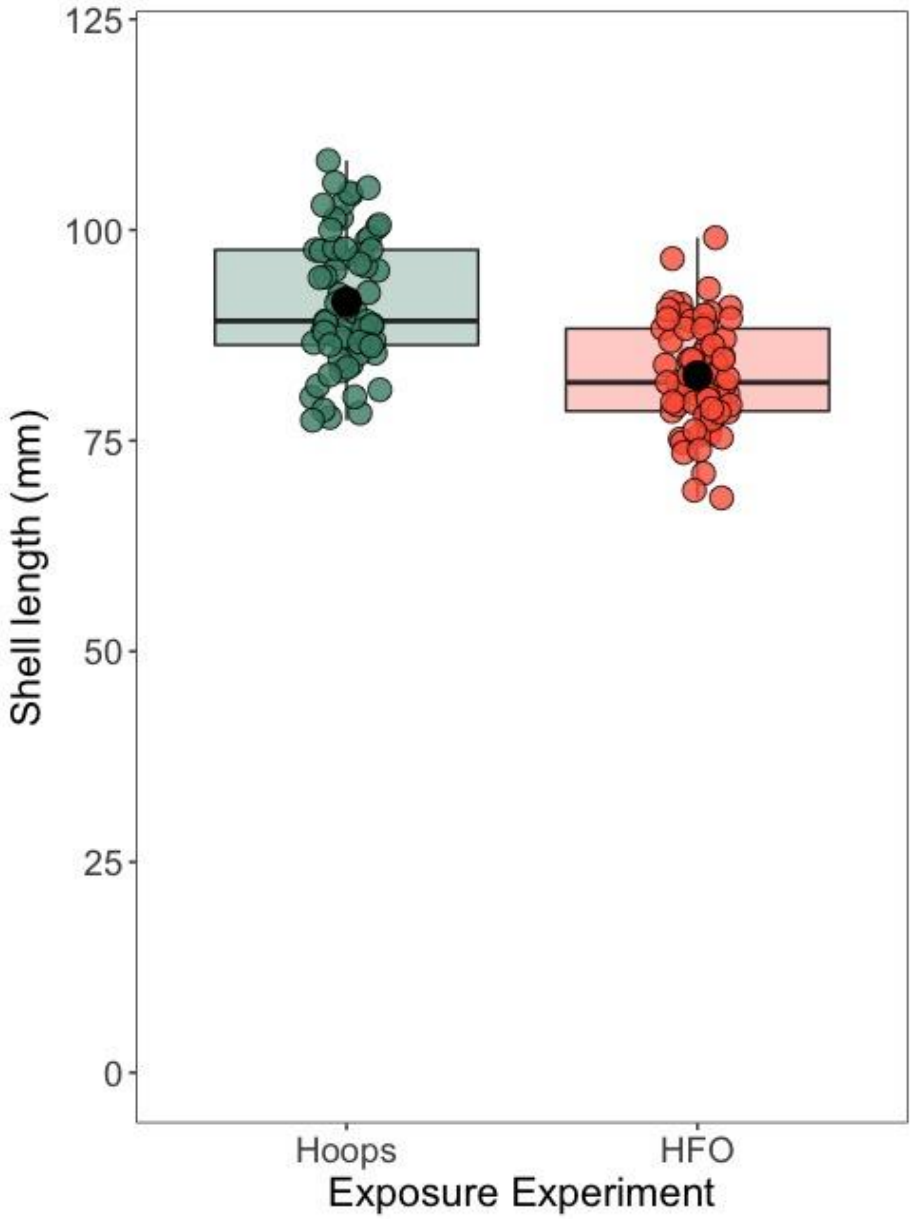

Figure S6. Comparison of shell length measurements for oysters used in the high dose WAF exposure to those used in the low dose WAF exposure. Conducting a Welch Two sample t-test, a significant difference in the means was found between groups (p-value < 0.05). Black point depicts the mean for each group. For interpretation of the boxplot: the filled area of the boxplot depicts the interquartile range, with the solid black line depicting the median for each group. Vertical lines (i.e. whiskers) extending from the box depict the upper and lower quartiles.

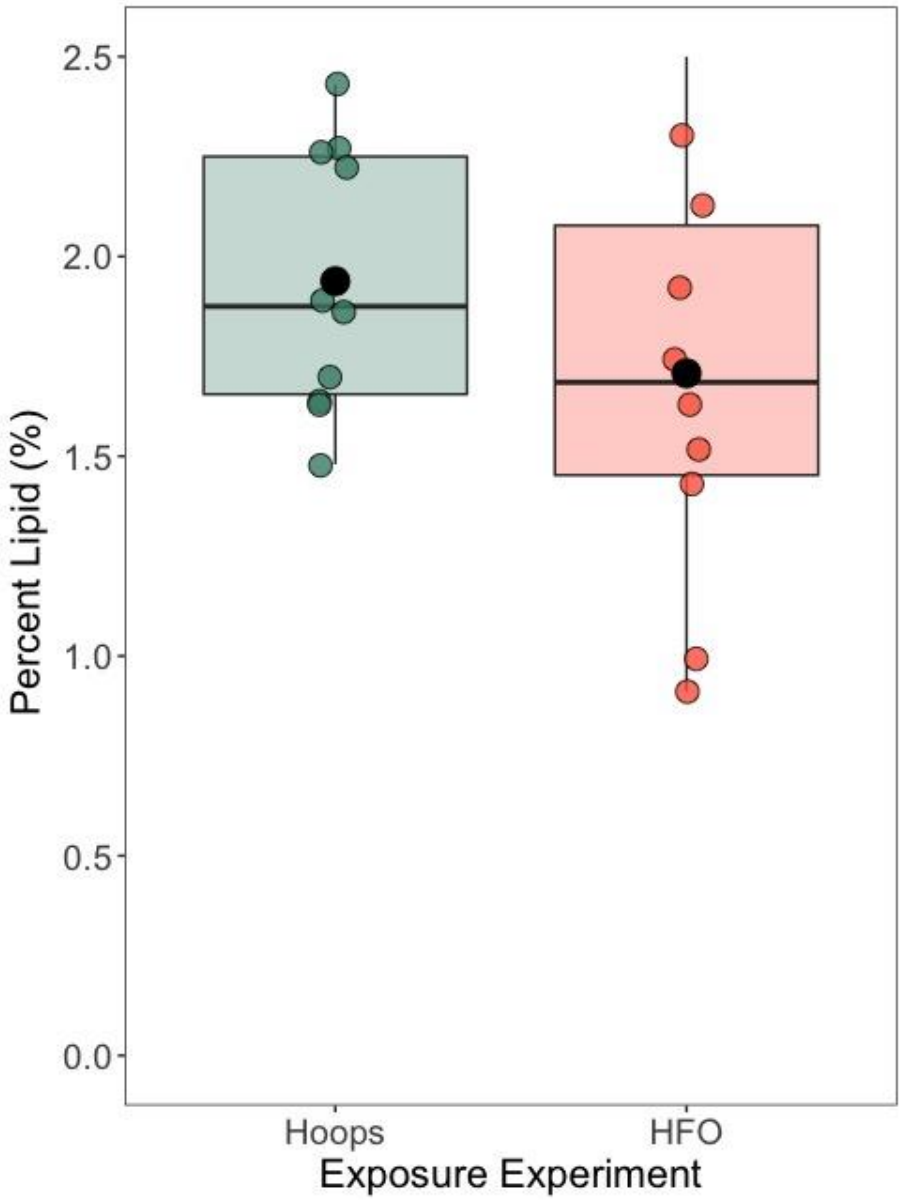

Figure S7. Comparison of extractable lipid percentage between oysters used in the high dose WAF exposure and those used in the low dose WAF exposure. Upon conducting a Welch Two sample t-test, no significant difference was observed in the means between groups (p-value=0.26,). The black point depicts the mean for each group. For interpretation of the boxplot: the filled area of the box depicts the interquartile range, with the solid black line depicting the median for each group. Vertical lines (i.e. whiskers) extending from the box depict the upper and lower quartiles.

Appendix C: Chapter 4 Supplementary Data

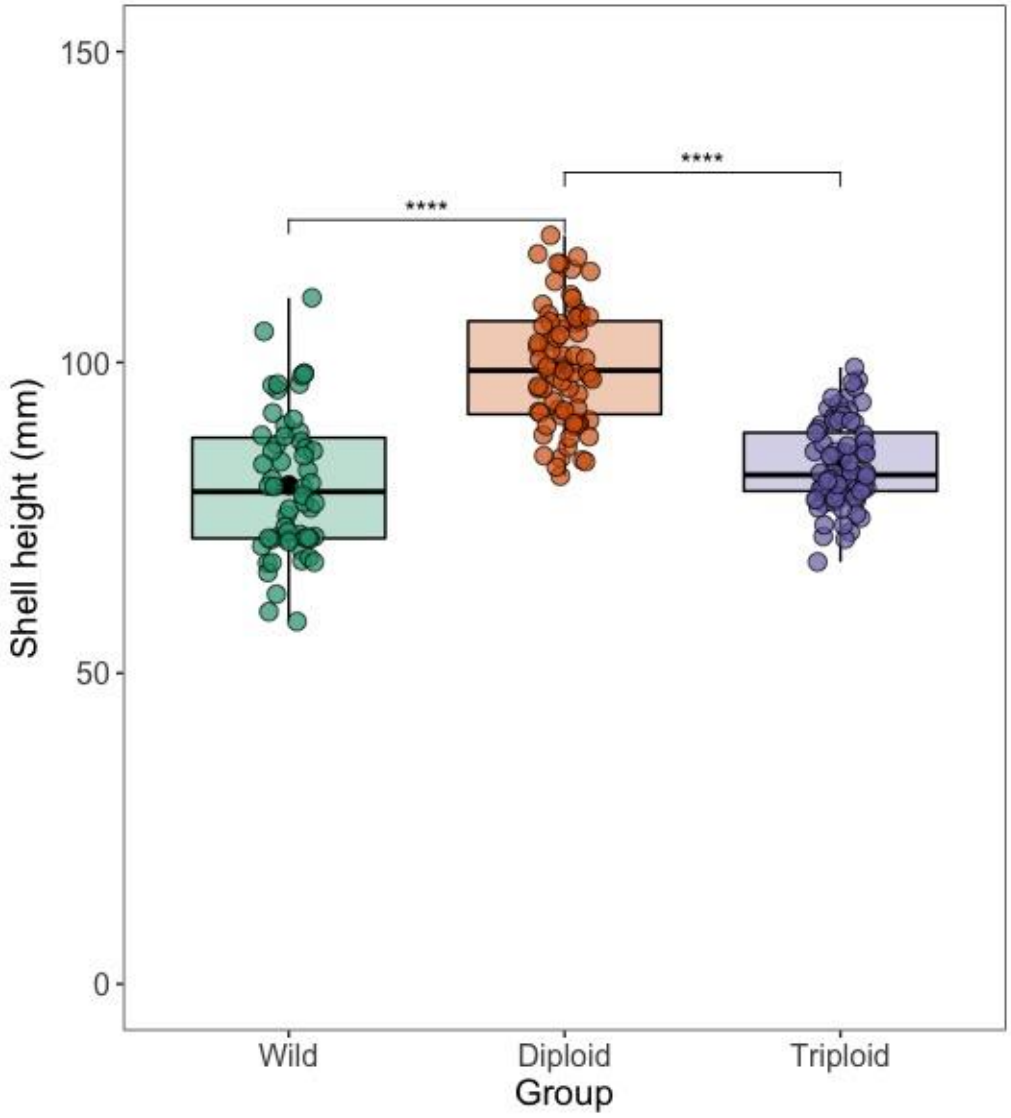

Figure S1. Shell height (mm) were measured by calipers and compared between wild oysters inhabiting Republic, transplanted diploid oysters, and transplanted triploid oysters. The black point depicts the mean. Brackets with asterisks depict significant results of Games-Howell post hoc comparison, conducted following a significant one-way ANOVA at each respective time point (p-value < 0.05). Non-significant results (p-value > 0.05) are not shown. For interpretation of the boxplot: the filled area of the boxplot depicts the interquartile range, with the solid black line depicting the median. Vertical lines (i.e. whiskers) extending from the box depict the upper and lower quartiles.

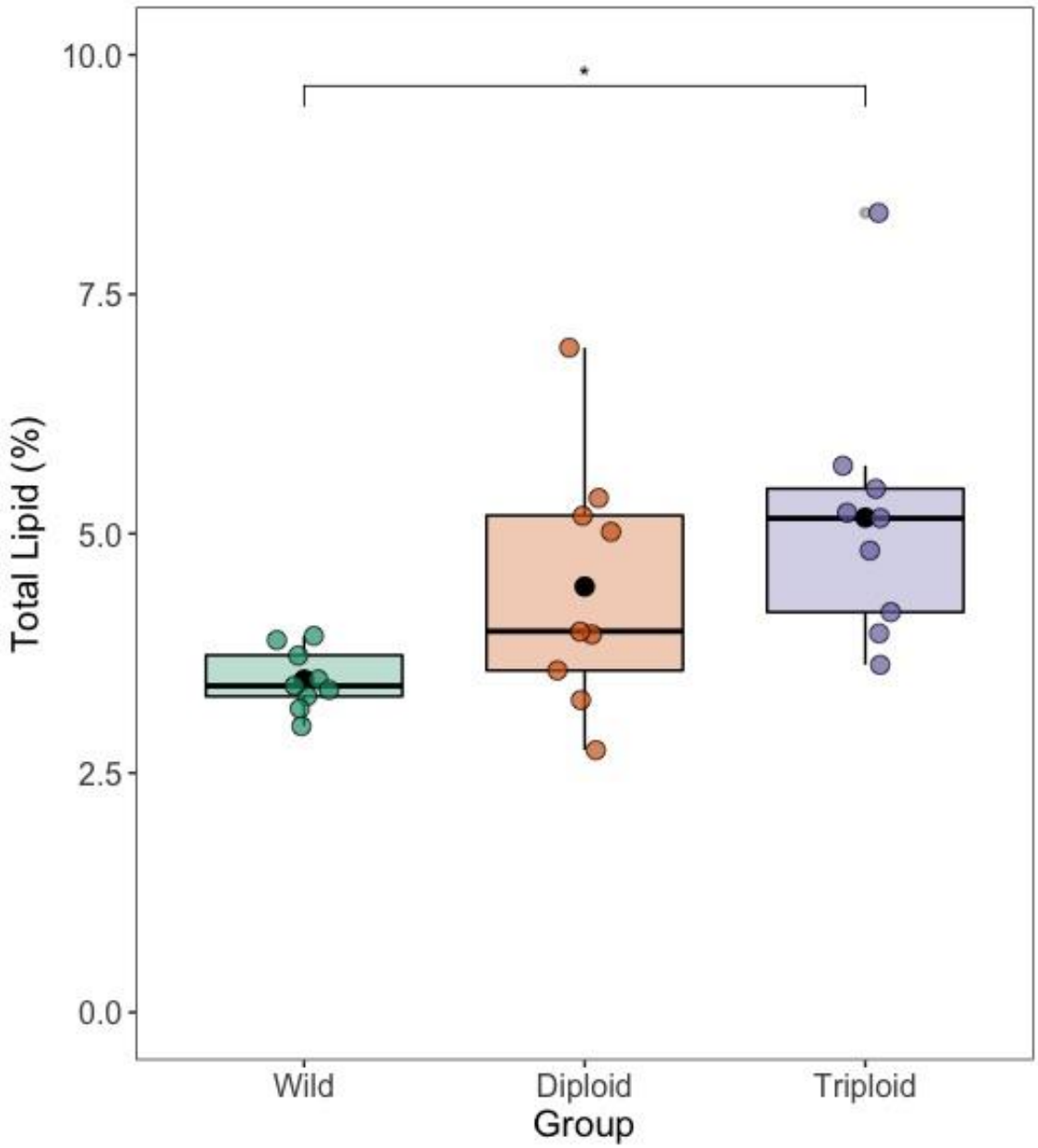

Figure S2. Total extractable lipid content was measured on a dry weight basis following HPLC-FLD. Lipid content was compared between wild oysters inhabiting Republic, transplanted diploid oysters, and transplanted triploid oysters. The black point depicts the mean. Brackets with asterisks depict significant results of Games-Howell post hoc comparison, conducted following a significant one-way ANOVA at each respective time point (p-value < 0.05). Non-significant results (i.e. p-value > 0.05) are not shown. For interpretation of the boxplot: the filled area of the boxplot depicts the interquartile range, with the solid black line depicting the median. Vertical lines (i.e. whiskers) extending from the box depict the upper and lower quartiles.

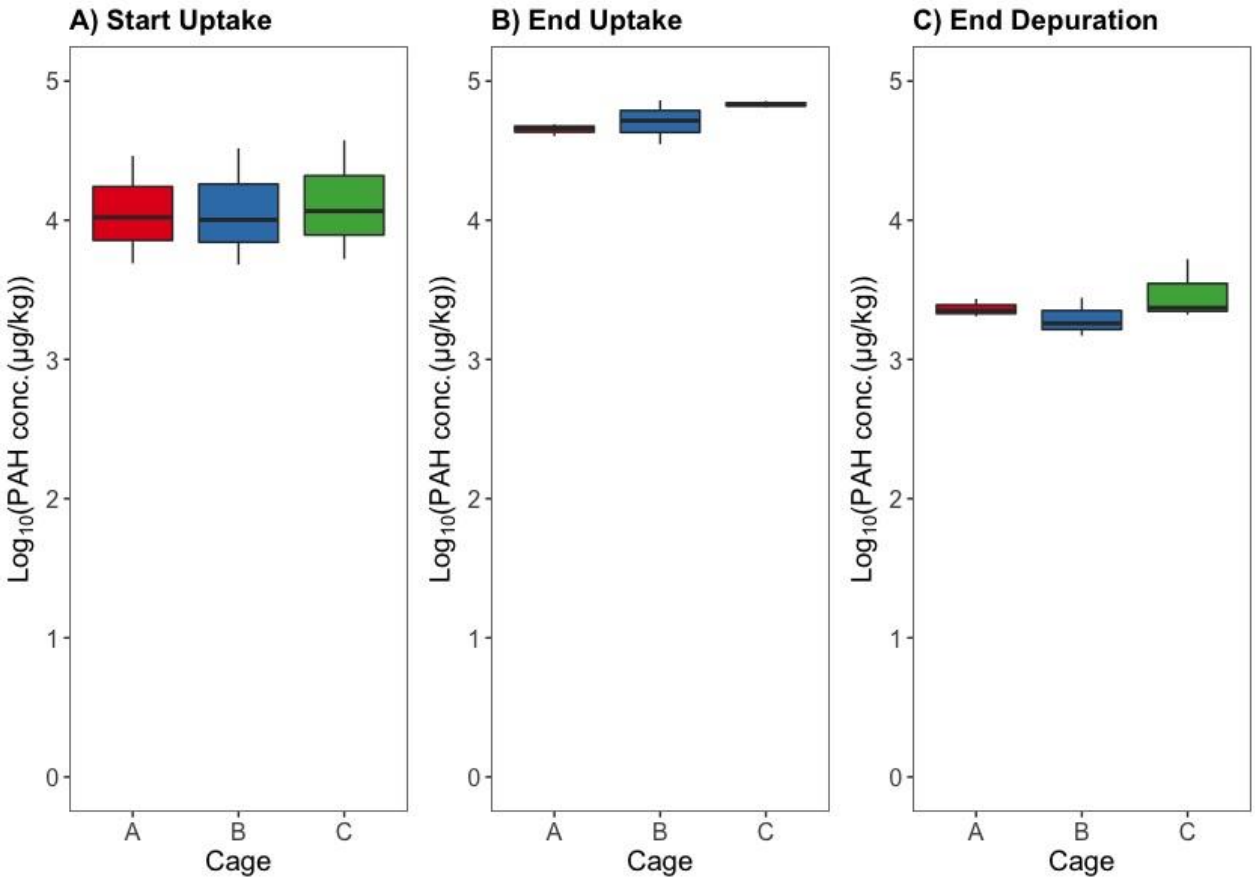

Figure S3. Comparison of log_{10}-transformed tissue concentrations between cages to assess potential cage effect at each time point: **A)** start of uptake phase (Day 0); **B)** end of uptake phase (Day 30); and **C)** end of depuration phase (Day 44). For GC–MS analysis, 3-5 oysters per cage were pooled to create a homogenized composite sample. Independent one-way ANOVAs at each time point determined that there were no significant differences in concentrations due to cage assignment.

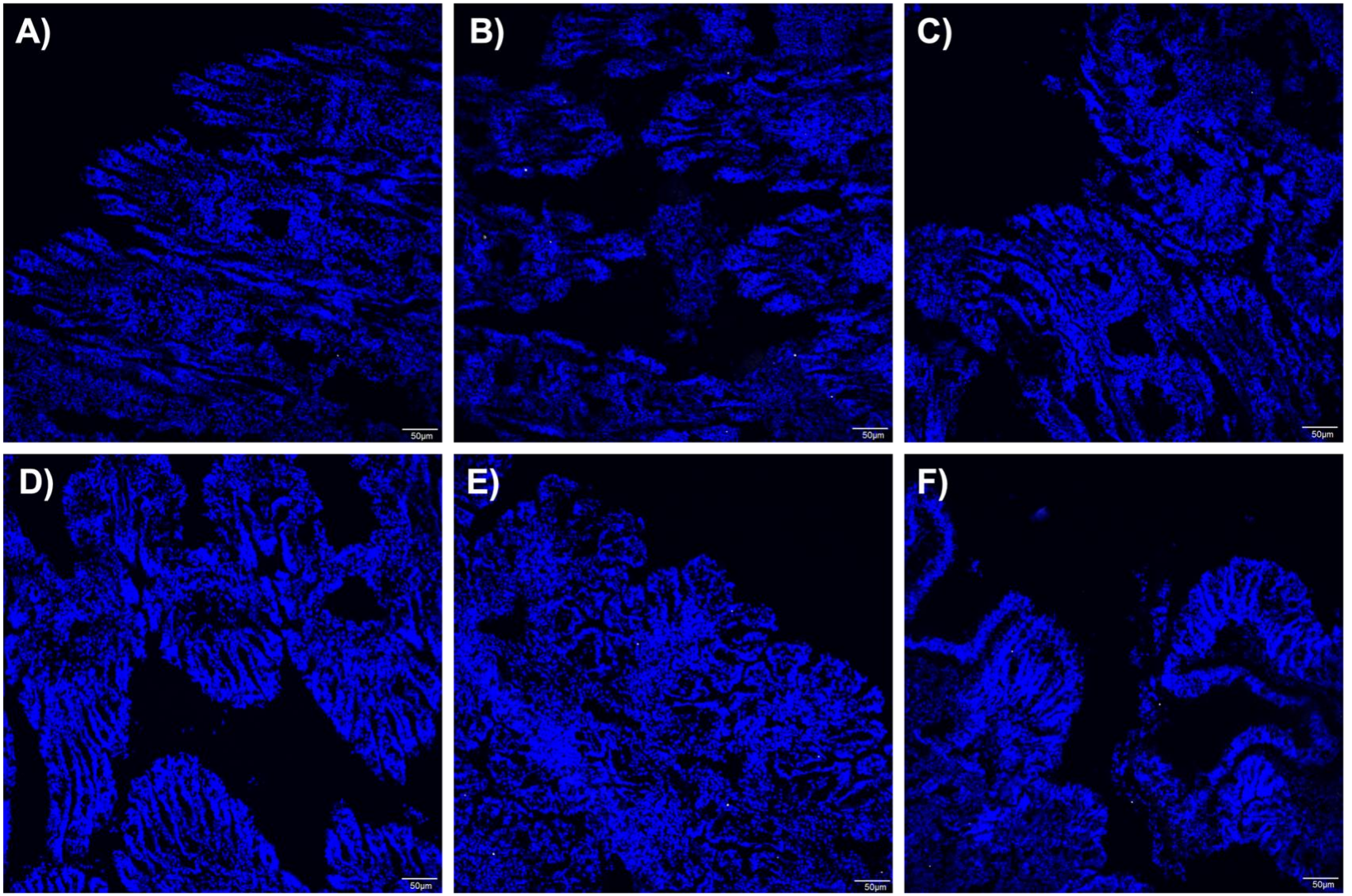
A)
B)
C)
D)
E)
F)
50µm

Figure S4. Negative control confocal microscope images of oyster gill tissue collected at each timepoint of the study. Oysters were held at PAH-impacted site in the Elizabeth River for uptake (30 days) and relocated to the York River for 14-day depuration period. **S4.A-C)** wild Republic oyster gill at **S4.A)** start of uptake (Day 0); **S4.B)** end of uptake (Day 30); **S4.C)** end of depuration (Day 44). **S4.D-F)** transplanted triploid oyster gill at **S4.D)** start of uptake; **S4.E)** end of uptake; **S4.F)** end of depuration. 4′,6-diamidino-2-phenylindole (DAPI) stain for cell nuclei depicted in blue; pl=gill plica, the target gill structure for throughout analysis, shown in S4A as reference.

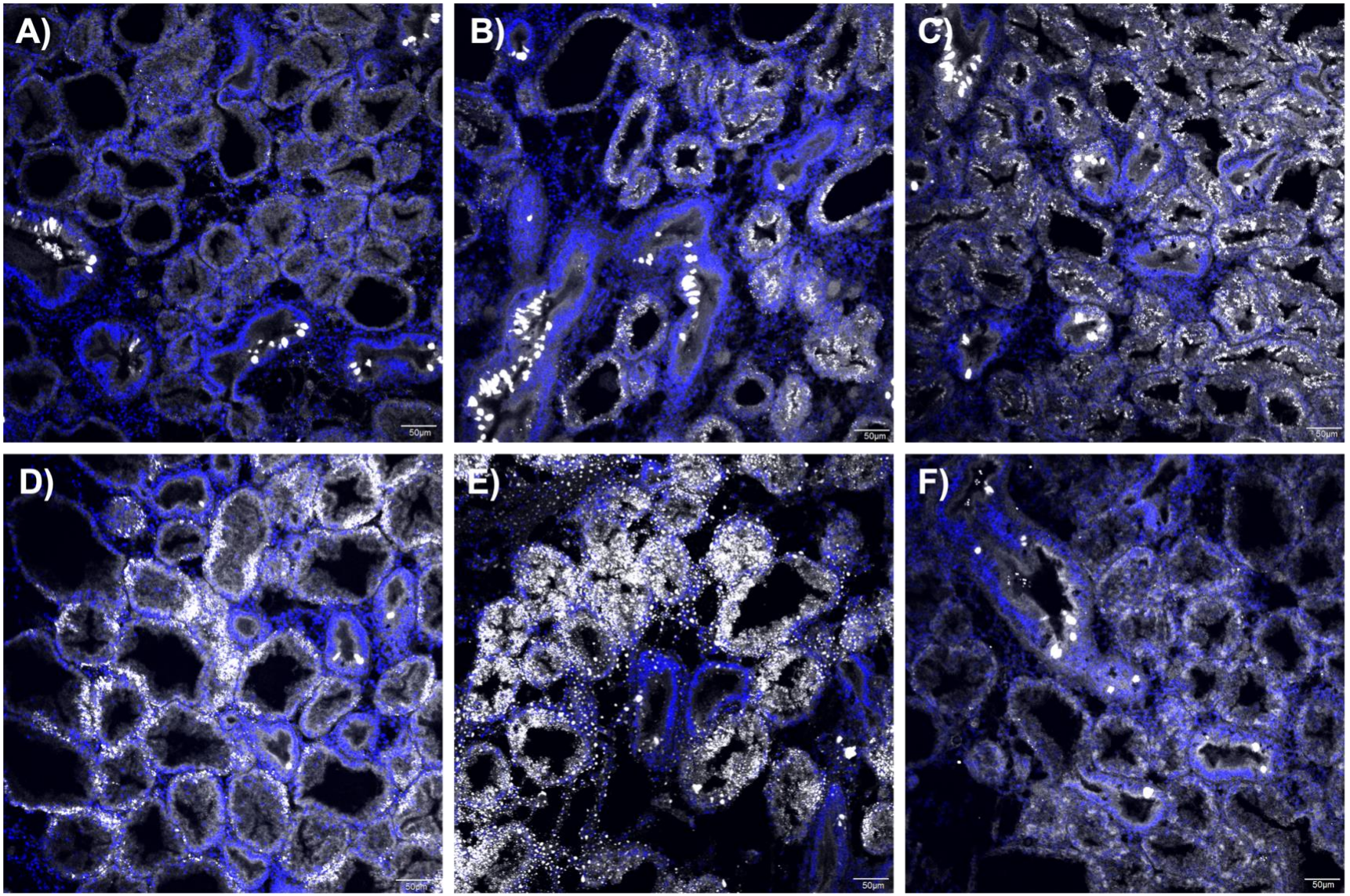
A)
B)
C)
D)
E)
F)
50µm

Figure S5. Positive control confocal microscope images of oyster digestive gland tissue collected at each timepoint of the study. Oysters were held at PAH-impacted site in the Elizabeth River for uptake (30 days) and relocated to the York River for 14-day depuration period. **S5.A-C)** wild Republic oyster digestive gland at **S5.A)** start of uptake (Day 0); **S5.B)** end of uptake (Day 30); **S5.C)** end of depuration (Day 44). **S5.D-F)** transplanted triploid oyster digestive gland at **S5.D)** start of uptake; **S5.E)** end of uptake; **S5.F)** end of depuration. AF647-tagged anti-PAH antibody (mAb 2G8) is depicted in white (however, autofluorescence is detected in the same wavelength, see Supplemental Figure S6.A-F); 4′,6-diamidino-2-phenylindole (DAPI) stain for cell nuclei depicted in blue.

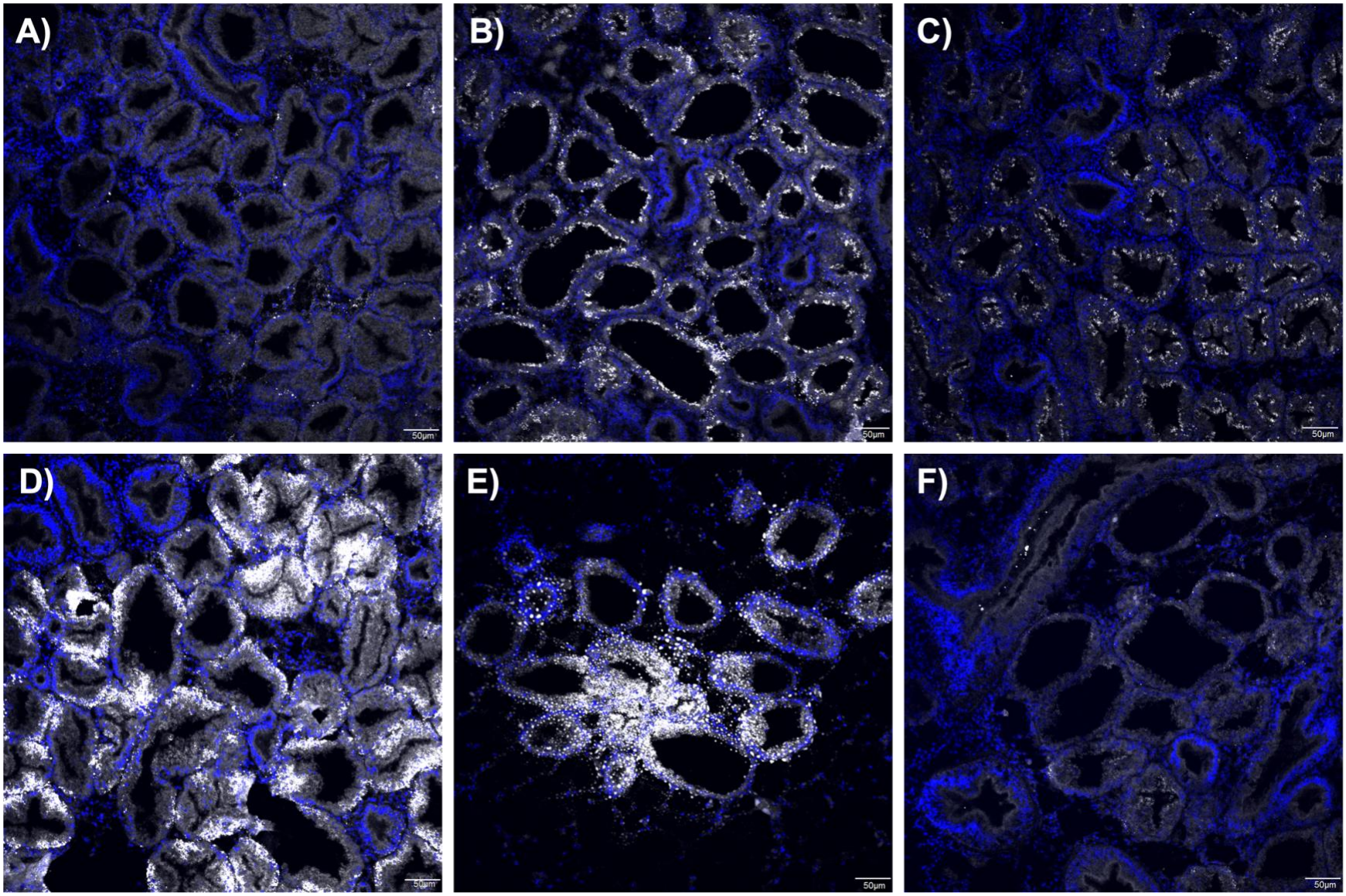
A)
B)
C)
D)
E)
F)
50µm

Figure S6. Negative control confocal microscope images of oyster digestive gland tissue collected at each timepoint of the study. Oysters were held at PAH-impacted site in the Elizabeth River for uptake (30 days) and relocated to the York River for 14-day depuration period. **S6.A-C)** wild Republic oyster digestive gland at **S6.A)** start of uptake (Day 0); **S6.B)** end of uptake (Day 30); **S6.C)** end of depuration (Day 44). **S6.D-F)** transplanted triploid oyster digestive gland at **S6.D)** start of uptake; **S6.E)** end of uptake; **S6.F)** end of depuration. Suspected autofluorescence (white) is detected in the same wavelength, as AF647-tagged mAB 2G8 see Supplemental Figure S5.A-F); 4′,6-diamidino-2-phenylindole (DAPI) stain for cell nuclei depicted in blue.

ANOVAs and Pairwise comparisons for Chapter 4

STAT.2: *One-Way ANOVAs for comparison oyster interstitial fluid concentration (measured via biosensor) between groups at each time point and post hoc comparisons reported in Figure 2*

A) Start of Uptake (Day 0)

```
T0.anova

## ANOVA Table (type II tests)
##
##   Effect DFn DFd      F        p p<.05   ges
## 1  Group   2  27 35.918 2.47e-08     * 0.727



## PAIRWISE COMPARISON (Games-Howell post hoc test)

pwc_T0

## # A tibble: 3 x 8
##   .y.        group1  group2   estimate conf.low conf.high       p.adj p.adj.signif
## * <chr>      <chr>   <chr>       <dbl>    <dbl>     <dbl>       <dbl> <chr>
## 1 conc_log10 Wild    Diploid    -0.594 -0.775      -0.413 0.000000612 ****
## 2 conc_log10 Wild    Triploid   -0.393 -0.584      -0.202 0.000211    ***
## 3 conc_log10 Diploid Triploid    0.201 -0.00825     0.411 0.061       ns
```

B) End of Uptake (Day 30)

```
T4.anova

## ANOVA Table (type II tests)
##
##   Effect DFn DFd      F        p p<.05   ges
## 1  Group   2  30 11.137 0.000241     * 0.426



## PAIRWISE COMPARISON (Games-Howell post hoc test)

pwc_T4

## # A tibble: 3 x 8
##   .y.        group1  group2   estimate conf.low conf.high p.adj p.adj.signif
## * <chr>      <chr>   <chr>       <dbl>    <dbl>     <dbl> <dbl> <chr>
## 1 conc_log10 Wild    Diploid     0.312   0.106     0.518  0.004 **
```

```
## 2 conc_log10 Wild    Triploid    0.208   0.0636    0.353  0.004 **
## 3 conc_log10 Diploid Triploid   -0.104  -0.306     0.0994 0.394 ns
```

C) End of Depuration (Day 44)

T6.anova

```
## ANOVA Table (type II tests)
##
##   Effect DFn DFd    F     p p<.05   ges
## 1  Group   2  30 3.79 0.034     * 0.202
```

```
## PAIRWISE COMPARISON (Games-Howell post hoc test)
```

pwc_T6

```
## # A tibble: 3 x 8
##   .y.        group1  group2   estimate conf.low conf.high p.adj p.adj.signif
## * <chr>      <chr>   <chr>       <dbl>    <dbl>     <dbl> <dbl> <chr>
## 1 conc_log10 Wild    Diploid    -0.147   -0.416    0.121  0.367 ns
## 2 conc_log10 Wild    Triploid   -0.301   -0.559   -0.0442 0.02  *
## 3 conc_log10 Diploid Triploid   -0.154   -0.375    0.0668 0.201 ns
```

STAT.3*: One-Way ANOVAs for comparison oyster tissue concentration (measured via GC–MS) between groups at each time point and pairwise comparisons reported in Figure 3*

A) Start of Uptake (Day 0)

```
GCT0.anova

## ANOVA Table (type II tests)
##
##   Effect DFn DFd      F     p p<.05   ges
## 1  Group   2   6 16.829 0.003     * 0.849



## PAIRWISE COMPARISON (Games-Howell post hoc test)

GCpwc_T0

## # A tibble: 3 x 8
##   .y.       group1  group2   estimate conf.low conf.high p.adj p.adj.signif
## * <chr>     <chr>   <chr>       <dbl>    <dbl>     <dbl> <dbl> <chr>
## 1 conc_log10 Wild    Diploid    -0.599   -1.22     0.0180 0.053 ns
## 2 conc_log10 Wild    Triploid   -0.710   -1.27    -0.150  0.03  *
## 3 conc_log10 Diploid Triploid   -0.112   -0.676    0.453  0.773 ns
```

B) End of Uptake (Day 30)

```
GCT4.anova

## ANOVA Table (type II tests)
##
##   Effect DFn DFd     F     p p<.05  ges
## 1  Group   2   6 1.165 0.374       0.28
```

C) End of Depuration (Day 44)

```
GCT6.anova

## ANOVA Table (type II tests)
##
##   Effect DFn DFd     F     p p<.05   ges
## 1  Group   2   6 0.609 0.574       0.169
```

STAT.4: *Two-Way ANOVAs for comparison of oyster gill and digestive gland fluid concentrations (via biosensor) between wild Republic oysters and transplanted triploid oysters reported in Figure 4*

A) Start of Uptake (Day 0)

```
IP.anova_T0

## ANOVA Table (type II tests)
##
##       Effect DFn DFd      F     p p<.05   ges
## 1      Group   1   7 17.066 0.004     * 0.709
## 2       Type   1   7  0.172 0.690       0.024
## 3 Group:Type   1   7  0.103 0.758       0.014
```

B) End of Uptake (Day 30)

```
IP.anova_T4

## ANOVA Table (type II tests)
##
##       Effect DFn DFd          F     p p<.05      ges
## 1      Group   1   8 13.7590000 0.006     * 6.32e-01
## 2       Type   1   8  5.5240000 0.047     * 4.08e-01
## 3 Group:Type   1   8  0.0000445 0.995       5.57e-06
```

C) End of Depuration (Day 44)

```
IP.anova_T6

## ANOVA Table (type II tests)
##
##       Effect DFn DFd     F     p p<.05   ges
## 1      Group   1   8 0.175 0.687       0.021
## 2       Type   1   8 9.163 0.016     * 0.534
## 3 Group:Type   1   8 1.189 0.307       0.129
```